Measures and dynamics of entangled states

Dissertation der Fakultät für Physik
der Ludwig-Maximilians-Universität München

vorgelegt von Florian Mintert
aus München

München, den 1. März 2004

1. Gutachter: PD Dr. Andreas Buchleitner
2. Gutachter: Prof. Dr. Herbert Spohn
Tag der mündlichen Prüfung: 7. Mai 2004

Zusammenfassung

Im ersten Teil der vorliegenden Arbeit entwickeln wir eine Theorie zur quantitativen Abschätzung der Verschränkung gemischter Quantenzustände von Zweiparteiensystemen. Wir leiten obere und untere Schranken der Concurrence für beliebige endliche Dimensionen her, was es insbesondere ermöglicht, ein endliches Intervall für deren tatsächlichen Wert anzugeben. Wir testen diese Schranken an unterschiedlichen Typen quantenmechanischer Zustände und erhalten verläßliche Beschreibungen. Ausserdem ist unsere untere Schranke in der Lage, die nichttriviale Verschränkung von Zuständen mit positiver partieller Transponierter zu erkennen. Im Hinblick auf konkrete experimentelle Anforderungen geben wir eine explizite Näherung für nahezu reine - d.h. schwach gemischte - Zustände an, die eine rein algebraische Abschätzung ermöglicht. Deren Vergleich mit den allgemeiner gültigen oberen und unteren Schranken zeigt, daß ihr Gültigkeitsbereich sich sogar auf Zustände mit relativ starkem Mischungsgrad erstreckt. Schließlich schlagen wir eine mögliche Verallgemeinerung der Concurrence für Systeme mit beliebig vielen Untersystemen vor. Es zeigt sich, daß diese verallgemeinerte Concurrence mit Hilfe derselben Methoden quantitativ gefaßt werden kann, die auch in unserer Behandlung von Zweiparteiensystemen zum Ziel führen.

Diese neuen Methoden zur Abschätzung des Verschränkungsgrades beliebiger gemischter Zustände ermöglichen es, die Erzeugung und den Zerfall von Verschränkung unter dem Einfluß kohärenter und inkohärenter Prozesse mit vergleichweise geringem Aufwand zu verfolgen, was wir mit der Anwendung unserer Theorie auf ein für Ionenfallenexperimente typisches Szenario zeigen.

Der zweite Teil der Arbeit liefert eine quantitative Charakterisierung reiner Zustände von Zweiparteiensystemen, die sich direkt auf Systeme mit einer beliebigen Anzahl von Unterteilungen verallgemeinern läßt. Hierzu benutzen wir geeignet definierte Quasiwahrscheinlichkeitsverteilungen und zeigen, daß deren statistische Momente oder Entropien, die ihre Lokalisierungseigenschaften beschreiben, unter lokalen Operationen und klassischer Kommunikation nicht anwachsen und somit Verschränkungsmonotone sind.

b

Abstract

In the first part of the present thesis, we derive a theory for quantifying entanglement of mixed bipartite quantum states. We derive upper and lower bounds for the concurrence of quantum states in arbitrary finite dimensions, such as to confine its actual value to a finite interval. We test these estimates for various sets of states with very satisfactory results. In particular, our lower bound detects entangled states with positive partial transpose. In view of the specific requirements of laboratory experiments, we derive an approximate expression for the concurrence of almost pure - *i.e.* weakly mixed - states. Comparison of this quasi-pure approximation with the above upper and lower bounds shows that its range of validity even comprises states with relatively large mixing. Finally, we propose a generalised concurrence for multipartite mixed states. For its quantitative characterisation, we can use the same strategies as in our treatment of bipartite systems.

These novel techniques for a quantitative description of the entanglement of mixed states allow to monitor the production and the decay of entanglement under coherent and incoherent forcing - as we show by applying our theory to a realistic scenario of ion trap experiments.

In the second part of the thesis, we introduce suitably defined quasi probability representations such as to quantify the entanglement of pure bipartite states, with an immediate generalisation for pure states of multipartite systems. It is shown that the statistical moments as well as various entropies of these representations - characterising their localisation properties - are non-increasing under local operations and classical communication, hence that they are proper entanglement monotones.

d

I am grateful for three inspiring, instructive and - most of all - wonderful years working with Andreas Buchleitner. I enjoy commemorating not only an encouraging and stimulating collaboration, but also lots of discussions about - and in particular also not about - my project.

I especially enjoyed and benefited from several visits to Kraków and Warszawa, funded by the project 'Entanglement measures and he influence of noise' by VW-foundation. In Kraków, I had the opportunity to benefit from a very nice collaboration with Karol Życzkowski, who - apart from our research project - also encouraged my attempts to learn Polish. In Warszawa, I benefited tremendously from numerous discussions and a joint project with Marek Kuś.

I am particularly thankful to my parents for a great support during all my studies.

Among all those people who made my last years a wonderful time, I am especially grateful to André Ricardo Ribeiro de Carvalho, Andreas Krug, Cord Müller, Javier Madroñero, Jim 'Jiminator' Hague, Kenfack 'Kenchen', Klaus Quedenbaum, Nilüfer 'Nili' Baba, Nils Hasselmann, Thomas 'Thomasito' Wellens and last but not least the 'Bios' Alex, Andi, Björn, Gernot, Tobias and Thomas.

f

Contents

Chapter 1

Introduction

Quantum entanglement is one of the central causes of the fundamental differences between quantum and classical mechanics. Whereas interference phenomena, which equally constitute a qualitatively different behaviour of quantum systems as compared to classical ones, are well understood, the knowledge about the nature of entangled states is still restricted - both regarding their physical as well as their mathematical aspects.

Entangled states exist in quantum systems that decompose into subsystems, whereas composite classical systems do not have any analogous states. Two or more classical, non-interacting subsystems are independent of each other - any exterior influence on one of the subsystems has no impact on the other subsystems at all. This also holds true for quantum systems, as long as the entire multipartite system is described by a separable state. However, if its state is entangled, the subsystems are not completely independent any more. For example, a measurement that is performed locally on one subsystem causes a state reduction [1] - not just of the subsystem state but of the state of the entire system. Thus, probabilities for a measurement result on any subsystem can change during a measurement on any other subsystem - irrespective of the absence of interactions between the subsystems.

Whereas this non-local behaviour caused severe criticisms during the founding period of quantum mechanics [2], it nowadays is even considered as the basis of various technical applications.

Discussions on the existence of entangled states in the 1930's rose doubts on whether quantum mechanics could provide a complete description of nature [2]. In particular, possible correlations of measurement results on different subsystems were widely discussed. In classical systems, all such possibly occuring correlations can be described in terms of classical probabilities. This is not possible for correlations characteristic of entangled states, what at that time contradicted common understanding of nature. As a consequence, there were attempts to find alternative theories that could explain the non-classical correlations of quantum systems. The most popular [2] -

that finally led to the first experimental evidence [3] for entangled states - postulates the existence of so-called hidden variables. These are assumed to determine the values of all local observables - without, however, being accessible to any kind of measurement, such that their deterministically fixed state remains unknown as a matter of principle.

Several inequalities - called *Bell inequalities* - capable of discriminating correlations of measurement results due to entanglement against those described by local hidden variable theories were proposed [4, 5]. Later, also criteria that use special three-partite states and do not involve inequalities were found [6]. Both kinds of criteria were tested experimentally [3, 7], and independently gave evidence that local hidden variable theories cannot describe all correlations that occur in quantum systems.

Nowadays, there is considerable interest in entangled states, because there are various potential applications that make use of these non-local properties. The most famous - and most controversially discussed - proposed technical application is the use of quantum systems as hard-ware for a new generation of computers that is based on the principles of quantum mechanics [8, 9]. All basic steps required for such a quantum computer are already experimentally demonstrated [10, 11, 12]. However, so far it is still unknown whether it will be possible to ever run a quantum computer that exceeds the performance of classical ones. Other potential applications, as for example, quantum teleportation [13] and quantum cryptography [14], that also are realised experimentally [15, 16] are more likely to be commercially usable in the near future.

Both, because of fundamental interest and because of their usefulness for the above applications, entangled states are the object of numerous experiments. There are several systems available in which entangled states can be prepared and investigated. For example, ion traps [17, 18, 19, 20] or micro-traps [21, 22, 23] allow to prepare entangled states of two or more subsystems using an interaction which is engineered with the help of coherent electro-magnetic radiation or using controlled collisions [24, 25].

Pure entangled states are best suited for technical applications because they bear strongest possible quantum correlations, and show no classical probabilistic correlations that could be detrimental to an application. However, there is no system that could be decoupled perfectly from environmental influences. Thus, non-unitary dynamics due to unavoidable environment coupling cannot be neglected completely, and one has to consider that initially pure states evolve into mixed ones. Since mixing always implies classical probabilistic behaviour, classical correlations can emerge at the expense of quantum correlations. This poses severe demands on experiments - in order to maintain quantum correlations, environment coupling has to be reduced as much as possible.

In addition, there are also fundamental problems in the theoretical de-

scription of mixed entangled states. Virtually the entire state of the art theory of entangled quantum states is based on so-called *entanglement measures*. An entanglement measure is a scalar quantity that quantifies quantum correlations, and distinguishes them from classical ones. Although several such measures have been proposed, no simple criterion of discriminating different kinds of correlations is known so far. All proposed measures that unambiguously discriminate classical against quantum correlations involve some optimisation procedure. The underlying idea is to represent given correlations as well as possible by classical probabilities. The extent to which non-classical properties are required for the representation of a state can provide a quantification of entanglement. A commonly used class of measures is, for example, based on straightforwardly computable measures for pure states, such that - among all ensembles represented by the considered mixed state - the ensemble with the minimum average entanglement quantifies the mixed state's entanglement.

As a consequence of the necessity of performing a - generally high dimensional - optimisation problem, hardly any formally defined measure actually can be computed so far. There are a few measures that can be calculated algebraically for states of smallest possible dimensions, namely of bipartite two-level systems [26, 27, 28]. Though none is known that unambiguously distinguishes quantum correlations from classical ones, and that could be calculated algebraically for arbitrary states of larger systems.

These difficulties of characterising mixed quantum states prevent a systematic investigation of entangled states that occur in real experiments. At least partially due to these problems, the interest in entangled states is divided into two nearly disjoint branches. The first one is the experimental approach of preparing entangled states and measuring non-local effects. The second branch is concerned with rather mathematical aspects of entangled states. In this field, general algebraic properties of states of composite quantum systems are investigated, but this general theory is hardly applicable to currently performed experiments - and in turn also experimental results do not influence the theoretical work significantly.

Here, we aim at providing theoretical means for the efficient characterisation of realistically occuring states of arbitrary finite-dimensional quantum systems. Applying these tools to realistic experimental scenarios we hope to build a bridge between experimental pragmatism and mathematical generality and rigour.

We will start out from the formal definition of concurrence, a widely accepted measure of entanglement of mixed bipartite states. A careful study of this quantity's algebraic properties will provide, step by step, a recipe for its numerical evaluation, as well as lower bounds thereof, and an estimate for a class of experimentally particularly interesting states. Whilst the exact evaluation of concurrence remains numerically demanding, at least in higher

dimensions, the lower bounds are given in purely algebraic form, and yet even allow to detect entangled states which remain undetected by standard indicators of entanglement.

We will show that, in general, these algebraic bounds provide excellent approximations of the actual value of concurrence of mixed states, and that in particular they allow to monitor the temporal evolution of entanglement in a typical experimental setting, including the unavoidable - and generally detrimental - influence of the environment. As we will see, this implies possible applications such as the optimisation of various experimental parameters, with the aim, *e.g.*, to maximise entanglement on experimentally relevant time scales, in the presence of environment coupling.

Finally, we will also consider entanglement measures for multi-partite systems. In this context we propose a generalisation of concurrence for mixed states of systems with arbitrarily many subsystems. It can be quantitatively characterised with the techniques that we will derive for bipartite systems. To end with, we present a new class of entanglement monotones for pure states that - unlike concurrence - have a straightforward generalisation for multi-partite systems.

However, before we outline our original approach, let us first summarise the present status of entanglement theory in the next chapter, as far as it is of relevance for our specific purposes.

Chapter 2

State of the art

2.1 Entangled states

A bipartite system is associated with a Hilbert space $\mathcal{H}$ that is given by the tensor product $\mathcal{H}_1 \otimes \mathcal{H}_2$ of the predefined subspaces.

For pure states one distinguishes two different kinds of states. A state $|\Psi\rangle$ is called a *product state* or *separable*, if it can be written as direct a product of subsystem states, *i.e.*

$$\exists\ |\varphi\rangle \in \mathcal{H}_1,\ |\phi\rangle \in \mathcal{H}_2\ , \quad \text{such that} \quad |\Psi\rangle = |\varphi\rangle \otimes |\phi\rangle\ . \tag{2.1}$$

Such a state describes a situation analogous to a classical one insofar as the system state contains exactly the information that is contained in the subsystem states. A state reduction [1] caused by a measurement performed on one subsystem has no influence on the state of the other subsystem. This means that measurement results on the different subsystems are uncorrelated. In contrast to this, they are correlated for *entangled* states, *i.e.* states that cannot be written as a direct product of subsystem states:

$$\nexists\ |\varphi\rangle \in \mathcal{H}_1,\ |\phi\rangle \in \mathcal{H}_2\ , \quad \text{such that} \quad |\Psi\rangle = |\varphi\rangle \otimes |\phi\rangle\ . \tag{2.2}$$

Here, a local measurement causes a state reduction of the entire, *i.e.* bipartite system state, and therefore changes the probabilities for potential future measurements on either subsystem.

For mixed states the situation is more complicated. Product- and separable states are not synonymous anymore. The former can be expressed as a direct product of subsystem states, *i.e.*

$$\exists\ \varrho^{(1)} \in \mathcal{B}(\mathcal{H}_1),\ \varrho^{(2)} \in \mathcal{B}(\mathcal{H}_2)\ , \quad \text{such that} \quad \varrho = \varrho^{(1)} \otimes \varrho^{(2)}\ , \tag{2.3}$$

with the set $\mathcal{B}(\mathcal{H})$ of bounded operators on $\mathcal{H}$ [29]. For the latter, a convex decomposition into product states exists

$$\exists\ \{p_i > 0,\ \varrho_i^{(1)} \in \mathcal{B}(\mathcal{H}_1),\ \varrho_i^{(2)} \in \mathcal{B}(\mathcal{H}_2)\}\ , \quad \text{s.t.} \quad \varrho = \sum_i\ p_i\ \varrho_i^{(1)} \otimes \varrho_i^{(2)}\ , \tag{2.4}$$

where convexity implies positive coefficients that sum up to unity, $\sum_i p_i = 1$. Such a state refers to a situation described above for classical systems. Correlations between different subsystems are due to incomplete knowledge about the system state. They are characterised completely by the classical probabilities p_i.

Quantum correlations, *i.e.* entanglement need now be distinguished from classical correlations - a problem which we will focus on throughout the largest part of this thesis. Formally, and in a rather non-constructive way, an entangled mixed state is defined through the non-existence [30] of a convex decomposition alike eq. (2.4), *i.e.*

$$\nexists \{p_i > 0,\ \varrho_1^i \in \mathcal{B}(\mathcal{H}_1),\ \varrho_2^i \in \mathcal{B}(\mathcal{H}_2)\} , \quad \text{s.t.} \quad \varrho = \sum_i p_i\ \varrho_1^i \otimes \varrho_2^i . \quad (2.5)$$

The correlations contained in such states cannot be characterised completely by a set of classical probabilities. Thus, entangled states contain correlations that do not exist in any classical system.

The definition of entangled states can straightforwardly be generalised to *multi-partite systems*, *i.e.* systems that decompose into more than two subsystems. A p-partite system is described by a Hilbert space $\mathcal{H}$ that decomposes into the tensor product of n subspaces $\mathcal{H}_1 \otimes \cdots \otimes \mathcal{H}_p$. A pure state is separable if it can be written as a direct product of p states, each of which describes one of the subsystems - any state that is not separable is entangled. A mixed state is separable if it can be written as a convex sum of product states, *i.e.* of direct products of states each acting on a single subsystem. If it cannot - it is entangled.

For multipartite systems it is also meaningful to distinguish between different degrees of separability: a pure state $|\Psi\rangle$ is called *ν-separable* if it can be written as a direct product of ν states $|\phi_i\rangle$, each of which is an element of one of the subspaces, or of the direct product of some subspaces. Thus a ν-separable state with $\nu < p$ can contain entanglement between some of the subsystems, whilst there also are subsystems that are completely uncorrelated. In this terminology, p-separability is equivalent to complete separability.

2.1.1 Schmidt decomposition

Pure bipartite states can be classified with the help of their *Schmidt decomposition*. Each bipartite pure state $|\Psi\rangle$ can be expressed in some product basis,

$$|\Psi\rangle = \sum_{ij} b_{ij}\ |\varphi_i\rangle \otimes |\phi_j\rangle . \quad (2.6)$$

The local bases $\{|\varphi_i\rangle \in \mathcal{H}_1\}$ and $\{|\phi_i\rangle \in \mathcal{H}_2\}$ can be chosen arbitrarily. However, referring to a given state, there is always one special basis. It can

be constructed with the following representations of the identity operators $\mathbb{1}_1 = \sum_i \mathcal{U}^\dagger|\varphi_i\rangle\langle\varphi_i|\mathcal{U}$ acting on the first subspace $\mathcal{H}_1$, and an analogous expression $\mathbb{1}_2 = \sum_i \mathcal{V}^\dagger|\phi_i\rangle\langle\phi_i|\mathcal{V}$ acting on the second subspace $\mathcal{H}_2$. $\mathcal{U}$ and $\mathcal{V}$ are some arbitrary, local unitary transformations acting on $\mathcal{H}_1$ and $\mathcal{H}_2$, respectively. Inserting these identities in eq. (2.6), the state $|\Psi\rangle$ can be expressed as

$$|\Psi\rangle = \sum_{ij} [ubv]_{ij}\ \mathcal{U}^\dagger|\varphi_i\rangle \otimes \mathcal{V}^\dagger|\phi_j\rangle\ , \tag{2.7}$$

where the unitary matrices u and v are defined as

$$u_{ij} = \langle\varphi_i|\mathcal{U}|\varphi_j\rangle \quad \text{and} \quad v_{ij} = \langle\phi_j|\mathcal{V}|\phi_i\rangle\ . \tag{2.8}$$

Now one can use the fact that every complex matrix b can be diagonalised by two unitary transformations u and v such that $ubv = \mathrm{diag}[\mathcal{S}_1, \ldots, \mathcal{S}_n]$, with real and non-negative diagonal elements $\mathcal{S}_i$, which provide the *singular value decomposition* of b [31]. Hence, any pure state can be represented in terms of its *Schmidt coefficients* $\lambda_i = \mathcal{S}_i^2$, and of the associated *Schmidt basis* $|\psi_i\rangle_1 \otimes |\psi_j\rangle_2 = \mathcal{U}^\dagger|\varphi_i\rangle \otimes \mathcal{V}^\dagger|\phi_j\rangle$:

$$|\Psi\rangle = \sum_i\ \sqrt{\lambda_i}\ |\psi_i\rangle_1 \otimes |\psi_i\rangle_2\ . \tag{2.9}$$

Given that the Schmidt basis comprises - by construction - only separable states, all information about entanglement of $|\Psi\rangle$ is now contained in the Schmidt coefficients λ_i. The characterisation of all correlations of a given pure state is therefore tantamount to the complete knowledge of all Schmidt coefficients. The normalisation condition $\langle\Psi|\Psi\rangle = 1$ implies that there are $n-1$ independent coefficients, in an n-dimensional system.

The Schmidt coefficients can easily be computed with the help of one of the *reduced density matrices* $\varrho_1 = \mathrm{Tr}_2|\Psi\rangle\langle\Psi|$, $\varrho_2 = \mathrm{Tr}_1|\Psi\rangle\langle\Psi|$. Assume, without loss of generality, $d = \dim(\mathcal{H}_1) \leq \dim(\mathcal{H}_2)$. Using eq. (2.9), one easily verifies that the spectrum of ϱ_1 is just given by the Schmidt coefficients - the spectrum of ϱ_2 is given by the Schmidt coefficients and $\dim(\mathcal{H}_2) - \dim(\mathcal{H}_1)$ vanishing eigenvalues.

The Schmidt coefficients also allow to distinguish separable from entangled states - a separable state is characterised by a vector of Schmidt coefficients with only one non-vanishing entry: $\vec{\lambda} = \vec{\lambda}_s = [1, 0, \ldots, 0]$, whereas the *Schmidt vector* of an entangled state has at least two non-vanishing components. A state is called *maximally entangled*, if its Schmidt vector reads $\vec{\lambda} = \vec{\lambda}^* = [1/d, \ldots, 1/d]$. In chapter 2.2.2 we will discuss in which respect this terminology is legitimate.

It follows that the concept of Schmidt coefficients allows to relate the degree of entanglement of pure bipartite states to the degree of mixing of the corresponding reduced density matrices - a pure reduced density matrix

corresponds to a separable state, whereas a maximally entangled state leads to a maximally mixed reduced density matrix.

Indeed, we will see in chapter 2.2.2 that the Schmidt coefficients do not only allow to distinguish between separable and entangled states: they are also useful to quantify entanglement.

2.1.2 Separability criteria

Whereas we have just seen that the separability of pure states can easily be checked, it turns out to be much more difficult to decide whether a given mixed state bears quantum entanglement. The above definition, eq. (2.5), for entangled mixed states is not constructive, and generically it is not clear whether there is a set of product states such that ϱ can be represented as a convex sum of its elements.

The standard approach to decide on the separability of a given mixed state relies on *positive maps*. A map $\Lambda : \mathcal{B}(\mathcal{H}) \to \mathcal{B}(\mathcal{H})$ is called *positive* if it maps positive operators on positive ones, *i.e.*

$$\Lambda(\varrho) \geq 0, \quad \text{for all} \quad \varrho \geq 0 \ , \tag{2.10}$$

where positivity of an operator ϱ is just a short hand notation stating that ϱ is positive semi-definite, *i.e.* it has only non-negative eigenvalues. A crucial property of positive maps is that a trivial extension $\Lambda \otimes \mathbb{1}$ is *not* necessarily positive. Consider a positive map $\Lambda : \mathcal{B}(\mathcal{H}_1) \mapsto \mathcal{B}(\mathcal{H}_1)$: if the trivial extension $\Lambda \otimes \mathbb{1}$, with $\mathbb{1}$ the identity map on $\mathcal{B}(\mathcal{H}_2)$, is not positive, it can be used to conclude on the separability of a mixed state ϱ, acting on $\mathcal{H}_1 \otimes \mathcal{H}_2$. Since the extended map $\Lambda \otimes \mathbb{1}$ is not positive, there are some states η such that $\big(\Lambda \otimes \mathbb{1}\big)(\eta) \ngeq 0$. However, if one assumes the considered state ϱ to be separable, its convex decomposition into product states (2.4) implies

$$\big(\Lambda \otimes \mathbb{1}\big)(\varrho) = \sum_i \ p_i \ \Lambda(\varrho_1^i) \otimes \varrho_2^i \ . \tag{2.11}$$

Obviously, any expectation value of this quantity is non-negative, such that $\big(\Lambda \otimes \mathbb{1}\big)(\varrho) \geq 0$. In turn, a state ϱ is necessarily entangled if $\big(\Lambda \otimes \mathbb{1}\big)(\varrho) \ngeq 0$.

However, the inverse statement does not hold in general. The mere fact that ϱ remains positive under the extended map does not necessarily imply that ϱ is separable. Only if

$$\big(\Lambda \otimes \mathbb{1}\big)(\varrho) \geq 0 \quad \textit{for all} \text{ positive maps } \Lambda \ , \tag{2.12}$$

one may conclude that ϱ is separable [32]. Note that for the complementary implication alone one only needs to find one positive map Λ with $\big(\Lambda \otimes \mathbb{1}\big)(\varrho) \ngeq 0$. This statement does not allow to derive a sufficient separability criterion for the very general case, since the classification of positive maps is still an unsolved problem. A large class of entangled states is detected by

the special choice of the transposition $T =: \Lambda$ [33] that indeed is a positive map. The *partial transpose* $\varrho^{pt} = \big(T \otimes \mathbb{1}\big)(\varrho)$ of a state ϱ is deduced as the relevant auxiliary quantity: if ϱ^{pt} has at least one negative eigenvalue,

$$\varrho^{pt} \not\geq 0 \ , \tag{2.13}$$

the state ϱ is entangled.

However, if ϱ^{pt} is positive, one can infer separability of ϱ only for low-dimensional, namely 2×2 and 2×3 systems. For these, the positive partial transpose (*ppt*) or *standard criterion* unambiguously distinguishes separable and entangled states [32]. However, in higher dimensions there exist entangled states [34, 35] that are not detected by the ppt criterion.

2.2 Entanglement monotones and measures

Since the definition of entangled states given in eq. (2.5) is not constructive, it turned out difficult to decide whether a given state is separable - and the general solution of this problem is still unknown. Moreover, the non-constructive definition also complicates finding a quantitative description of entanglement rather than the purely qualitative given so far. How can you measure something, if you don't even know what it is?

The basic idea for a quantitative description is to classify all kinds of operations that in principle can be applied to quantum systems and that can create or increase only classical correlations, but none of quantum nature. Any number assigned to a state that does not increase under such operations can serve for a quantification of entanglement [36].

In our subsequent discussion of such operations, we will not distinguish between operations describing the time evolution of a real system, and those which serve just as a mathematical tool. In the latter case one can always have in mind a Gedankenexperiment where the considered operation is implemented. For the following considerations it is not crucial whether one has the technical prerequisites and experimental skills to perform a considered operation - but rather that the operation is in principal allowed by the laws of quantum mechanics. Therefore, we do not consider technical problems - as long as we do not refer to real experiments.

2.2.1 Quantum operations and LOCC

A map $\mathcal{E} : \ \mathcal{B}(\mathcal{H}_i) \to \mathcal{B}(\mathcal{H}_f)$ describing the evolution of a quantum system has to be linear,

$$\mathcal{E}(\lambda_1 \varrho_1 + \lambda_2 \varrho_2) = \lambda_1 \ \mathcal{E}(\varrho_1) + \lambda_2 \ \mathcal{E}(\varrho_2) \ , \tag{2.14}$$

due to the underlying linear Schrödinger equation. Moreover, in order to ensure positivity of ϱ, any map $\mathcal{E}$ has to be positive. However, this requirement is not strong enough to ensure positivity of ϱ in all cases. Since one

can always consider a system as a subsystem of a larger one, one has to allow for extensions $\mathcal{E} \otimes \mathbb{1}$ of $\mathcal{E}$. The extended map acts on the entire system in such a way that the original map affects the considered subsystem, whereas the identity map acts on the residual system degrees of freedom. As already mentioned in chapter 2.1.2, such a trivial extension is *not* necessarily a positive map again. In order to assure positivity of the entire system state, one has to require that the described extension be a positive map for identity maps $\mathbb{1}$ in any dimension, *i.e.* that $\mathcal{E}$ is *completely positive*. Accordingly, any evolution consistent with the general rules of quantum mechanics can be described by a linear, completely positive map called *quantum operation*.

A unitary evolution is just a special case of such a quantum operation - but a general quantum operation can also describe non-unitary evolutions, *e.g.* due to environment coupling or measurements. Any such quantum operation can be composed from three elementary operations [37, 38]:

- unitary transformations, $\mathcal{E}_1(\varrho) = U \varrho \, U^\dagger$;
- addition of an auxiliary system, $\mathcal{E}_2(\varrho) = \varrho \otimes \sigma$, where ϱ is the original system and σ is the auxiliary state;
- trace over a part (p) of the system, $\mathcal{E}_3(\varrho) = \mathrm{Tr}_p \varrho$,

and any such combination can be expressed as an operator sum [39, 40]

$$\mathcal{E}(\varrho) = \sum_i E_i \varrho E_i^\dagger \ , \quad \text{with} \quad \sum_i E_i^\dagger E_i = \mathbb{1} \ , \tag{2.15}$$

with suitably defined linear operators E_i.

Quantum operations can be interpreted in terms of the reduced dynamics of a system initially prepared in the state $\varrho(0)$, coupled to an environment with initial state $|\Psi_0\rangle$. If we allow for an interaction between system and environment, we will have a unitary evolution $\mathcal{U}(t)$ in both system and environment. The system state after time t is obtained by evolving the system-bath state over t, followed by a trace over the environment:

$$\varrho(t) = \mathrm{Tr}_{\mathrm{env}} \Big(\ \mathcal{U}(t) \ |\Psi_0\rangle\langle\Psi_0| \otimes \varrho(0) \, \mathcal{U}^\dagger(t) \ \Big) \ . \tag{2.16}$$

Expressing the trace over the environmental degrees of freedom by a sum over an orthonormal basis $\{|\chi_i\rangle\}$, one immediately obtains the above operator sum representation

$$\varrho(t) = \sum_i E_i(t) \ \varrho(0) \ E_i^\dagger(t) \ , \quad \text{with} \quad E_i = \langle \chi_i | \mathcal{U}(t) | \Psi_0 \rangle \ , \tag{2.17}$$

where the operators $E_i(t)$ satisfy the resolution of the identity required in eq. (2.15).

For our purposes it is useful to distinguish the following types of quantum operations:

- local operations,
- global operations,
- local operations and classical communication (LOCC).

Local operations An operation is called *local* if under its action the subsystems evolve independently from each other. In terms of operator sums this is expressed as

$$\mathcal{E}_{loc}(\varrho) = \sum_{ij} E_i \otimes F_j \; \varrho \; F_j^\dagger \otimes E_i^\dagger, \quad \text{with} \quad \sum_{i,j} E_i^\dagger E_i \otimes F_j^\dagger F_j = \mathbb{1}_{\mathcal{H}_1 \otimes \mathcal{H}_2} \; . \tag{2.18}$$

Local unitary evolutions $\mathcal{U}_{loc} = \mathcal{U}_1 \otimes \mathcal{U}_2$ are just special cases of general local operations. Since both subsystems evolve independently from each other, possibly preexisting correlations remain unaffected, but can neither grow nor increase. A product state will remain a product state,

$$\mathcal{E}_l(\varrho_1 \otimes \varrho_2) = \Big(\sum_i E_i \varrho_1 E_i^\dagger\Big) \otimes \Big(\sum_i F_i \varrho_2 F_i^\dagger\Big), \tag{2.19}$$

and any separable state will remain separable under local operations:

$$\mathcal{E}_l\Big(\sum_i \; p_i \; \varrho_1^i \otimes \varrho_2^i\Big) = \sum_i \; p_i \; \Big(\sum_i E_i \varrho_1^i E_i^\dagger\Big) \otimes \Big(\sum_i F_i \varrho_2^i F_i^\dagger\Big). \tag{2.20}$$

Therefore, starting from a separable state no correlations - neither classical nor quantum - can be created by local operations alone.

Global transformations If two subsystems are interacting with each other, their evolution will in general not derive from purely local operations. Any operation that is not local is called *global*. Under this type of operations all kinds of correlations can grow, as well as decrease. Therefore, entangled states can be created from initially separable states and vice versa. The most prominent and natural way of creating entangled states is a global unitary evolution due to an interaction between subsystems.

Local operations and classical communication (LOCC) A prominent subclass of global operations are *local operations and classical communication* (LOCC). They comprise general local operations, and also allow for correlations between them. The idea behind is to allow arbitrary local operations and, in addition, to admit all classical means to correlate their application. Hence, parties having access to different subsystems can use means of classical communication to exchange information about their locally performed operations and the respective outcomes, such that other

parties can apply some further local operations *conditioned* on the information communicated to them.

In terms of operator sums this is expressed as

$$\mathcal{E}_{\mathrm{LOCC}}(\varrho) = \sum_i E_i \otimes F_i \ \varrho \ F_i^\dagger \otimes E_i^\dagger, \quad \text{with} \quad \sum_i E_i^\dagger E_i \otimes F_i^\dagger F_i = \mathbb{1}_{\mathcal{H}_1 \otimes \mathcal{H}_2} \ . \tag{2.21}$$

In contrast to eq. (2.18), only a single sum is involved in the description of LOCC operations. This is a manifestation of the correlated application of the respective operations on the subsystems: if the operator E_i is applied to the first subsystem, the operator F_i is applied to the second subsystem.

LOCC operations can be used to create classical correlations between subsystems. In general, a product state will not remain a direct product under the action of an LOCC operation:

$$\mathcal{E}_{\mathrm{LOCC}}(\varrho_1 \otimes \varrho_2) = \sum_i \left(E_i \varrho_1 E_i^\dagger\right) \otimes \left(F_i \varrho_2 F_i^\dagger\right) = \sum_i \ p_i \ \varrho_1^i \otimes \varrho_2^i \ , \tag{2.22}$$

with $\varrho_1^i = \dfrac{E_i \varrho_1 E_i^\dagger}{\mathrm{Tr}\left(E_i \varrho_1 E_i^\dagger\right)}$, $\varrho_2^i = \dfrac{F_i \varrho_2 F_i^\dagger}{\mathrm{Tr}\left(F_i \varrho_2 F_i^\dagger\right)}$, and $p_i = \mathrm{Tr}\left(E_i \varrho_1 E_i^\dagger\right) \mathrm{Tr}\left(F_i \varrho_2 F_i^\dagger\right)$. Thus classical, probabilistic correlations can change under the action of LOCC operations. However, any separable state will always remain separable under LOCC operations. Accordingly, entangled states cannot be created with LOCC operations.

2.2.2 Entanglement monotones

Since we have argued that entanglement cannot be created using LOCC operations, our discussion at the beginning of this chapter suggests to consider quantities that do not increase under LOCC operations. Any scalar valued function that satisfies this criterion is called an *entanglement monotone* [36] and can be used to quantify entanglement. Later, in chapter 2.2.3, we will refine this approach and introduce *entanglement measures* that satisfy some additional properties - important in particular for mixed states.

Pure states

For pure states there exists a simple criterion that allows for the characterisation of entanglement monotones. It was shown that a state $|\Psi\rangle$ can be prepared starting from a second state $|\Phi\rangle$ and using only LOCC, if and only if the vector $\vec{\lambda}_\Psi$ of Schmidt coefficients of $|\Psi\rangle$ is majorised by $\vec{\lambda}_\Phi$ [41]

$$\vec{\lambda}_\Psi \prec \vec{\lambda}_\Phi \ . \tag{2.23}$$

Majorisation means that the components $[\lambda_\Psi]_i$ and $[\lambda_\Phi]_i$ of both vectors, listed in increasing order, satisfy $\sum_{i=1}^{j} [\lambda_\Psi]_i \leq \sum_{i=1}^{j} [\lambda_\Phi]_i$ for $0 < j \leq d$.

Since any vector $\vec{\lambda}$ is majorised by the Schmidt vector $\vec{\lambda}^*$ with equal components $1/d$ as introduced in chapter 2.1.1, any bipartite state can be prepared with LOCC starting out from a state $|\Psi^*\rangle$ with Schmidt vector $\vec{\lambda}^*$. This justifies calling $|\Psi^*\rangle$ maximally entangled.

Since entanglement cannot increase under LOCC operations, any monotone $\mathcal{M}$ has to satisfy

$$\mathcal{M}(\Psi) \; > \; \mathcal{M}(\Phi) \; , \quad \text{for} \quad \vec{\lambda}_\psi \prec \vec{\lambda}_\phi \; . \tag{2.24}$$

This condition is known as *Schur concavity*. It is satisfied if and only if [42] $\mathcal{M}$ given as a function of the Schmidt coefficients is invariant under permutations of any two arguments and satisfies

$$(\lambda_1 - \lambda_2)\left(\frac{\partial \mathcal{M}}{\partial \lambda_1} - \frac{\partial \mathcal{M}}{\partial \lambda_2}\right) \leq 0 \; . \tag{2.25}$$

Due to the invariance mentioned above, there is nothing peculiar about the first two components of $\vec{\lambda}$ - if eq. (2.25) holds true for λ_1 and λ_2, it is also satisfied for any two components of $\vec{\lambda}$. Any quantity is called *Schur convex* if it gets Schur concave when multiplied with a negative number.

The above characterisation allows to derive several entanglement monotones for pure states. Very useful quantities in this context are the reduced density matrices ϱ_1 or ϱ_2 obtained by tracing over one subsystem

$$\varrho_1 = \mathrm{Tr}_2 |\Psi\rangle\langle\Psi| \; , \qquad \varrho_2 = \mathrm{Tr}_1 |\Psi\rangle\langle\Psi| \; . \tag{2.26}$$

The basic idea is that the degree of mixing of a reduced density matrix is directly related to the amount of entanglement of the pure state $|\Psi\rangle$. Any function $g(\varrho_r)$ of a reduced density matrix that is

- invariant under unitary transformations, $g(\varrho_r) = g(\mathcal{U}\varrho_r\,\mathcal{U}^\dagger)$, and
- concave, $g(\varrho_r) \geq \lambda g(\varrho_\alpha) + (1-\lambda) g(\varrho_\beta)$, for any $0 \leq \lambda \leq 1$, and states ϱ_α and ϱ_β such that $\varrho_r = \lambda\varrho_\alpha + (1-\lambda)\varrho_\beta$,

is Schur concave, and therefore provides an entanglement monotone $\mathcal{M}(\Psi) = g(\varrho_r)$ [36]. The most prominent choice of g is the von Neumann entropy

$$S(\varrho_r) = -\mathrm{Tr}\varrho_r \ln \varrho_r \tag{2.27}$$

of the reduced density matrix, often simply called *the* entanglement $E(\Psi) = S(\varrho_r)$ of the pure state $|\Psi\rangle$.

Note that due to the invariance of g under unitary transformations, g can only be a function of unitary invariants, and this is the spectrum of ϱ_r. Accordingly, it is not necessary to distinguish between ϱ_1 and ϱ_2, since they have the same non-vanishing eigenvalues. If both subsystems have the

same dimensions, the spectrum of ϱ_1 equals that of ϱ_2. If the dimensions are not equal the reduced density matrix of the larger subsystem has some additional vanishing eigenvalues. That is why one often does not distinguish between ϱ_1 and ϱ_2, but rather expresses $\mathcal{M}(\Psi)$ as

$$\mathcal{M}(\Psi) = g(\varrho_r) \ , \quad \text{with} \quad \varrho_r = \mathrm{Tr}_p|\Psi\rangle\langle\Psi|, \tag{2.28}$$

with 'the' reduced density matrix, where the partial trace Tr_p does not specify explicitly which subsystem is traced out. However, in chapter 3.4 we will discuss a situation where the proper choice of the subsystem over which the trace is performed is not completely arbitrary.

Yet a single monotone is not always sufficient to completely characterise the quantum correlations contained in a given pure state. For such a characterisation, knowledge of *all* Schmidt coefficients is required. Since there are $d-1$ independent Schmidt coefficients, where $d = \min(\dim(\mathcal{H}_1), \dim(\mathcal{H}_2))$ a single scalar quantity is only sufficient for $d = 2$. In general, a set of $d-1$ independent monotones is required.

Mixed states

For pure states it is rather simple to find some entanglement monotones - any unitarily invariant, concave function of the reduced density matrix defines one. This is due to the fact that there are no classical probabilistic correlations contained in pure states. For mixed states the situation is much more involved, because there are both classical and quantum correlations that have to be discriminated against each other by an entanglement monotone. It is by no means obvious to devise a unique generalisation of a pure state monotone $\mathcal{M}(\Psi)$ to a mixed state monotone $\mathcal{M}(\varrho)$, such that

- $\mathcal{M}(\varrho)$ reduces to the original pure state definition when applied to pure states, and
- $\mathcal{M}(\varrho)$ is a good entanglement monotone, *i.e.* non-increasing under LOCC.

We will follow one special generalisation that applies to any pure state monotone [36, 43], and therefore is the most commonly used one. It can easily be formulated but leaves severe problems when it comes to its quantitative evaluation. Any mixed state can be expressed as a convex sum of pure states:

$$\varrho = \sum_i \ p_i \ |\Psi_i\rangle\langle\Psi_i| \ . \tag{2.29}$$

On a first glance, it might appear as a self-evident generalisation to sum up the entanglement assigned by a certain monotone to the pure states in eq. (2.29), weighted by the prefactors p_i. Unfortunately, the decomposition into pure states is not unique, and different decompositions in general lead

to different values for a given entanglement monotone. The proper, unambiguous generalisation of a pure state monotone, that also we will use in the following, therefore uses the infimum over all decompositions into pure states - the so-called *convex roof* [44]:

$$\mathcal{M}(\varrho) = \inf_{\{p_i,\Psi_i\}} \sum_i \; p_i \; \mathcal{M}(\Psi_i) \; , \quad \text{with } \; p_i > 0 \; , \quad \text{s.t. } \; \varrho = \sum_i \; p_i \; |\Psi_i\rangle\langle\Psi_i| \; . \tag{2.30}$$

An explicit evaluation of this quantity for a specific state - one has to find the infimum over all possible decompositions into pure states - implies a high dimensional optimisation problem - in general a very hard computational task.

To ease this enterprise, it is convenient to make use of the following characterisation of all ensembles of pure states which represent a certain mixed state. Using *subnormalised states*

$$|\psi_i\rangle = \sqrt{p_i} \; |\Psi_i\rangle \tag{2.31}$$

allows to reduce the number of involved quantities. Since the p_i are positive, one has $|\psi_i\rangle\langle\psi_i| = p_i|\Psi_i\rangle\langle\Psi_i|$. Assume one ensemble $\{|\psi_i\rangle\}$ is known such that $\varrho = \sum_i |\psi_i\rangle\langle\psi_i|$ - *e.g.* the eigensystem of ϱ . New ensembles defined as

$$|\phi_i\rangle = \sum_j V_{ij}|\psi_j\rangle, \qquad \text{with} \qquad \sum_i V^\dagger_{ki} V_{ij} = \delta_{jk} \; , \tag{2.32}$$

represent the same mixed state $\varrho = \sum_i |\psi_i\rangle\langle\psi_i| = \sum_i |\phi_i\rangle\langle\phi_i|$, and any ensemble representing ϱ can be constructed in this way [13, 45]. In the following, any matrix V satisfying eq. (2.32) will be referred to as *left unitary*. The number, *cardinality*, of ensemble members of the decomposition of ϱ is not fixed by the rank of the considered state. There is no *a priori* maximum cardinality, though it is sufficient to consider ensembles with cardinality not larger than the square of the considered state's rank [46]. However, there is no evidence that it is necessary to employ ensembles of this maximum cardinality. There is no proof that the infimum in eq. (2.30) cannot be found with ensembles of smaller cardinality. Nonetheless, without a sharper bound on the length of the decomposition we need to find the optimal left-unitary matrix $V \in \mathbb{C}^{n^2 \times n}$, which implies an n^3-dimensional optimisation procedure to compute the entanglement $\mathcal{M}(\varrho)$ of a given state ϱ of rank n. Since there is no simple parametrisation of arbitrary left-unitary matrices, the constraint $\sum_i V^\dagger_{ki} V_{ij} = \delta_{jk}$ even complicates the numerical implementation.

2.2.3 Entanglement measures

Entanglement monotones that satisfy some additional axioms are called *entanglement measures* E. So far, however, there is no uniquely accepted list of axioms, hence there is no commonly accepted distinction between

monotones and measures [47, 48]. We do not attribute too much relevance to this question of terminology, and just present here a list of potential axioms:

- $E(\varrho)$ vanishes exactly for separable states.
- *additivity*: the entanglement of several copies of a state adds up to n times the entanglement of a single copy, $E(\varrho^{\otimes n}) = nE(\varrho)$.
- *subadditivity*: the entanglement of two states is not larger than the sum of the entanglement of both individual states, $E(\varrho_1 \otimes \varrho_2) \leq E(\varrho_1) + E(\varrho_2)$.
- *convexity*: $E(\lambda\varrho_1 + (1-\lambda)\varrho_2) \leq \lambda E(\varrho_1) + (1-\lambda)E(\varrho_2)$, for $0 \leq \lambda \leq 1$.

Some authors additionally require that an entanglement measure has to be invariant under local unitary transformations. However, this is already implied by monotonicity under LOCC (chapter 2.2.2), since monotonicity implies invariance under transformations that are invertible within the class of LOCC operations [49]. Local unitaries and their inverses are LOCC operations. Thus, any entanglement monotone and -measure has to be non-increasing under both the former and the latter. Since non-increasing behaviour under the latter implies non-decreasing behaviour under the former and vice versa, any monotone or -measure has to be invariant under local unitaries.

There are attempts to find a distinct set of axioms that leads to a unique measure [50]. On the other hand, it sometimes is necessary to relax some of the above listed constraints, in order to find a measure that is computable. For example, *negativity* [51] - that we will discuss in more detail in chapter 2.3.3 - has become a commonly used quantity although it vanishes for a class of entangled states [51]. Though, compared to other measures it has the major advantage that it can be computed straight-forwardly.

2.3 Algebraically computable measures

As mentioned earlier most entanglement measures for mixed states, as for example eq. (2.30), involve an optimisation procedure. This hampers finding an analytic solution. However, for 2×2 systems - the smallest ones of interest - solutions are known in closed form for some specific measures [26, 43, 51, 52]. There are also some measures - as for example negativity to be defined in chapter 2.3.3 - that involve no optimisations and can be calculated in any dimensions. However, they assign vanishing entanglement to some non-separable states. In the following, we will briefly discuss those algebraically given entanglement monotones or -measures that will be relevant for our subsequent analysis.

2.3.1 Concurrence

Concurrence was originally introduced as an auxiliary quantity, used to calculate the *entanglement of formation* of 2×2 systems. However, concurrence can also be considered as an independent entanglement measure [26]. For systematic reasons we first introduce concurrence, and discuss entanglement of formation in chapter 2.3.2 hereafter.

For the definition of concurrence [43, 53] in 2×2 systems a special basis

$$|e_1\rangle = |\Phi^+\rangle \ , \quad |e_2\rangle = i|\Phi^-\rangle \ , \quad |e_3\rangle = i|\Psi^+\rangle \ , \quad |e_4\rangle = |\Psi^-\rangle \ , \tag{2.33}$$

defined in terms of the *Bell states* [43]

$$|\Phi^\pm\rangle = \frac{1}{\sqrt{2}}\left(|00\rangle \pm |11\rangle\right) \qquad |\Psi^\pm\rangle = \frac{1}{\sqrt{2}}\left(|01\rangle \pm |10\rangle\right) \tag{2.34}$$

is used. With this at hand, the concurrence c of a pure state $|\Psi\rangle$ is defined as

$$c(\Psi) = \left|\sum_i \langle e_i|\Psi\rangle^2\right| \ . \tag{2.35}$$

Writing this definition more explicitly, $c(\Psi) = \left|\sum_i \langle\Psi^*|e_i^*\rangle\langle e_i|\Psi\rangle\right|$, one ends up, after summation, with the alternative formulation [26]

$$c(\Psi) = \left|\langle\Psi^*|\sigma_y\otimes\sigma_y|\Psi\rangle\right| \ , \tag{2.36}$$

where σ_y is the second Pauli matrix, and $|\Psi^*\rangle$ is the complex conjugate of $|\Psi\rangle$ with the conjugation performed in the standard basis $\{|00\rangle,\ |01\rangle,\ |10\rangle,\ |11\rangle\}$. Since a scalar product implies a complex conjugation anyway, the second conjugation cancels the first one such that $\langle\Psi^*| = \sum_{ij}\Psi_{ij}\langle ij|$ is the transpose and not the adjoint of $|\Psi\rangle = \sum_{ij}\Psi_{ij}|ij\rangle$. Eq. (2.36) is the most commonly used formulation and is often considered as the definition of concurrence rather than eq. (2.35).

The concurrence of mixed states is given by the corresponding convex roof, alike eq. (2.30):

$$c(\varrho) = \inf_{\{p_i,\Psi_i\}} \sum_i \ p_i\ c(\Psi_i) \ , \ \text{with}\ p_i > 0 \ , \ \text{s.t.}\ \varrho = \sum_i p_i|\Psi_i\rangle\langle\Psi_i| \ . \tag{2.37}$$

Concurrence of a pure state $|\psi\rangle$ can be expressed as $c(\psi) = f_c(\psi,\psi)$, in terms of the function

$$f_c(\psi_1,\psi_2) = \langle\psi_2^*|\sigma_y\otimes\sigma_y|\psi_1\rangle \ , \tag{2.38}$$

that it is linear in the first argument and anti-linear in the second. This linearity properties, together with the parametrisation of all decompositions of ϱ into pure states as given in eq. (2.32), allows to write eq. (2.37) as

$$c(\varrho) = \inf_V \sum_i \left|\sum_{j,k} V_{ij} f_c(\psi_j,\psi_k)\left[V^T\right]_{ki}\right| \ . \tag{2.39}$$

The quantities $f_c(\psi_j, \psi_k)$ can be understood as elements τ_{jk} of a complex symmetric matrix τ. Hence one can use the compact matrix notation

$$c(\varrho) = \inf_V \sum_i \left| \left[V \tau V^T \right]_{ii} \right| . \tag{2.40}$$

The infimum of this quantity is known [26] to be given by

$$c(\varrho) = \max\Big(\mathcal{S}_1 - \sum_{i=2}^{4} \mathcal{S}_i,\ 0 \Big) , \tag{2.41}$$

where the $\mathcal{S}_i$ are the singular values of τ, in decreasing order. They can be obtained as the square roots of the eigenvalues of the positive hermitian matrix $\tau\tau^\dagger$.

Since we will refer to infima of expressions similar to that given in eq. (2.40) several times later-on, we discuss the derivation of this infimum in some detail. Though, we do not follow here the original derivation [26], but rather present a generalisation [44] valid in arbitrary dimensions - which we will need for later reference when considering subsystems with more than two levels. Thus, the following considerations do not only apply to the hitherto discussed 2×2 case, but also to systems of arbitrary finite dimensions.

Any complex matrix $M \in \mathbb{C}^{n_1 \times n_2}$ can be diagonalised [31] as

$$M = U_l D U_r , \tag{2.42}$$

where $U_l \in \mathbb{C}^{n_1 \times d}$ and $U_r \in \mathbb{C}^{d \times n_2}$ with $d = \min(n_1, n_2)$ are left- and right unitary, *i.e.* $U_l^\dagger U_l = \mathbb{1}$ and $U_r U_r^\dagger = \mathbb{1}$, and $D \in \mathbb{C}^{d \times d}$ is a diagonal matrix with real and positive diagonal elements, refered to as singular values of M. Moreover, U_l and U_r can always be chosen such that the singular values are arranged in decreasing order along the diagonal.

Applying this to the above quadratic, complex symmetric matrix τ, one concludes that τ can be diagonalised with a unitary transformation U as

$$U \tau U^T = \mathrm{diag}\big[\mathcal{S}_1, \ldots, \mathcal{S}_n \big] =: \tau_d . \tag{2.43}$$

Given this diagonal representation, one defines a transformation V_H with the help of *Hadamard Matrices* H [54]. They exist in dimensions $n \times 2^k$ with $2^k \geq n$. Their rows are given by n mutually orthogonal real vectors, with the same absolute value $1/(2^{k/2})$ of all elements. Due to the rows' orthogonality, H is left unitary, $H^\dagger H = \mathbb{1}$.

The transformation matrix V_H is a modification of a Hadamard matrix. Namely the i-th ($i = 2, \ldots, n$) element of any row is multiplied by a phase

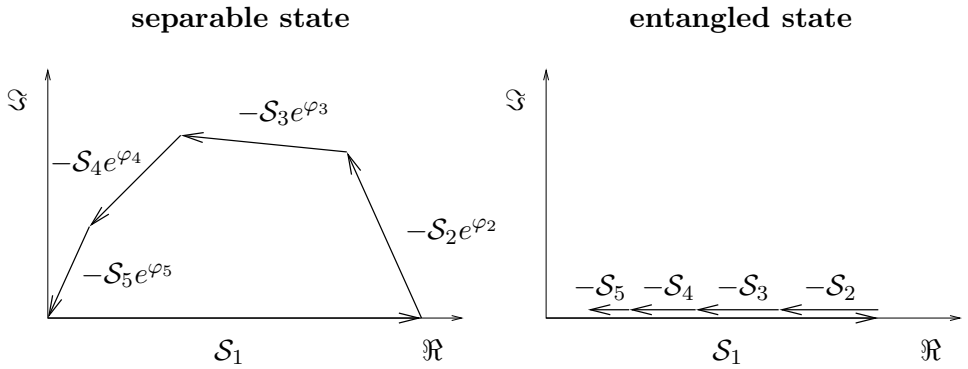

Figure 2.1: Complexified singular values $\mathcal{S}_1$ and $-\mathcal{S}_i e^{i\varphi_i}$ $(i > 1)$ - see eq. (2.44) - plotted in the complex plane. For a separable state (left) one can always find appropriate phase factors such that all terms add up to 0. However, for an entangled state (right) this is not possible. The minimum of eq. (2.44) can be obtained for $e^{i\varphi_j} = 1$ for all j.

factor $ie^{i\varphi_i}$. The latter does not affect left-unitarity, $V_H^\dagger V_H = \mathbb{1}$. However, since V_H^T enters eq. (2.40) instead of $V_H^\dagger$, the phase factors are indeed important. Carrying out the transformation, one obtains

$$\left[V_H \tau_d V_H^T\right]_{ii} = \frac{1}{2^k}\left(\mathcal{S}_1 - \sum_{i>1} \mathcal{S}_i e^{i\varphi_i}\right) , \tag{2.44}$$

where one needs not care about the non-diagonal entries, since only diagonal elements are summed up in the end.

So far we found a transformation $V_H U$ such that

$$\sum_i \left| \left[V_H U \tau U^T V_H^T\right]_{ii} \right| = \left| \mathcal{S}_1 - \sum_{j>1} \mathcal{S}_j e^{i\varphi_j} \right| . \tag{2.45}$$

Now one has to distinguish two cases. In the first case one has $\mathcal{S}_1 \leq \sum_{i>1} \mathcal{S}_i$. In that case one can always find phases φ_i such that $\mathcal{S}_1 - \sum_{i>1} \mathcal{S}_i e^{i\varphi_i} = 0$, as depicted in figure 2.1. In the second case, where $\mathcal{S}_1 > \sum_{i>1} \mathcal{S}_i$, the optimal choice for all phases is $\varphi_i = 0$, and one gets $\mathcal{S}_1 - \sum_{i>1} \mathcal{S}_i$. All-together, we found a transformation such that

$$\sum_i \left| \left[V_H U \tau U^T V_H^T\right]_{ii} \right| = \max\Big(\mathcal{S}_1 - \sum_{i>1} \mathcal{S}_i, 0\Big) . \tag{2.46}$$

It is now easy to show that there is no left unitary transformation leading to a smaller result. We can restrict ourselves to the second case above, $\mathcal{S}_1 > \sum_{j>1} \mathcal{S}_j$, since 0 is the smallest possible value of a non-negative quantity anyway. To do so, we start with the diagonal form τ^d of τ, and transform it with $U_p = \mathrm{diag}(1, i, \ldots, i)$ such that we obtain

$$\tilde{\tau}^d = U_p \tau^d U_p^T = \mathrm{diag}\big[\mathcal{S}_1, -\mathcal{S}_2, \ldots, -\mathcal{S}_m\big] . \tag{2.47}$$

Now one has

$$\sum_i \Big| \sum_{jk} V_{ij} \tilde{\tau}^d_{jk} V^T_{ki} \Big| = \Big| \sum_i \big(V^2_{i1} \mathcal{S}_1 - \sum_{j>1} V^2_{ij} \mathcal{S}_j \big) \Big| \ . \tag{2.48}$$

One can always choose V in such a way that the V_{i1} are real for any i. Then one has $\sum_i V^2_{i1} = 1$, and $\sum_i |V_{i1}|^2 \leq 1$. Therefore:

$$\sum_i \Big| \sum_{jk} V_{ij} \tilde{\tau}^d_{jk} V^T_{ki} \Big| \geq \sum_i |V^2_{i1}| \mathcal{S}_1 - \sum_{j>1} |V^2_{ij}| \mathcal{S}_j \geq \mathcal{S}_1 - \sum_{i>1} \mathcal{S}_i \ . \tag{2.49}$$

Thus we have shown that eq. (2.41) really is the infimum corresponding to eq. (2.40).

2.3.2 Entanglement of formation

Entanglement of formation is our second example for an entanglement measure defined as a convex roof alike eq. (2.30). In contrast to the previously discussed concurrence, entanglement of formation is defined for bipartite systems of arbitrary dimensions. As we have seen in chapter 2.2.2 above, the entanglement $E(\Psi)$ of a pure state $|\Psi\rangle$ can be quantified by the von Neumann entropy $S(\varrho)$ of the reduced density matrix, eq. (2.27). Entanglement of formation of a mixed state then follows as the convex roof [43]

$$E(\varrho) = \inf_{\{p_i, \Psi_i\}} \sum_i \ p_i \ E(\Psi_i) \ , \ \text{ with } \ p_i > 0 \ , \ \text{ s.t. } \ \varrho = \sum_i \ p_i \ |\Psi_i\rangle\langle\Psi_i| \ . \tag{2.50}$$

In higher dimensions the underlying optimisation problem is unsolved - apart from a few known solutions for particular states [55]. Only for 2×2 systems an algebraic solution is known for general states. For these low dimensional systems, the entanglement of a pure state can be expressed as a function of its concurrence, $E(\Psi) = \mathcal{E}(c(\Psi))$, with [26]

$$\mathcal{E}(c) = - \sum_{\alpha = -1,1} \frac{1}{2}(1 + \alpha \sqrt{1 - c^2})) \log_2 \frac{1}{2}(1 + \alpha \sqrt{1 - c^2})) \ . \tag{2.51}$$

The function $\mathcal{E}(c)$ is monotonically increasing and convex. Thus, the entanglement of formation can be estimated as

$$E(\varrho) = \inf \ \sum_i \ p_i \ \mathcal{E}(c_i) \ \geq \ \inf \ \mathcal{E}\Big(\sum_i \ p_i \ c_i \Big) = \mathcal{E}(c(\varrho)) \ . \tag{2.52}$$

Consequently, concurrence provides a lower bound for the entanglement of formation. In general, the decomposition that provides the infimum is not unique. In the present case of 2×2 systems, the manifold on which the infimum is adopted always contains a set of pure states all of which

have the same concurrence [26]. For these special decompositions one has $\sum_i p_i \mathcal{E}(c_i) = \mathcal{E}\big(\sum_i p_i c_i\big)$. Thus, equality holds in the above inequality. Therefore, in 2×2 systems, one can always express entanglement of formation in terms of concurrence. Since an algebraic expression, eq. (2.41), for concurrence is available for arbitrary 2×2 states, also entanglement of formation can be computed purely algebraically.

2.3.3 Negativity

For both, concurrence and entanglement of formation, solutions for arbitrary mixed states are known only in 2×2 systems. Negativity has the great advantage that it can be calculated algebraically in any dimensions. However, it vanishes for some entangled states and thus is not an entanglement measure in the strict sense. But since it is non-increasing under LOCC, it is an entanglement monotone [51]. Its definition is closely related to the above mentioned ppt criterion. *Negativity* $\mathcal{N}$ of a state ϱ is defined as

$$\mathcal{N}(\varrho) = \|\varrho^{pt}\|_1 - 1 \ , \tag{2.53}$$

where $\|.\|_1$ is the 1-norm, given by the sum of the moduli of the eigenvalues. Since transposition is trace-preserving, *i.e.* $\mathrm{Tr}\varrho^{pt} = 1$, it is obvious that $\mathcal{N}(\varrho)$ is larger than zero exactly for states with non-positive partial transpose. As mentioned above there exist entangled states with positive partial transpose for systems larger than 2×3. Consequently, negativity assigns a vanishing amount of entanglement to these states, although they are indeed entangled.

Chapter 3

Concurrence

In the following chapter we will focus on the concurrence of systems of arbitrary dimension. We prefer concurrence to the entanglement of formation, since - as we will see in chapter 3.2 - it can be expressed in terms of a function that is linear in some of its arguments, and anti-linear in the others. Such a representation is not available for entanglement of formation, because of the logarithmic dependence on ϱ in eq. (2.50), together with eq. (2.27), which, however, is crucial for the construction of convex roofs. Negativity, on the other hand, can be calculated algebraically in arbitrary dimensions, though assigns vanishing entanglement to some non-separable states, as we have already seen above in chapter 2.3.3. Hence, we will concentrate on concurrence which is both distinctive and, as we will see below, computationally operational.

The quantitative estimation of the concurrence of a mixed state is often achieved by numerical means [56, 57, 58] which essentially solve a high dimensional optimisation problem when searching for the minimum that defines the convex roof, eq. (2.30). However, such an approach can only provide an upper bound of concurrence rather than its actual value, since a numerical optimisation procedure can never guarantee convergence into the global rather than a local minimum. Hence, besides an efficient numerical implementation of such an optimisation procedure it is most desirable to derive a lower bound of concurrence that possibly can be evaluated purely algebraically, since the numerical effort increases rapidly with the dimension of the underlying Hilbert space. In the present chapter, we will derive an approach to characterise concurrence of general mixed states in arbitrary, finite dimensions, and we will

- not only provide a framework for an efficient numerical implementation to compute an upper bound of concurrence in chapter 3.3, but also

- formulate lower bounds of concurrence in chapter 3.4, some of which can be computed purely algebraically.

- Moreover, in chapter 3.5 we will derive an approximation of concurrence that is valid for most states describing current experiments and can also be evaluated purely algebraically.

- Finally, in chapter 3.6, we will propose a generalisations of concurrence to multi-partite systems.

Both, upper and lower bounds, will allow to confine the actual value of concurrence to a finite interval, providing reliable information for arbitrary states. In a second step, we will specialise our approach to typical experimental requirements, which do not necessarily need a completely general treatment. In most experiments (see for example [59, 60]), the evolution of pure into mixed states occurs on a time-scale which is much longer than the time required to prepare or to manipulate entangled states. Therefore, quantum states which arise in such experiments exhibit rather small degrees of mixing. This a priori assumption allows a further approximation in our general treatment which yields a purely algebraic, and therefore very efficient and easily implemented estimation of concurrence, as we will see in chapter 3.5.

Since we have neither an a priori estimate of the tightness of our lower bounds, nor one for the range of validity of our approximation, we will compare our estimations from below with the corresponding upper bound in chapter 4. For this purpose, we will use random states, as well as states under scrutiny in real experiments [59].

3.1 Extension to higher dimensional systems

The definition of concurrence given in chapter 2.3.1 only applies to two-level systems. Since Bell states used in the original definition in eq. (2.35), and the spin flip operation used in eq. (2.36) do not have unique generalisations to higher dimensions, there is no straight-forward generalisation of concurrence to higher dimensions. So far, two *inequivalent* generalisations for systems comprising more than two levels have been formulated, which both coincide with the original one, if restricted to two-level systems.

Θ-concurrence One possible generalisation is Θ-*concurrence* [44]. The complex conjugation that is used in eq. (2.36) is an anti-linear operation. Θ concurrence is based on anti-linear operators, where anti-linearity of an operator θ is defined by the property

$$\theta\big(\alpha_1|\Psi_1\rangle + \alpha_2|\Psi_2\rangle\big) = \alpha_1^*\theta|\Psi_1\rangle + \alpha_2^*\theta|\Psi_2\rangle \ . \tag{3.1}$$

An anti-linear operator Θ is called a *conjugation* if it is unitary $\Theta^\dagger = \Theta^{-1}$ and if it satisfies $\Theta^2 = \mathbb{1}$. In terms of such a conjugation Θ, one can define

Θ-concurrence $c_\Theta(\psi)$ of a pure state $|\psi\rangle$ that is not necessarily normalised to unity as

$$c_\Theta(\psi) = \left|\langle\psi|\Theta|\psi\rangle\right| . \tag{3.2}$$

Of course, $c_\Theta(\psi)$ does not only depend on $|\psi\rangle$, but also on the choice of Θ. Thus Θ-concurrence is not a single, uniquely defined quantity, but rather a family of quantities, depending on the choice of Θ. In systems larger than two-level systems, no conjugation Θ is known such that $c_\Theta(\psi)$ vanishes for all separable states and is strictly larger than zero for all entangled states. However, in the case of two-level systems there is one. For $\Theta = \sigma_y \otimes \sigma_y \; C_*$ [44, 61], $c_\Theta(\psi)$ is non-vanishing if and only if $|\psi\rangle$ is entangled. For this special choice, Θ-concurrence coincides with regular concurrence as defined in eq. (2.36).

Θ-concurrence can easily be extended to mixed states using the concept of convex roofs. Given a complex symmetric matrix τ_Θ with elements

$$[\tau_\Theta]_{jk} = \langle\psi_j|\Theta|\psi_k\rangle \; , \tag{3.3}$$

one easily finds for the Θ-concurrence $c_\Theta(\varrho) = \inf \sum_i p_i c_\Theta(\psi_i)$ of a mixed state ϱ:

$$c_\Theta(\varrho) = \inf_V \sum_i \left| \left[V \tau_\Theta V^T\right]_{ii} \right| . \tag{3.4}$$

As discussed in chapter 2.3.1, the infimum can be expressed as

$$c_\Theta(\varrho) = \max\Big(\mathcal{S}_1^\Theta - \sum_{i>1} \mathcal{S}_i^\Theta, \; 0\Big) \; , \tag{3.5}$$

with the singular values $\mathcal{S}_i^\Theta$ of τ_Θ in decreasing order. Thus, Θ-concurrence can be easily evaluated for arbitrary mixed states. However, since, apart from $\Theta = \sigma_y \otimes \sigma_y \; C_*$ in 2×2 systems, no conjugation is known that is positive exactly for entangled states, it has the disadvantageous property that c_Θ vanishes for some entangled states - similar to negativity discussed in chapter 2.3.3 above.

I-concurrence *I-concurrence* [62] is defined in terms of operators I_1 and I_2 acting on $\mathcal{H}_1$ and $\mathcal{H}_2$ as

$$c_I(\Psi) = \sqrt{\langle\Psi|(I_1 \otimes I_2|\Psi\rangle\langle\Psi|)|\Psi\rangle} \; . \tag{3.6}$$

The operators I_i are required to satisfy the following properties [62]

a) $I_i H = (I_i H)^\dagger$ $(i = 1, 2)$, for all hermitian operators H, which ensures that I-concurrence is real.

b) $[I_i, \mathcal{U}] = 0$ $(i = 1, 2)$ for all unitary $\mathcal{U}$, which ensures that I-concurrence is invariant under local unitary transformations.

c) $\langle\Psi|(I_1 \otimes I_2|\Psi\rangle\langle\Psi|)|\Psi\rangle \geq 0$, for all states $|\Psi\rangle$, where equality holds if and only if $|\Psi\rangle$ is separable .

Up to scaling, there is a unique operator satisfying these requirements [62], namely

$$I(|\Psi\rangle\langle\Psi|) = \mathbb{1} - |\Psi\rangle\langle\Psi| \tag{3.7}$$

that maps $|\Psi\rangle\langle\Psi|$ onto its orthogonal space. Thus - in contrast to Θ-concurrence - I-concurrence is a quantity that is uniquely defined up to a multiplicative constant. With eq. (3.7), I-concurrence $c_I(\Psi)$ of a pure state $|\Psi\rangle$ can also be expressed in terms of reduced density matrices

$$c_I(\varrho) = \sqrt{2\big|\langle\Psi|\Psi\rangle\big|^2 - \mathrm{Tr}\varrho_1^2 - \mathrm{Tr}\varrho_2^2} \ . \tag{3.8}$$

As argued right before eq. (2.28), the last two terms are equal, such that there is no need to explicitly distinguish between the two reduced density matrices. It therefore became a wide spread convention to define concurrence using only one of the two reduced density matrices

$$c(\Psi) = \sqrt{2\big(\big|\langle\Psi|\Psi\rangle\big|^2 - \mathrm{Tr}\varrho_r^2\big)} \ , \tag{3.9}$$

where ϱ_r can be either one. However, in chapter 3.2 we will encounter circumstances where the definition in eq. (3.8) is advantageous compared to that in eq. (3.9).

If we now use the Schmidt form eq. (2.9) of an arbitrary pure states $|\Psi\rangle$, its I-concurrence reads

$$c_I(\Psi) = \sum_{i\neq j} \mathcal{S}_i\mathcal{S}_j \ , \tag{3.10}$$

and it is easily verified that I-concurrence coincides with the original definition given in eq. (2.36), for two-level systems. Note that I-concurrence cannot exceed a given maximum value $\sqrt{2(1-1/d)}$, with the dimension d of the smallest subsystem.

3.2 Mixed states in higher dimensions

In contrast to I-concurrence, Θ-concurrence has the advantage that an analytic solution is known for the very general case [44]. However, Θ-concurrence vanishes for some entangled states, and consequently does not satisfy one of the most important requirements for an entanglement measure listed in chapter 2.2.3. We therefore focus on I-concurrence, given by eq. (3.9)

$$c(\psi) = \sqrt{2\big(\big|\langle\psi|\psi\rangle\big|^2 - \mathrm{Tr}\ {\varrho_r}^2\big)} \ , \tag{3.11}$$

and call it simply concurrence, for brevity. For mixed states it is defined as the corresponding convex roof defined in eq. (2.30). For convenience, we introduce the following auxiliary quantity $\mathcal{C}_{\{\psi_i\}}$:

$$\mathcal{C}_{\{\psi_i\}}(\varrho) = \sum_i \, c(\psi_i) \;, \quad \text{with} \quad \varrho = \sum_i |\psi_i\rangle\langle\psi_i| \;, \tag{3.12}$$

such that the concurrence $c(\varrho)$ is the infimum of $\mathcal{C}(\varrho)$ over all sets $\{|\psi_i\rangle\}$.

For our further analysis, which aims at a transparent construction of the convex roof, it is convenient to introduce a function f of four arguments,

$$f(\psi_1,\psi_2,\psi_3,\psi_4) = \langle\psi_2|\psi_1\rangle\langle\psi_4|\psi_3\rangle - \mathrm{Tr}_1\Big(\big(\mathrm{Tr}_2|\psi_1\rangle\langle\psi_2|\big)\big(\mathrm{Tr}_2|\psi_3\rangle\langle\psi_4|\big)\Big) \;, \tag{3.13}$$

that is linear in the first and in the third argument, and anti-linear in the second and the third one. The concurrence of a pure state can be expressed as $c(\psi) = \sqrt{f(\psi,\psi,\psi,\psi)}$, such that one obtains

$$\mathcal{C}_{\{\psi_i\}}(\varrho) = \sum_i \sqrt{2 \; f(\psi_i,\psi_i,\psi_i,\psi_i)} \tag{3.14}$$

for a mixed state ϱ. Now one can use the fact that all decompositions of ϱ into pure states can be parametrised by a left unitary matrix V as in eq. (2.32). Using the characterisation of all ensembles representing ϱ, and making use the aforementioned linearity and anti-linearity of f, we obtain

$$\mathcal{C}_{\{\psi_i\}}(\varrho) = \mathcal{C}_V(\varrho) = \sum_i \left(\Big[V\otimes V A \; V^\dagger \otimes V^\dagger \Big]^{ii}_{ii} \right)^{\frac{1}{2}} \;, \tag{3.15}$$

where V is left-unitary and the tensor A is defined as

$$A^{lm}_{jk} = 2 \; f(\phi_j,\phi_l,\phi_k,\phi_m) \;, \tag{3.16}$$

with the set of states $\{|\phi_i\rangle\}$ a valid decomposition of ϱ. According to its definition, A is hermitian and symmetric with respect to a simultaneous exchange of both its co- and contravariant indices,

$$A^{lm}_{jk} = \big(A^{jk}_{lm}\big)^* \;, \qquad A^{lm}_{jk} = A^{ml}_{kj} \;. \tag{3.17}$$

A crucial pre-requisite for the derivation of an analytic expression for the concurrence of a two-level system [26] is the fact that a complex symmetric matrix τ can be diagonalised by a unitary transformation, as $\mathcal{U}\tau\mathcal{U}^T$ [31]. Similarly, a hermitian matrix H can be diagonalised by a unitary transformation, as $\mathcal{U}H\mathcal{U}^\dagger$ [31]. Since eq. (3.15) restricts these transformations to those that decompose into a tensor product $V\otimes V$ of a transformation

V with itself, it is in general not possible to diagonalise A. However, the symmetry of $V \otimes V$ under exchange of the subsystems of A implies another symmetry, in addition to those of eq. (3.17) - one can replace A in eq. (3.15) by the symmetrised quantity $\mathcal{A}$ with elements

$$\mathcal{A}^{lm}_{jk} = \frac{1}{2}\left(A^{lm}_{jk} + A^{lm}_{kj}\right) \ , \tag{3.18}$$

without affecting the value of $\mathcal{C}_V(\varrho)$. The reader may wonder why this additional symmetry has to be enforced and is not a result of the analysis. This is due to the asymmetric definition of concurrence with respect to the subsystems $\mathcal{H}_1$ and $\mathcal{H}_2$, in eq. (3.9). In the definition of concurrence in eq. (3.11), there is some arbitrariness in the sequence of traces which first yield ϱ_r and then $c(\psi)$. One has to choose whether to trace over the first or the second subsystem to obtain the reduced density matrix ϱ_r. If, on the other hand, one starts out with the symmetric version in eq. (3.8), one immediately obtains $\mathcal{A}$ instead of A, as we will show in chapter 3.2.1. Our initial choice of starting out with eq. (3.9) was motivated by its wide-spread use. In fact, the symmetric version eq. (3.8) is hardly used in the literature at all.

3.2.1 Algebraic properties of A and $\mathcal{A}$

Before we continue, we will discuss some algebraic properties of A and $\mathcal{A}$. Not only will these properties be crucial for our further analysis. They will also suggest a potential generalisation of concurrence to multi-partite systems that we will sketch in chapter 3.6.

For this purpose, we consider the function f defined in eq. (3.13) as a map $f : \mathcal{H} \otimes \mathcal{H}^* \otimes \mathcal{H} \otimes \mathcal{H}^* \to \mathbb{C}$. Since f is linear in the first and third argument, and anti-linear in the second and fourth, it defines a linear map $A : \ \mathcal{H} \otimes \mathcal{H} \to \mathcal{H} \otimes \mathcal{H}$, with elements

$$\langle \psi_2 \otimes \psi_4 | A | \psi_1 \otimes \psi_3 \rangle = 2 \ f(|\psi_1\rangle, \langle \psi_2|, |\psi_3\rangle, \langle \psi_4|) \ . \tag{3.19}$$

In the local bases $\{|\phi_a\rangle \in \mathcal{H}_1\}$ and $\{|\chi_b\rangle \in \mathcal{H}_2\}$ they are denoted by

$$\langle \phi_c| \otimes \langle \chi_\gamma| \otimes \langle \phi_d| \otimes \langle \chi_\delta| \ A \ |\phi_a\rangle \otimes |\chi_\alpha\rangle \otimes |\phi_b\rangle \otimes |\chi_\beta\rangle = A^{c\gamma \ d\delta}_{a\alpha \ b\beta} \ . \tag{3.20}$$

Now, the space $\mathcal{K} := \mathcal{H} \otimes \mathcal{H} = \mathcal{H}_1 \otimes \mathcal{H}_2 \otimes \mathcal{H}_1 \otimes \mathcal{H}_2$ is, in a natural manner, isomorphic to $\tilde{\mathcal{K}} = \big(\mathcal{H}_1 \otimes \mathcal{H}_1\big) \otimes \big(\mathcal{H}_2 \otimes \mathcal{H}_2\big) =: \mathcal{K}_1 \otimes \mathcal{K}_2$, such that the mapping A induces a linear map $\tilde{A}$ on $\tilde{\mathcal{K}} = \mathcal{K}_1 \otimes \mathcal{K}_2$. The elements of $\tilde{A}$ in the above local bases

$$\langle \phi_c| \otimes \langle \phi_d| \otimes \langle \chi_\gamma| \otimes \langle \chi_\delta| \ \tilde{A} \ |\phi_a\rangle \otimes |\phi_b\rangle \otimes |\chi_\alpha\rangle \otimes |\chi_\beta\rangle = \tilde{A}^{cd \ \gamma\delta}_{ab \ \alpha\beta} \ . \tag{3.21}$$

can be computed straight-forwardly and read

$$\tilde{A}^{cd \ \gamma\delta}_{ab \ \alpha\beta} = A^{c\gamma \ d\delta}_{a\alpha \ b\beta} = 2 \ \big(\delta_{ac}\delta_{bd} - \delta_{ad}\delta_{bc}\big)\delta_{\alpha\gamma}\delta_{\beta\delta} \ , \tag{3.22}$$

with δ_{ij} the usual Kronecker symbol. Thus A and $\mathcal{A}$ are completely antisymmetric in the first subsystem, *i.e.* A and $\mathcal{A}$ change their sign under exchange of a and b as well as under exchange of c and d. However, they do not incorporate this symmetry in the second subsystem. This distinction between the first subsystem and the second one reflects the different roles of the two subsystems in eq. (3.9).

The map $\mathcal{A}$, *i.e.* the symmetrised version of A, does not exhibit this distinction between the respective subsystems any more. By virtue of eq. (3.18), it is defined as

$$\begin{aligned}\langle\psi_2\otimes\psi_4|\mathcal{A}|\psi_1\otimes\psi_3\rangle &= \frac{1}{2}\big(\langle\psi_2\otimes\psi_4|A|\psi_1\otimes\psi_3\rangle + \langle\psi_4\otimes\psi_2|A|\psi_1\otimes\psi_3\rangle\big)\\ &= f(|\psi_1\rangle,\langle\psi_2|,|\psi_3\rangle,\langle\psi_4|) + f(|\psi_1\rangle,\langle\psi_4|,|\psi_3\rangle,\langle\psi_2|)\end{aligned} \tag{3.23}$$

and analogously for the matrix elements of $\tilde{\mathcal{A}}$, which is the symmetrised version of $\tilde{A}$. It easily follows that $\mathcal{A}$ and $\tilde{\mathcal{A}}$ are completely antisymmetric in both subsystems

$$\mathcal{A}^{c\gamma\ d\delta}_{a\alpha\ b\beta} = \tilde{\mathcal{A}}^{cd\ \gamma\delta}_{ab\ \alpha\beta} = \big(\delta_{ac}\delta_{bd}-\delta_{ad}\delta_{bc}\big)\big(\delta_{\alpha\gamma}\delta_{\beta\delta}-\delta_{\alpha\delta}\delta_{\beta\gamma}\big)\ . \tag{3.24}$$

Given the matrix elements of $\mathcal{A}$ with respect to a product basis, one can also compute the matrix elements with respect to a set of general states $|\psi_j\rangle$. Decomposing $|\psi_j\rangle$ into a product basis $|\psi_j\rangle = \sum_{a\alpha}\psi^j_{a\alpha}|\phi_a\rangle\otimes|\chi_\alpha\rangle$, one obtains all elements of $\mathcal{A}$, summing over all basis states

$$\mathcal{A}^{lm}_{jk} = \sum_{\substack{abcd\\ \alpha\beta\gamma\delta}} \psi^j_{a\alpha}\left(\psi^k_{b\beta}\right)^*\psi^k_{c\gamma}\left(\psi^l_{d\delta}\right)^*\big(\delta_{ac}\delta_{bd}-\delta_{ad}\delta_{bc}\big)\big(\delta_{\alpha\gamma}\delta_{\beta\delta}-\delta_{\alpha\delta}\delta_{\beta\gamma}\big)\ , \tag{3.25}$$

and verifies that $\mathcal{A}$ can be expressed in terms of partial traces

$$\begin{aligned}\mathcal{A}^{lm}_{jk} &= \mathrm{Tr}_1\big(\mathrm{Tr}_2\big(|\psi_j\rangle\langle\psi_k|\big)\big)\mathrm{Tr}_1\big(\mathrm{Tr}_2\big(|\psi_j\rangle\langle\psi_k|\big)\big)\\ &- \mathrm{Tr}_1\big(\mathrm{Tr}_2\big(|\psi_j\rangle\langle\psi_k|\big)\mathrm{Tr}_2\big(|\psi_l\rangle\langle\psi_m|\big)\big)\\ &- \mathrm{Tr}_2\big(\mathrm{Tr}_1\big(|\psi_j\rangle\langle\psi_k|\big)\mathrm{Tr}_1\big(|\psi_l\rangle\langle\psi_m|\big)\big)\\ &+ \mathrm{Tr}_1\big(\mathrm{Tr}_2\big(|\psi_j\rangle\langle\psi_k|\psi_l\rangle\langle\psi_m|\big)\big)\ .\end{aligned} \tag{3.26}$$

Here it is clear that $\mathcal{A}$ represents the symmetric definition of concurrence, as given in eq. (3.8), insofar as there is no distinguished subsystem - in contrast to eq. (3.9).

Eq. (3.24) also implies that $\tilde{\mathcal{A}}$ is supported only on the tensor product of the antisymmetric parts of $\mathcal{K}_1$ and $\mathcal{K}_2$, *i.e.* on $\big(\mathcal{H}_1\wedge\mathcal{H}_1\big)\otimes\big(\mathcal{H}_2\wedge\mathcal{H}_2\big)$. The

antisymmetric space $\mathcal{H}\wedge\mathcal{H}$ contains all states $|\chi_\wedge\rangle$ that can be expressed as $|\chi_\wedge\rangle = \sum_{ij} c_{ij}(|\Phi_i\rangle\otimes|\Phi_j\rangle - |\Phi_j\rangle\otimes|\Phi_i\rangle)$, with $|\Phi_i\rangle \in \mathcal{H}$. This means that all elements of $\tilde{\mathcal{A}}$ with respect to fully symmetric linear combinations of product states vanish. Since the space $\big(\mathcal{H}_1\wedge\mathcal{H}_1\big)$ has dimension $n_1(n_1-1)/2$, and $\big(\mathcal{H}_2\wedge\mathcal{H}_2\big)$ has dimension $n_2(n_2-1)/2$, $\tilde{\mathcal{A}}$, and consequently also $\mathcal{A}$, cannot have more than $n_1(n_1-1)n_2(n_2-1)/4$ non-vanishing eigenvalues.

Finally, one can show quite easily that $\mathcal{A}$ is also positive definite, *i.e.* each expectation value of $\mathcal{A}$ is non-negative. Expanding an arbitrary pure state $|\zeta\rangle \in \mathcal{K}$ in terms of local basis states

$$|\zeta\rangle = \sum_{a,b,\alpha\beta} \zeta_{a\alpha b\beta}\ |\phi_a\rangle\otimes|\chi_\alpha\rangle\otimes|\phi_b\rangle\otimes|\chi_\beta\rangle\ , \tag{3.27}$$

one obtains for the corresponding expectation values

$$\begin{aligned}\langle\zeta|\mathcal{A}|\zeta\rangle &= \sum_{a,\alpha,b,\beta}\big(\zeta^*_{a\alpha b\beta} - \zeta^*_{b\alpha a\beta} - \zeta^*_{a\beta a\alpha} + \zeta^*_{b\beta a\alpha}\big)\zeta_{a\alpha b\beta} \\ &= \sum_{a,\alpha,b,\beta}\big|\zeta_{a\alpha b\beta} - \zeta_{b\alpha a\beta} - \zeta_{a\beta a\alpha} + \zeta_{b\beta a\alpha}\big|^2\ \geq 0\ ,\end{aligned} \tag{3.28}$$

where we used the fact that symmetric part of $\zeta_{a\alpha b\beta}$ drops out when summed with the antisymmetric expression $\zeta^*_{a\alpha b\beta} - \zeta^*_{b\alpha a\beta} - \zeta^*_{a\beta a\alpha} + \zeta^*_{b\beta a\alpha}$.

In particular positivity - but also the reduced rank $n_1(n_1-1)n_2(n_2-1)/4$ of $\mathcal{A}$ - will soon turn out to be crucial for constructing concurrence of mixed states.

3.2.2 Expansion of $\mathcal{A}$

Since $\mathcal{A}$ is invariant under exchange of its covariant as well as of its contravariant indices, it can be expanded in terms of a basis of real symmetric matrices $\Lambda^\alpha \in \mathbb{R}^{n\times n}$, according to

$$\mathcal{A}^{lm}_{jk} = \sum_{\alpha,\beta}\ B_{\alpha\beta}\ \Lambda^\alpha_{jk}\ \Lambda^\beta_{lm}\ . \tag{3.29}$$

Here, the Λ^α are orthonormal with respect to the Hilbert-Schmidt scalar product [31] $\mathrm{Tr}\ \Lambda^\alpha\big(\Lambda^\beta\big)^\dagger = \delta_{\alpha,\beta}$, with $\big(\Lambda^\beta\big)^\dagger$ the adjoint of Λ^β. Since $\mathcal{A}$ is hermitian, also the matrix B with elements

$$B_{\alpha\beta} = \sum_{jklm}\ \Lambda^\alpha_{jk}\ \mathcal{A}^{lm}_{jk}\ \Lambda^\beta_{lm} \tag{3.30}$$

is hermitian, and due to the positivity of $\mathcal{A}$ also B is positive. Consequently, B has real, non-negative eigenvalues μ_α, and the associated eigenvectors

$\vec{x}^\alpha \in \mathbb{C}^{n(n+1)/2}$ form a complete orthonormal set.

Yet, there is an ambiguity left in the choice of the phases of $B's$ eigenvectors. Under most circumstances, the phases are not important and their choice is arbitrary. However, in chapter 3.4 the proper choice of phases will reveal as a vital ingredient. Therefore, we will explicitely incorporate this ambiguity by denoting the eigenvectors as $\vec{x}^\alpha e^{i\varphi_\alpha}$.

Given the eigensystem of B, we can construct an eigensystem T^α of $\mathcal{A}$

$$T^\alpha e^{i\varphi_\alpha} = \sqrt{\mu_\alpha}\ e^{i\varphi_\alpha}\ \sum_\beta [x^\alpha]_\beta\ \Lambda^\beta\ , \tag{3.31}$$

where $[x^\alpha]_\beta$ denotes the β-th component of the vector $\vec{x}^\alpha$. The matrices T^α are not normalised to 1, but rather subnormalised

$$\text{Tr}\ T^\alpha (T^\beta)^* = \mu_\alpha \delta_{\alpha,\beta}\ . \tag{3.32}$$

Since the eigenvalues μ_i are positive, $\mathcal{A}$ can be expanded in terms of its sub-normalised eigensystem as

$$\mathcal{A}^{lm}_{jk} = \sum_{\alpha=1}^{m}\ T^\alpha_{jk}\ \left(T^\alpha_{lm}\right)^*\ . \tag{3.33}$$

Hence, eq. (3.15) can be rewritten as

$$\begin{aligned}
\mathcal{C} &= \sum_{i=1}^{N} \left(\sum_{jklm} V_{ij} V_{ik} A^{lm}_{jk} V^\dagger_{li} V^\dagger_{mi} \right)^{\frac{1}{2}} \\
&= \sum_{i=1}^{N} \left(\sum_{\alpha=1}^{m} \sum_{jklm} V_{ij} T^\alpha_{jk} V_{ik} V^\dagger_{li} T^\alpha_{lm} V^\dagger_{mi} \right)^{\frac{1}{2}} \\
&= \sum_{i=1}^{N} \left(\sum_{\alpha=1}^{m} \sum_{jk} \left| V_{ij} T^\alpha_{jk} V_{ik} \right|^2 \right)^{\frac{1}{2}} \\
&= \sum_{i=1}^{N} \left(\sum_{\alpha=1}^{m} \left| \left[V T^\alpha e^{i\varphi_\alpha} V^T \right]_{ii} \right|^2 \right)^{\frac{1}{2}}\ ,
\end{aligned} \tag{3.34}$$

the infimum of which gives the concurrence of the mixed state ϱ.

Eq. (3.34) is now much more reminiscent of eq. (2.40) than eq. (3.15). The tensorial structure of the transformation is eliminated, the hermitian quantity $\mathcal{A}$ is replaced by a set of complex symmetric matrices T^α, and the transpose of the transformation matrix V enters, instead of the hermitian

conjugate. The remaining difference with respect to eq. (2.40) is that the sum over α in general implies a non-linear dependence of $\mathcal{C}$ on T^α.

For the derivation of eq. (2.41) from eq. (2.40), it was crucial that τ could be diagonalised. Two complex symmetric matrices T^α and T^β can be diagonalised simultaneously by a unitary matrix *if and only if* $\left(T^\alpha\right)^{-1}T^\beta$ is symmetric [31]. In general, this condition is not satisfied for all pairs in a set $\{T^\alpha\}$, so that not all matrices T^α can be diagonalised simultaneously, which complicates the derivation of a closed expression for the infimum of eq. (3.34). However, as we will discuss in chapter 3.4, our above approach allows to derive of a lower bound of concurrence, valid in arbitrary dimensions. Moreover, the original derivation of concurrence [26] is naturally embedded in our theory, as we will see in chapter 3.4.2.

3.3 Gradient

Before we derive a lower bound for the concurrence of mixed states, we first perform a maybe more self-evident analysis, namely we consider eq. (3.15) for infinitesimal transformations $V \otimes V$. This will lead to an efficient numerical recipe to evaluate the convex roof defined in eq. (2.30).

As mentioned in chapter 2.2.2, the cardinality of the ensemble that realises the infimum in eq. (2.30) can exceed that of the initial ensemble used do construct A, what is the cause for the appearance of a rectangular left-unitary matrix V instead of a quadratic unitary matrix U in eq. (3.15). In the present chapter, however, matrices of the latter type are more convenient. Therefore we will fix the cardinality of the considered ensembles. If it turns out that the assumed cardinality is not large enough, one can always add some null-vectors to the ensemble, and thereby increase the cardinality.

According to eq. (3.15) and eq. (3.18), the concurrence of a mixed state ϱ is given by

$$c(\varrho) = \inf_U \mathcal{C}(U) \ , \quad \text{with} \quad \mathcal{C}(U) = \sum_i \left(\left[U \otimes U A \, U^\dagger \otimes U^\dagger \right]_{ii}^{ii} \right)^{\frac{1}{2}} \ . \tag{3.35}$$

If one considers an infinitesimal transformation $dU = \mathbb{1} + i\epsilon H$, with ϵ infinitesimally small, and uses the symmetry of A with respect to an exchange of co- and contra-variant indices, this simplifies to

$$\mathcal{C}(dU) \simeq \sum_i \left(\left(A_{ii}^{ii} + 2i\epsilon \left[H \otimes \mathbb{1} \ A \ \mathbb{1} \otimes \mathbb{1} - \mathbb{1} \otimes \mathbb{1} \ A \ H \otimes \mathbb{1} \right]_{ii}^{ii} \right)^{\frac{1}{2}} \right) \ . \tag{3.36}$$

With an expansion of the square root function to lowest order in ε, this can be approximated as

$$\mathcal{C}(dU) \simeq \sum_i \sqrt{A_{ii}^{ii}} + \frac{i\epsilon}{\sqrt{A_{ii}^{ii}}} \left[H \otimes \mathbb{1} \ A \ - A \ H \otimes \mathbb{1} \right]_{ii}^{ii} \ . \tag{3.37}$$

Since the power series of $\sqrt{x}$ is defined only for $x \neq 0$, one has to take care that A^{ii}_{ii} be non-vanishing for all i, what is the case if and only if there are only non-separable pure states $|\Psi_i\rangle$ in the decomposition of ϱ, since by eq. (3.13) and eq. (3.16) the elements A^{ii}_{ii} are the squares of the concurrences of the states $|\Psi_i\rangle$. This demands some caution in numerical implementations, which we will address later.

Disregarding this problem for a while, eq. (3.37) can be rephrased as

$$\mathcal{C}(dU) = \sum_i \sqrt{A^{ii}_{ii}} + \varepsilon \sum_{ij} H_{ij} G_{ji} \ , \quad \text{with} \quad G_{ij} = i \left(\frac{A^{ii}_{ji}}{\sqrt{A^{ii}_{ii}}} - \frac{A^{ij}_{jj}}{\sqrt{A^{jj}_{jj}}} \right) \ . \tag{3.38}$$

The hermitian matrix G can be considered as a gradient, since the increment of $\mathcal{C}$ reads

$$\mathcal{C}(dU) - \mathcal{C}(\mathbb{1}) = \varepsilon \ \mathrm{Tr} \ HG \ , \tag{3.39}$$

what is just a Hilbert-Schmidt scalar product [31]. Accordingly, the direction of steepest descent of $\mathcal{C}$ is given by $H = -\epsilon G$. Minima of $\mathcal{C}$ can therefore be found by repeated application of the transformation $dU = \exp(-i\epsilon H)$. However, no a priori information is provided on whether the minimum reached by that procedure is a local or the global one. Though, one may start the iteration with different initial conditions parametrised by U. The comparison of the final values of the different runs eventually gives some intuition about the nature of the detected minima.

A drawback of the gradient procedure is the occurrence of rather large matrices - A is quadratically bigger than ϱ. However, using the symmetrised quantity $\mathcal{A}$ instead of A, we can use eq. (3.33) and express all quantities in terms of the matrices T^α, such as to decrease the number of matrix elements that have to be stored. Consequently, one obtains, for the elements of the gradient G in eq. (3.38):

$$G_{ij} = i \left(\frac{\sum_\alpha T^\alpha_{ji} T^\alpha_{ii}}{\sqrt{\sum_\alpha \left(T^\alpha_{ii}\right)^2}} - \frac{\sum_\alpha T^\alpha_{jj} \left(T^\alpha_{ij}\right)^*}{\sqrt{\sum_\alpha \left(T^\alpha_{jj}\right)^2}} \right) \ . \tag{3.40}$$

We already mentioned above that special care hat to be taken when A^{ii}_{ii} vanishes for some i. In the case of two-level systems, the summation over α in eq. (3.40) reduces to only one single non-vanishing matrix T. Therefore, the gradient simplifies to

$$G_{ij} = i \left(T_{ij} - T^*_{ij} \right) \ . \tag{3.41}$$

Wherever a denominator vanishes in eq. (3.40), also the corresponding numerator behaves accordingly, so that the gradient is non-singular, and can be expressed by eq. (3.41).

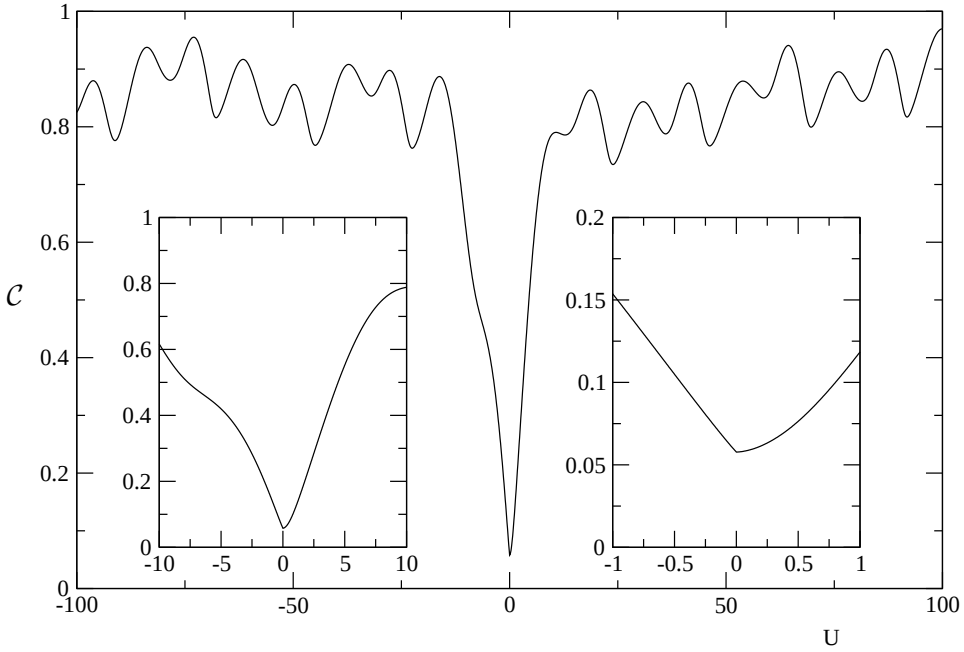

Figure 3.1: Profile of the manifold $\mathcal{C}(U)$ cut along the direction of steepest descent, evaluated at $\xi = 0$ (see eq. (3.43)), where one element A^{ii}_{ii} in eq. (3.40) vanishes. Although the square root function has an infinitely large increment, the gradient remains finite. Still - as also shown in the insets which zoom into the region around the origin of the abscissa - the curvature of $\mathcal{C}(U)$ gets very large, what complicates the iterative execution of the gradient procedure.

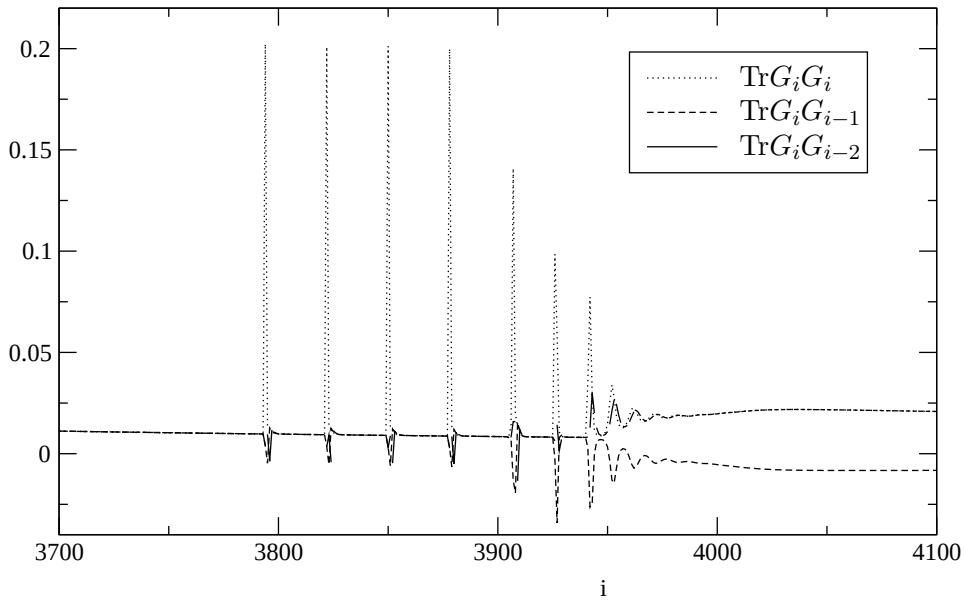

Figure 3.2: The dotted line shows the square of the trace norm Tr G_iG_i of the gradient after i iterations. The dashed and the solid line show the overlap of the gradient G_i with the gradient G_{i-1} and with G_{i-2} of the $i-1$st and $i-2$nd step. Initially all three values coincide. This means that the gradient does not change significantly from one step to the next. Later-on, a few sudden changes in the gradient appear. The iteration jumps between regions where the gradient changes drastically between two successive steps, and regimes where the gradient behaves rather smoothly. In the end, all three quantities exhibit a smooth behaviour again. The square of the trace norm of the gradient and the overlap of G_i with G_{i-2} coincide. However, the overlap of G_i with G_{i-1} significantly differs from the other two quantities. This is a clear signature that the iteration jumps back and forth due to the strong curvature of $\mathcal{C}(U)$.

For higher dimensional systems, however, there is generically more than one non-vanishing matrix T^α. Consider a path on the manifold $\mathcal{C}(U)$, parametrised by a real parameter ξ that leads to a point $\mathcal{C}_0$ where at least one of the elements $\mathcal{A}_{ii}^{ii}$ vanishes, *i.e.*

$$\lim_{\xi\to 0} \mathcal{C}(U(\xi)) = \mathcal{C}_0 \ . \tag{3.42}$$

The gradient nonetheless remains finite for $\xi \to 0$, if

$$\lim_{\xi\to 0} \frac{\sum_\alpha T_{ji}^\alpha T_{ii}^\alpha}{\sqrt{\sum_\alpha (T_{ii}^\alpha)^2}} < \infty \ , \ \forall \ i,j \ . \tag{3.43}$$

The following discussion can be restricted to those values of i for which $\mathcal{A}_{ii}^{ii}$ vanishes. Since $\mathcal{A}_{ii}^{ii}$ is given by $\sum_\alpha (T_{ii}^\alpha)^2$, the diagonal element T_{ii}^α vanishes for each α in these cases. Thus, for $\xi \simeq 0$, each element T_{ii}^α is proportional to ξ^{p_α}, where the p_α are real and non-negative. For $\xi \simeq 0$, the denominator behaves as ξ^{p_β}, where $p_\beta = \min(\{p_\alpha\})$. Since the elements T_{ji}^α do not diverge, the numerator behaves as $T_{ji}^\beta T_{ii}^\beta \sim T_{ji}^\beta \xi^{p_\beta}$, if $T_{ji}^\beta \neq 0$. If $T_{ji}^\beta = 0$, the numerator approaches 0 not slower than ξ^{p_β}, since $\xi^{p_\beta} \leq \xi^{p_\alpha}$. Thus, in any case, eq. (3.43) does not diverge!

However, it turns out that there can be points where the manifold $\mathcal{C}(U)$ can exhibit a very large curvature. An example of such a point of large curvature is given in fig. 3.1. Once such a point is reached, convergence of the gradient algorithm cannot be guaranteed for finite step size. It is likely that the iteration will start to jump back and forth between two regions separated by a region of large curvature. Fig. 3.2 shows that an iteration can get trapped between two points. The iteration depicted in fig. 3.2 refers to the manifold of fig. 3.1. However, such critical situations are in general only reached near the minimum we are seeking for, and the algorithm always produces satisfactory results. In chapter 4 we will compare the upper bound of concurrence provided by the gradient procedure with the lower bound that we will derive hereafter, such as to illustrate the quantitative reliability of both estimates.

3.4 Lower bound

Eq. (3.34) above is our starting point for the derivation of the promised lower bound for the concurrence of arbitrary mixed states. As already mentioned in chapter 3.2.2, the non-linear dependence of $\mathcal{C}$ on T^α complicates the deduction of an analytic expression for the infimum of eq. (3.15). However, the said dependence on T^α can be linearised with help of the Cauchy-Schwarz

inequality [63]

$$\Big(\sum_\alpha x_\alpha^2\Big)^{\frac{1}{2}}\Big(\sum_\alpha y_\alpha^2\Big)^{\frac{1}{2}} \geq \sum_\alpha x_\alpha y_\alpha \ . \tag{3.44}$$

Applying this to each term in the sum over i in eq. (3.34), with $x_\alpha := \big|\big[VT^\alpha e^{i\varphi_\alpha}V^T\big]_{ii}\big|$, we conclude that

$$\mathcal{C}(\varrho) \geq \sum_{i=1}^{N}\sum_{\alpha=1}^{m} y_\alpha \Big|\Big[VT^\alpha e^{i\varphi_\alpha}V^T\Big]_{ii}\Big| , \quad \text{for all} \quad \{y_\alpha \in \mathbb{R}\} \quad \text{s.t.} \quad \sum_\alpha y_\alpha^2 = 1 \ . \tag{3.45}$$

Now $\mathcal{C}$ is bounded from below by an expression which is linearised in the T^α. Though there is still the appearance of several matrices T^α that in general cannot be diagonalised simultaneously, what still causes trouble finding the desired infimum. However, one can make use of a second inequality,

$$\sum_\alpha |z_\alpha| \geq \Big|\sum_\alpha z_\alpha\Big| \ , \tag{3.46}$$

valid for arbitrary complex numbers z_α. For $z_\alpha := y_\alpha\big[VT^\alpha e^{i\varphi_\alpha}V^T\big]_{ii}$, and $y_\alpha \geq 0$, one obtains

$$\mathcal{C}(\varrho) \geq \sum_{i=1}^{N}\left|\Big[V\Big(\sum_{\alpha=1}^{m} y_\alpha T^\alpha e^{i\varphi_\alpha}\Big)V^T\Big]_{ii}\right| =: W \ , \tag{3.47}$$

an expression for which the infimum is given analytically by eq. (2.46) - the lower bound of concurrence of ϱ finally reads

$$c(\varrho) \geq \inf_V W = \max\Big(\mathcal{S}_1 - \sum_{i>1}\mathcal{S}_i,\ 0\Big) \ , \tag{3.48}$$

with the singular values $\mathcal{S}_j$ of $\mathcal{T} = \sum_\alpha Z_\alpha T_\alpha$, $Z_\alpha = y_\alpha e^{i\varphi_\alpha}$, and $\sum_\alpha |Z_\alpha|^2 = 1$.

The bound in eq. (3.48) still depends on the choice of the Z_α, what allows to tighten the bound. Consequently, one is left with an optimisation problem on an m-dimensional parameter space [64]. Note that the constraint $\sum_\alpha |Z_\alpha|^2 = 1$ is by far simpler to implement than the constraint of left unitarity according to eq. (2.32), since it can be parametrised easily. Moreover, the dimension $n_1(n_1-1)n_2(n_2-1)/4$ of the optimisation space is significantly reduced with respect to the dimension $n_1^3 n_2^3$ of the original optimisation problem defined by eqs. (2.30) and (3.12).

Still, if one aims at reducing numerical effort one can also use purely algebraic bounds that are implied by eqs. (3.47) and (3.48). Instead of optimising over the Z_α, one can set one of these coefficients equal to unity,

and all others equal to zero. In that case, the singular values of any of the matrices $\mathcal{T}^\alpha$ provide an algebraic bound

$$c \geq \max\Big(\mathcal{S}_1^\alpha - \sum_{i>1} \mathcal{S}_i^\alpha,\ 0\Big)\ . \tag{3.49}$$

The states we investigated - and that we will discuss in chapters 3.4.4 and 4 - suggest that in general there is one matrix $\mathcal{T}^\alpha$ that provides the main contribution to the optimised lower bound. The bound associated with this distinguished matrix often yields a satisfactory approximation of the optimised bound. In fact, the state defined in eq. (3.54) hereafter is the only exception we encountered, as much as it has no distinguished matrix $\mathcal{T}^\alpha$.

3.4.1 Lower bound versus concurrence vector

Previously to our - though independent - work, the *concurrence vector* $\vec{\mathcal{C}}$ was proposed in [57], to distinguish separable and entangled states. Its elements $\mathcal{C}_i$ are constructed with the help of some complex symmetric matrices T_i as

$$\mathcal{C}_i = \sum_j \Big| \big[V T_i V^T\big]_{jj} \Big|\ , \tag{3.50}$$

where V is left-unitary. This equation is strongly reminiscent of eq. (3.47). A given state is separable if and only if there is a left unitary matrix V that makes all elements of $\vec{\mathcal{C}}$ vanish simultaneously. This - necessary and sufficient - separability criterion is, in general, inoperational - mainly because general matrices T_i cannot be diagonalised simultaneously. Nevertheless, it is the basis for some operational, but only necessary criteria. It implies that a given state is entangled if the singular values $\mathcal{S}_j^{(i)}$ of one matrix T_i satisfy $\mathcal{S}_1^{(i)} - \sum_j \mathcal{S}_j^{(i)} > 0$. A further - in general stronger - criterion is obtained with the help of linear combinations $\sum_i z_i T_i$ of all matrices T_i with complex prefactors z_i. For a suitably chosen set $\{z_i\}$, the expression $\mathcal{S}_1 - \sum_j \mathcal{S}_j$ can be significantly larger than the corresponding expression for a single matrix T_i.

Similar criteria can also be formulated with recourse to our lower bounds. Then, the criteria that use a single matrix T_i or linear combinations thereof are analogous to our algebraic, eq. (3.49), or optimised bound, eq. (3.48), respectively. Though, let us stress once more that our bound does *not only* serve as a separability criterion, but - beyond that - also yields a quantitative description, as will be illustrated by various examples in chapter 4.

3.4.2 Concurrence of two-level systems

In this chapter, we would like to relate our approach to earlier results on 2×2 systems [26]. As already observed in chapter 3.2.1, the maximum number

m of non-vanishing eigenvalues of $\mathcal{A}$ is given by $m = n_1(n_1-1)n_2(n_2-1)/4$, in terms of the dimensions n_1 and n_2 of the underlying Hilbert spaces. In the case of two-level systems, where the dimension of both spaces equals two, there is at most one single non-vanishing eigenvalue of $\mathcal{A}$. Accordingly, there is at maximum one finite matrix $T = T^\alpha$, and the summation over α in eq. (3.34) contains only one term. Therefore, the square and the square root cancel each other, and eq. (3.34) simplifies to

$$c(\varrho) = \inf_V \left| \left[VTV^T \right]_{ii} \right| . \tag{3.51}$$

This expression has exactly the same structure as eq. (2.40). The analytic solution given in eq. (2.41) therefore also applies in the present case. Consequently, the concurrence for two-level systems can be expressed as

$$c(\varrho) = \max\Big(\mathcal{S}_1 - \sum_{i=2}^{4} \mathcal{S}_i,\ 0 \Big) , \tag{3.52}$$

where the $\mathcal{S}_i$ are the singular values of T in decreasing order. One easily verifies that T coincides with the matrix τ defined in eq. (2.40), by evaluating both quantities in a product basis. Hence, the analysis restricted to two-level systems [26] is naturally embedded in ours.

3.4.3 Tightness of the lower bound

Of course, the significance of our lower bound, eq. (3.48) strongly depends on its tightness. In its derivation, we were using two inequalities both of which can be saturated for some parameters.

Equality in the Cauchy-Schwarz inequality, eq. (3.44), holds if and only if $\vec{x} \sim \vec{y}$. Therefore, the bound can only coincide with the exact solution if $y_\alpha \sim \left| \left[VT^\alpha e^{i\varphi_\alpha} V^T \right]_{ii} \right|$ for all $i \in [1, N]$. A priori it is not clear whether one can find a left unitary matrix V such that this proportionality is satisfied for all values of i,

The second inequality, eq. (3.46), we have used is saturated if and only if the phases of all terms $z_\alpha = y_\alpha \left[VT^\alpha e^{i\varphi_\alpha} V^T \right]_{ii}$ are equal, for all $i \in [1, N]$. The freedom to choose the free phases $e^{i\varphi_\alpha}$ of the eigenvectors of the matrix B can be exploited to adjust the phases of the z_α. However, it is not clear whether this freedom is sufficient to attain the above equality, whilst it does become clear why the choice of phases is important for the tightness of the bound.

Thus, in general, we cannot make any predictions whether our lower bound, eq. (3.48), provides the exact value of the concurrence for a given state with finite mixing, or how large a possible difference between the bound and the exact value may be. Therefore, we will test the bound numerically in the next chapter and in chapter 4, applying it to various families of mixed quantum states.

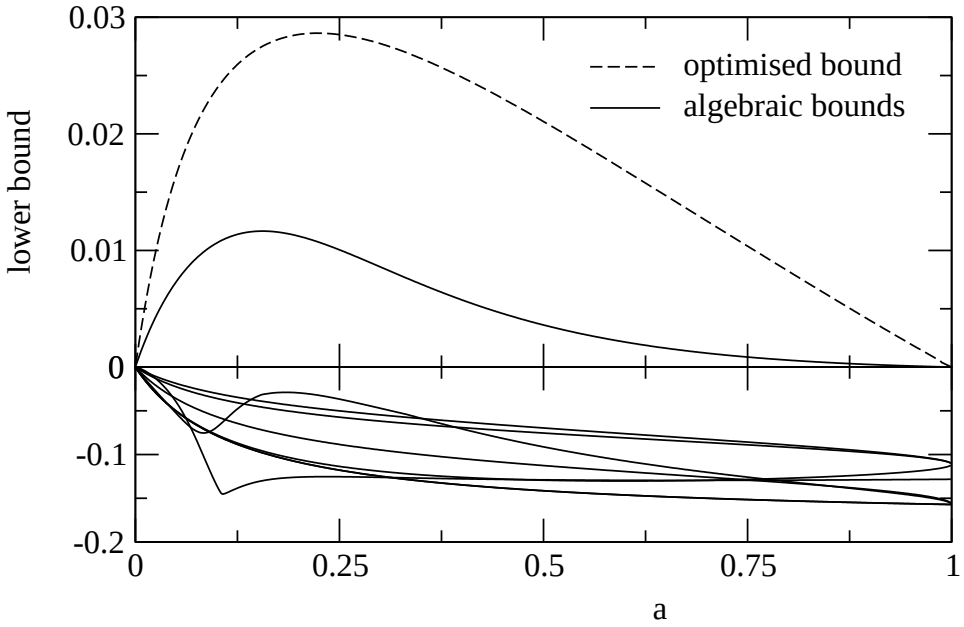

Figure 3.3: Numerically optimised lower bound (dashed line) of the concurrence of the family of bipartite spin-1 states ϱ_a [65] as defined in eq. (3.53), together with the algebraic bounds given in eq. (3.49) (solid lines). Both the optimised bound and the largest algebraic bound are positive, such that the state is detected as entangled in the entire parameter range $a = [0, 1]$. All other algebraic lower bounds are negative. Note that the scale is different for positive and negative bounds.

3.4.4 Some exemplary ppt states

One of the main requirements imposed on an entanglement measure is that it be able to distinguish entangled states from separable ones. Whereas a large class of entangled states is detected by the ppt criterion defined in eq. (2.13), no operational criterion is known so far that can detect all states with positive partial transpose. In general it turns out rather demanding to decide whether such states are entangled or not. Therefore - albeit our bound, eq. (3.47), is capable of more than just checking separability - we use it, as a first test of its pertinence, as a separability criterion for some families of entangled states with positive partial transpose [34, 35, 65].

The first class of states describes a bipartite spin-1 system. The state ϱ_a

acting on $\mathbb{C}^3 \otimes \mathbb{C}^3$ is given [34, 65] for $a \in [0,1]$ as

$$\varrho_a = \frac{1}{1+8a} \begin{bmatrix} a & 0 & 0 & 0 & a & 0 & 0 & 0 & a \\ 0 & a & 0 & 0 & 0 & 0 & 0 & 0 & 0 \\ 0 & 0 & a & 0 & 0 & 0 & 0 & 0 & 0 \\ 0 & 0 & 0 & a & 0 & 0 & 0 & 0 & 0 \\ a & 0 & 0 & 0 & a & 0 & 0 & 0 & a \\ 0 & 0 & 0 & 0 & 0 & a & 0 & 0 & 0 \\ 0 & 0 & 0 & 0 & 0 & 0 & \beta & 0 & \gamma \\ 0 & 0 & 0 & 0 & 0 & 0 & 0 & a & 0 \\ a & 0 & 0 & 0 & a & 0 & \gamma & 0 & \beta \end{bmatrix}, \quad \text{with} \quad \begin{cases} \beta = \dfrac{1+a}{2}\,, \\ \\ \gamma = \dfrac{\sqrt{1-a^2}}{2}\,, \end{cases} \tag{3.53}$$

and has a positive partial transpose as defined in eq. (2.13) in the entire range of a. The algebraic lower bounds attained from eq. (3.49) are plotted in fig. 3.3 as solid lines. One of them is positive for all values of the parameter a, and the non-separability of ϱ_a is therefore detected by a *purely algebraic criterion*. All other algebraic bounds are negative, and therefore do not provide any information on their own.

The dashed line in fig. 3.3 shows the lower bound that is numerically optimised over the Z_α in eq. (3.47), using a *downhill simplex method* [66]. It is significantly larger than the positive algebraic bound, and shows a qualitatively different behaviour for large a, where its first derivative is finite, whilst that of the largest algebraic bound vanishes for $a = 1$.

A second class of states ϱ_a [65] acts on $\mathbb{C}^4 \otimes \mathbb{C}^2$, and once again has a positive partial transpose, eq. (2.13), for $a \in [0,1]$:

$$\varrho_a = \frac{1}{1+7a} \begin{bmatrix} a & 0 & 0 & 0 & 0 & a & 0 & 0 \\ 0 & a & 0 & 0 & 0 & 0 & a & 0 \\ 0 & 0 & a & 0 & 0 & 0 & 0 & a \\ 0 & 0 & 0 & a & 0 & 0 & 0 & 0 \\ 0 & 0 & 0 & 0 & \beta & 0 & 0 & \gamma \\ a & 0 & 0 & 0 & 0 & a & 0 & 0 \\ 0 & a & 0 & 0 & 0 & 0 & a & 0 \\ 0 & 0 & a & 0 & \gamma & 0 & 0 & \beta \end{bmatrix}, \quad \text{with} \quad \begin{cases} \beta = \dfrac{1+a}{2}\,, \\ \\ \gamma = \dfrac{\sqrt{1-a^2}}{2}\,. \end{cases} \tag{3.54}$$

Fig 3.4 shows the algebraic lower bounds obtained from eq. (3.49), which are all negative. Thus, none of them detects ϱ_a as entangled. In fact, some eigenvalues of B, eq. (3.30), are degenerate. Therefore, the matrices T^α, and, consequently, also the algebraic lower bounds, are not uniquely determined. However, we did not find any matrices T^α in the degenerate subspaces that provide positive lower bounds. Yet, the numerically optimised lower bound - also shown in fig. 3.54 - *is* positive in the entire parameter range. Hence, also this state is detected as entangled by our lower bound, eq. (3.48).

A third class of states ϱ_a [35] acting on $\mathbb{C}^3 \otimes \mathbb{C}^3$ is defined for $a \in$

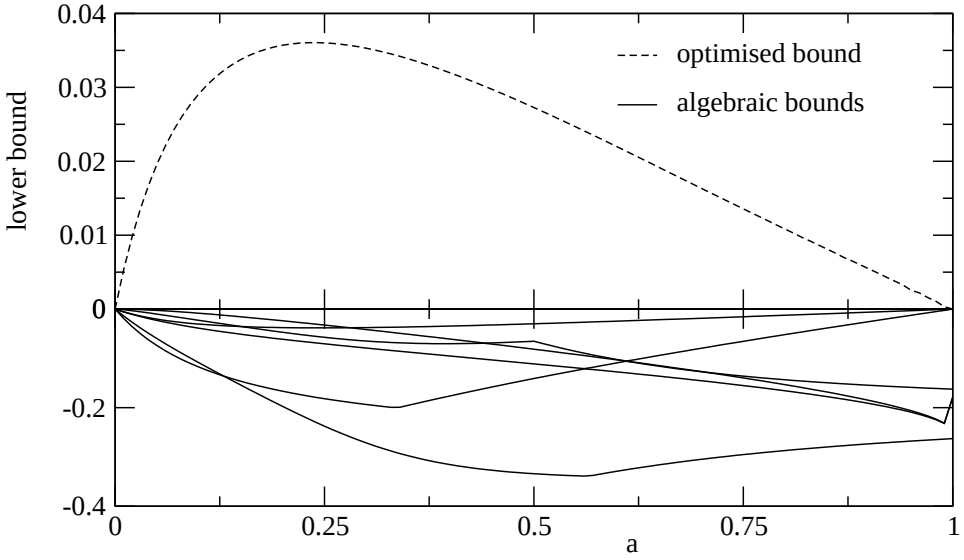

Figure 3.4: Algebraic lower bounds, eq. (3.49), of the concurrence of a family of 4×2 states [65] defined by eq. (3.54), plotted as a function of the parameter a. Although none of these bounds is positive, the optimised bound (dashed line), eq. (3.48), *is* positive. Thus the state is detected as entangled in the entire parameter range of a.

$[-5/2, 5/2]$,

$$\varrho_a = \frac{1}{21}\begin{bmatrix} 2 & 0 & 0 & 0 & 2 & 0 & 0 & 0 & 2 \\ 0 & \beta_- & 0 & 0 & 0 & 0 & 0 & 0 & 0 \\ 0 & 0 & \beta_+ & 0 & 0 & 0 & 0 & 0 & 0 \\ 0 & 0 & 0 & \beta_+ & 0 & 0 & 0 & 0 & 0 \\ 2 & 0 & 0 & 0 & 2 & 0 & 0 & 0 & 2 \\ 0 & 0 & 0 & 0 & 0 & \beta_- & 0 & 0 & 0 \\ 0 & 0 & 0 & 0 & 0 & 0 & \beta_- & 0 & 0 \\ 0 & 0 & 0 & 0 & 0 & 0 & 0 & \beta_+ & 0 \\ 2 & 0 & 0 & 0 & 2 & 0 & 0 & 0 & 2 \end{bmatrix}, \quad \text{with} \quad \beta_\pm = \frac{5}{2} \pm a \ . \tag{3.55}$$

Since replacing a by $-a$ is equivalent to exchanging the subsystems, we will discuss this state only for $a \in [0, 5/2]$. The state ϱ_a has a non-positive partial transpose for $a \in [3/2, 5/2]$, is entangled with positive partial transpose for $a \in [1/2, 3/2]$ and is separable for $a \in [0, 1/2]$ [35]. As depicted in fig. 3.5, ϱ_a is detected as entangled in its domain of negative partial transpose already by the best algebraic lower bound. In the regime where ϱ_a has positive partial transpose all of the algebraic bounds are negative, such that the optimised lower bound is required for distinguishing ϱ_a from separable states. However, even the optimised bound cannot detect ϱ_a in the entire interval $a \in [1/2, 3/2]$. For $a \lesssim 1.02$, the lower bound seems to fail as a sufficient separability criterion. At the present, we have no conclusive evi-

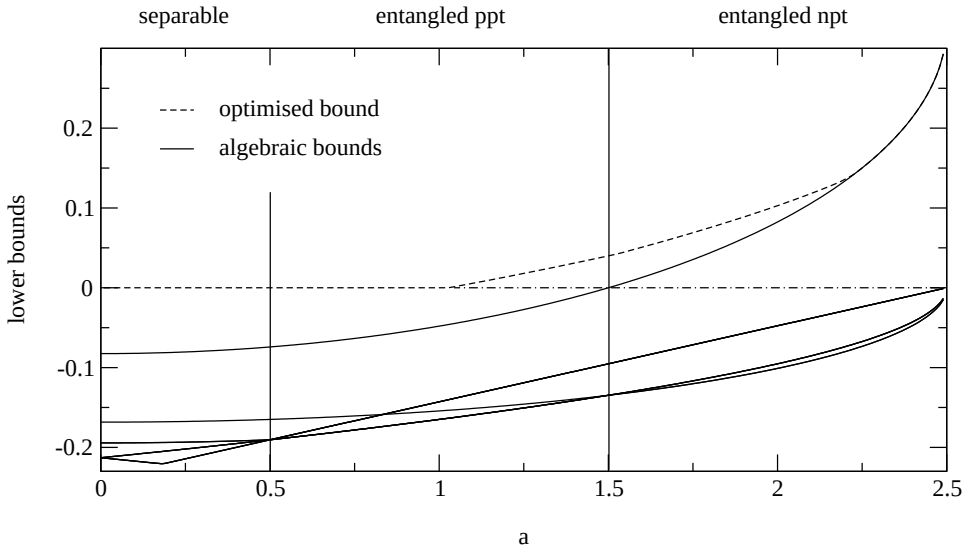

Figure 3.5: Algebraic lower bounds, eq. (3.49), of a family of 3×3 states [35] defined in eq. (3.55), as a function of the parameter a. For $a \leq 1/2$, ϱ_a is separable, and for $a > 1/2$ it is entangled [35]. It has positive partial transpose for $a \leq 3/2$, and non-positive partial transpose for $a > 3/2$. The dashed line shows the numerically optimised lower bound, eq. (3.48). The state ϱ_a is detected as entangled by the algebraic bound exactly in that parameter range where it has non-positive partial transpose. It is detected as entangled by the optimised bound in approximately half the parameter range with positive partial transpose, what might be due to a failure of our numerical optimisation routine.

dence from our optimisation to decide whether the bound itself is not good enough, or whether the numerically found maximum is just a local and not the global one.

The above exemplary *ppt* states show that our lower bound, eq. (3.48), is capable to detect entangled states which are not recognised by the *ppt* criterion. For some states it even is not necessary to evaluate the optimised bound, since already one of the algebraic bounds, eq. (3.49), is positive. However, there are also states with only negative algebraic bounds, though positive optimised bound. Our last example above showed a case of entangled states that we have so far been unable to detect for a small subset of parameters, though it remains hitherto undecided whether this is a failure of our numerical optimisation routine or of our lower bound, eq. (3.48)),itself.

3.5 Quasi-pure approximation

Nowadays, a large number of experiments is performed in which entangled states are prepared and investigated. An increase of mixing - *i.e.* of classical correlations - decreases quantum correlations and can lead to their complete destruction. Therefore - in particular for technical applications - mainly pure entangled states are of interest, such that it is crucial to decouple the investigated systems as well as possible from the environment.

In general, it is not possible to achieve a perfect decoupling, but experimental techniques are sufficiently advanced [18, 22, 25] to preserve entanglement over some period of time. However, very little is known on the temporal evolution of entanglement for a given environment coupling. One of the principal obstacles that prevent a systematic study of this question is the lack of computable entanglement measures for arbitrary states.

On the other hand, since environmental influences can be assumed to be small, it is not even necessary to have a solution that applies to arbitrary states. Since the evolution of an initially pure state into a mixed one occurs on a rather long time scale, the states that appear in experiments are - though not exactly pure - at least *quasi-pure*, *i.e.* they have one single eigenvalue μ_1 that is much larger than all the other ones. In order to provide a means to investigate the problems posed above, we derive an analytic approximation of concurrence for such quasi-pure states in the present chapter. This approximation will allow to efficiently characterise non-classical correlations that arise in most of the currently performed experiments.

The elements of $\mathcal{A}$ defined in eqs. (3.16) and (3.18) obey the proportionality relation

$$\mathcal{A}_{jk}^{lm} \sim \sqrt{\mu_j \mu_k \mu_l \mu_m} \ , \tag{3.56}$$

where the μ_i are the eigenvalues of the considered state ϱ. Consequently,

we can classify the elements of $\mathcal{A}$ according to their relative magnitude determined by the eigenvalues μ_j. This classification will serve as a basis for the approximate evaluation of concurrence in our subsequent treatment.

The above proportionality leads to a natural order of the elements of $\mathcal{A}$, in terms of powers of square roots of the real eigenvalues μ_i of ϱ, which we assume to be numbered in decreasing order, *i.e.* $\mu_1 \gg \mu_2 \geq \ldots \geq \mu_n$. Hence, if we consider terms proportional to either one of the μ_j, with $j \geq 2$, as perturbations of the dominant term $\mathcal{A}^{ii}_{ii} \sim \mu_1^2$, we obtain the following classification:

- the element $\mathcal{A}^{1,1}_{1,1}$ is lowest order,
- all elements with one index different from 1, *i.e.* $\mathcal{A}^{1,1}_{j,1}$, $\mathcal{A}^{1,1}_{1,j}$, $\mathcal{A}^{j,1}_{1,1}$ and $\mathcal{A}^{1,j}_{1,1}$, are first order, and
- elements with two indices different from 1, alike $\mathcal{A}^{1,1}_{j,k}$ or $\mathcal{A}^{k,1}_{j,1}$, are second order.

Yet, this classification is not yet a sufficient basis for our approximation. In fact, the element $\mathcal{A}^{1,1}_{1,1}$ is lowest order, though still it could vanish. This is the case if and only if the eigenstate $|\psi_1\rangle$ to the largest eigenvalue μ_1 of ϱ is separable, since A^{ii}_{ii} is the square of the concurrence of $|\psi_1\rangle$ - see eqs. (3.13) and (3.16). Therefore, as a requirement additional to quasi-purity we have to impose that $|\psi_1\rangle$ be entangled. Since the desired approximation is supposed to be applied to states that occur in the experiments mentioned above, this is not too stringent a restriction - if an ideal experiment without any environment coupling led to a pure state with non-negligible entanglement, it is reasonable to assume that the eigenstate $|\psi_1\rangle$ to this largest eigenvalue μ_1 of ϱ is not separable either.

We wish to approximate $\mathcal{A}$ by a matrix product

$$\mathcal{A}^{lm}_{jk} \simeq \mathcal{T}_{jk}\mathcal{T}^*_{lm} \,, \tag{3.57}$$

with a complex symmetric matrix $\mathcal{T} \in \mathbb{C}^{n\times n}$. Such replacement allows for an analytic solution, since the sum over α in eq. (3.34) reduces to a single term, and the analytic expression for the infimum derived in chapter 2.3.1 can be employed.

Considering eq. (3.57) for the lowest order term $\mathcal{A}^{11}_{11}$, one obtains $\mathcal{T}_{11} = \sqrt{\mathcal{A}^{11}_{11}}\exp(i\varphi)$, where $\exp(i\varphi)$ is an arbitrary phase - which we set equal to unity for convenience. In the next step, we evaluate eq. (3.57) for the first order elements. Together with the already determined value of $\mathcal{T}_{11}$, this leads to $\mathcal{T}_{j1} = \mathcal{A}^{11}_{j1}/\sqrt{\mathcal{A}^{11}_{11}}$. Now there is still the freedom to fix $\mathcal{T}_{jk}$ for $j,k \neq 1$. For this purpose we use eq. (3.57) for $\mathcal{A}^{11}_{jk}$, which leads to $\mathcal{T}_{jk} = \mathcal{A}^{11}_{jk}/\sqrt{\mathcal{A}^{11}_{11}}$, such that $\mathcal{T}$ reads

$$\mathcal{T}_{jk} = \frac{\mathcal{A}^{11}_{jk}}{\sqrt{\mathcal{A}^{11}_{11}}} \,. \tag{3.58}$$

With this choice of $\mathcal{T}$, eq. (3.57) is exact in lowest and first order, and - in addition - the second order elements $\mathcal{A}^{11}_{jk}$ are taken into account correctly. Note that, using only one single matrix $\mathcal{T}$, it is not possible to describe accurately *all* second order elements, as for example $\mathcal{A}^{k1}_{j1}$. All terms of third and fourth order are dropped in our approximation.

Since we were assuming $|\psi_1\rangle$ to be entangled, *i.e.* $\mathcal{A}^{1,1}_{1,1}$ finite by virtue of eq. (3.13), $\mathcal{T}$ is well defined. Approximating $\mathcal{A}$ in terms of this matrix $\mathcal{T}$, eq. (3.15) can be approximated as

$$c(\varrho) \approx c_{\mathrm{qp}}(\varrho) = \inf_V \sum_i \left| \left[V \mathcal{T} V^T \right]^{ii}_{ii} \right| \ , \tag{3.59}$$

following the same steps as in the derivation of eq. (3.34). As formulated in eq. (2.46), the infimum can be expressed in terms of the decreasingly ordered singular values $\mathcal{S}_i$ of $\mathcal{T}$,

$$c_{\mathrm{qp}}(\varrho) = \max\Big(\mathcal{S}_1 - \sum_{i>1} \mathcal{S}_i,\ 0 \Big) \ . \tag{3.60}$$

A priori, it is not clear up to which degree of mixing the quasi-pure approximation provides reliable estimates. The fact that not all second order elements are taken into account may reduce our expectations about a wide range of applicability for this approximation. However, in chapter 4 we will show that for many states the above ansatz provides very good results, even for states with a substantial degree of mixing.

A major advantage of the quasi-pure approximation in comparison with the lower bound presented in chapter 3.4 is that it requires less computational resources, and therefore enables the investigation of larger sets of states, or of states of systems with larger dimensions. Since only second order terms are taken into account in our approximation, only $O(n^2)$ elements of $\mathcal{A}$ have to be evaluated in contrast to $O(n^4)$ elements needed for the computation of $\mathcal{A}$ as given in eq. (3.16). Whereas for the evaluation of the lower bound, eq. (3.48), the matrix B defined in eq. (3.30), of size $n(n-1)/2 \times n(n-1)/2$, has to be diagonalised, the largest matrix to be diagonalised for the quasi-pure approximation is of dimension $n \times n$. Furthermore, the latter requires no numerical optimisation.

A drawback of the quasi-pure approximation is that we do not know whether it is smaller or larger than the exact value - though, the data presented in chapter 4 strongly suggest that the quasi-pure approximation indeed is a lower bound.

3.6 Concurrence in multi-partite systems

In the present chapter, we propose a potential generalisation of our quantitative description of concurrence for systems comprising more than just

two subsystems. In such multi-partite systems, many different kinds of states may appear, such that even for pure states of two-level systems $|\Psi\rangle \in \mathbb{C}^2 \otimes \mathbb{C}^2 \otimes \ldots \otimes \mathbb{C}^2$ more than a single scalar quantity is required for a complete characterisation of all quantum correlations.

In bi-partite systems any state could be prepared with LOCC only, starting with a distinguished, maximally entangled state (see chapter 2.2.2). This is no longer true in multi-partite systems - where inequivalent kinds of multi-partite entanglement exist [67]. Consider for example a *Greenberger-Horne-Zeilinger state* (GHZ-state) [6]

$$|\Psi_{\mathrm{GHZ}}\rangle = \frac{1}{\sqrt{2}}\big(|000\rangle + |111\rangle\big) \;\in\; \mathbb{C}^2 \otimes \mathbb{C}^2 \otimes \mathbb{C}^2 \,, \tag{3.61}$$

and a W-state [67]

$$|\Psi_{\mathrm{W}}\rangle = \frac{1}{\sqrt{3}}\big(|001\rangle + |010\rangle + |100\rangle\big) \;\in\; \mathbb{C}^2 \otimes \mathbb{C}^2 \otimes \mathbb{C}^2 \,. \tag{3.62}$$

Both states contain fundamentally different correlations, such that none of the two can be created from the other one using LOCC alone [67]. Thus, one cannot expect that a single scalar quantity can describe p-particle correlations completely.

Nevertheless, a generalisation of concurrence for multi-partite systems can describe some of the correlations. There is already a generalisation of concurrence [68] for tri-partite two-level systems that characterises all tri-partite correlations of pure states. Here we propose a potential generalisation of concurrence to systems with an arbitrary number of subsystems that even applies to mixed states. So far, we did not yet rigorously prove that our generalisation really is an entanglement monotone for arbitrary multi-partite systems. However, the formal analogies with the bipartite case are rather suggestive that it really is one.

Favourably, our *multi-partite concurrence* C satisfies all formal equivalences with regular bipartite concurrence, required for the application of the hitherto derived theory, *i.e.* it defines a positive tensor $\mathcal{A}$ with the symmetries of eq. (3.17). Thus, its value can be confined by the upper and lower bounds derived in chapters 3.3 and 3.4, and it can be approximated by the quasi-pure approximation of chapter 3.5. In some cases of multi-partite two-level systems its value can even be determined by purely algebraic means, as we will see in a specific case treated below.

Concurrence as defined in eq. (3.8) or eq. (3.9) does not have an immediate generalisation to multi-partite systems. However, eq. (3.24) is rather suggestive for a generalisation. Just consider a linear map $\mathcal{A}$ on $\big(\mathcal{H}_1 \otimes \mathcal{H}_1\big) \otimes \cdots \otimes \big(\mathcal{H}_p \otimes \mathcal{H}_p\big)$ with the following elements in some arbitrary

product basis:

$$\mathcal{A}^{c\gamma\ldots C\ d\delta\ldots D}_{a\alpha\ldots A\ b\beta\ldots B} = \big(\delta_{ac}\delta_{bd} - \delta_{ad}\delta_{bc}\big)\big(\delta_{\alpha\gamma}\delta_{\beta\delta} - \delta_{\alpha\delta}\delta_{\beta\gamma}\big)\ldots\big(\delta_{AC}\delta_{BD} - \delta_{AD}\delta_{BC}\big)\ . \tag{3.63}$$

The corresponding multi-partite concurrence C of a pure state $|\psi\rangle$, *i.e.* the square root of an element alike $\mathcal{A}^{ii}_{ii}$, can easily be expressed in terms of partial traces

$$\begin{aligned} C^2(\psi) \;&=\; \mathrm{Tr}_{1\ldots p}\left(|\psi\rangle\langle\psi|\right)^2 \\ &-\; \mathrm{Tr}_{1\ldots p-1}\left(\mathrm{Tr}_p|\psi\rangle\langle\psi|\right)^2 - \ldots - \mathrm{Tr}_{2\ldots p}\left(\mathrm{Tr}_1|\psi\rangle\langle\psi|\right)^2 \\ &+\; \mathrm{Tr}_{1\ldots p-2}\left(\mathrm{Tr}_{p-1\ p}|\psi\rangle\langle\psi|\right)^2 + \ldots \\ &-\; \vdots \\ &(-1)^p\ \left(\mathrm{Tr}_{1\ldots p}|\psi\rangle\langle\psi|\right)^2\ . \end{aligned} \tag{3.64}$$

All occuring terms have the structure $\mathrm{Tr}_{\{i\}}\left(\mathrm{Tr}_{\{j\}}|\psi\rangle\langle\psi|\right)^2$, with $\{i\}\cup\{j\} = \{1,\ldots,p\}$. Since $\mathrm{Tr}_{\{i\}}\left(\mathrm{Tr}_{\{j\}}|\psi\rangle\langle\psi|\right)^2 = \mathrm{Tr}_{\{j\}}\left(\mathrm{Tr}_{\{i\}}|\psi\rangle\langle\psi|\right)^2$, all terms cancel each other pairwise for an odd number of subsystems, and C vanishes identically. However, also when we replace some anti-symmetric parts, *e.g.* $\big(\delta_{AC}\delta_{BD}-\delta_{AD}\delta_{BC}\big)$ in eq. (3.63) by the corresponding symmetric expression $\big(\delta_{AC}\delta_{BD}+\delta_{AD}\delta_{BC}\big)$, a suitable tensor $\mathcal{A}$ can be defined. Thus, any combination of symmetric and anti-symmetric terms, with the number of the latter even, defines a multi-partite concurrence C_i. Different multi-partite concurrences C_i are in general independent quantities, and are sensitive to different kinds of correlations. We will illustrate this statement in an example below.

The generalisation of C_i to mixed states, using the concept of convex roofs, directly leads to an expression that is identical to eq. (3.15). Since the symmetries of $\mathcal{A}$ are not changed in its multi-partite generalisation, the theory derived in the chapters 3.3, 3.4 and 3.5 is applicable also in the multi-partite case.

The maximum number of non-vanishing eigenvalues of $\mathcal{A}$ - crucial in particular for the lower bound, since it coincides with the maximum number of matrices T^α in eq. (3.47) - is given by $n_1(n_1 \pm 1)/2 \ldots n_p(n_p \pm 1)/2$, where n_i are the dimensions of the subsystems, and the positive sign holds if the considered concurrence is symmetric in the respective subsystem, whereas the negative sign holds in the opposite case. This implies that for mixed states of p-partite two level systems, with p even, the multi-partite concurrence that is anti-symmetric in all subspaces can be evaluated purely algebraically, since it is described by a single matrix T.

To be more specific, we will sketch some properties of the four-partite concurrence $C^{(4)}$ that is anti-symmetric in all subsystems. In the case of

two-level systems, it is a straight forward generalisation of eq. (2.36), namely

$$C^{(4)}(\varrho) = \inf \sum_i \; p_i \; C(\psi_i) \; , \quad \text{with} \quad C^{(4)}(\psi) = \left| \langle \psi^* | \sigma_y^{\otimes 4} | \psi \rangle \right| \; . \tag{3.65}$$

This equivalence can easily be verified by considering the corresponding tensor $\mathcal{A}$ and the matrix $\tau_{ij} = \langle \varphi_i^* | \sigma_y^{\otimes 4} | \varphi_j \rangle$ for a product basis $\{|\varphi_i\rangle\}$. Doing so, one obtains that $\mathcal{A}$ can be expressed as $\mathcal{A}_{jk}^{lm} = \tau_{jk} \tau_{lm}^*$, which proves the equivalence of the concurrence defined with the help of eq. (3.63) and the concurrence given in eq. (3.65).

In the following we will sketch what kind of correlations are classified using the discussed multi-partite concurrence $C^{(4)}$. In this context we will drop the restriction to two-level systems and discuss systems of arbitrary dimensions. Though, we will restrict our discussion to the case of pure states. This however, is no real restriction, since - thanks to the concept of convex roofs, eq. (2.30) - the properties of $C^{(4)}$ concerning pure states directly carry over to mixed states.

The four-partite concurrence $C^{(4)}$ is completely insensitive to bi-separable and tri-separable pure states - *i.e.* it vanishes identically for all states that can be written as a direct product of at least two terms, even if the state does contain a finite amount of entanglement between some of the subsystems. Moreover, there are also states with real four-partite correlations that lead to a vanishing multi-partite concurrence $C^{(4)}$ - consider for example the generalisation

$$\sqrt{\alpha_1} \, | \, \psi_1 0 \, 0 \, 0 \rangle + \sqrt{\alpha_2} \, | \, 0 \, \psi_2 \, 0 \, 0 \rangle + \sqrt{\alpha_3} \, | \, 0 \, 0 \, \psi_3 \, 0 \rangle + \sqrt{\alpha_4} \, | \, 0 \, 0 \, 0 \, \psi_4 \rangle \tag{3.66}$$

of a W-state, where the $|\psi_i\rangle$ $(i = 1, \ldots, 4)$ are arbitrary states of the respective single subsystems. For such a state, $C^{(4)}$ vanishes identically. However, for a generalisation of a GHZ-state

$$|\Psi_{\text{GHZ}}\rangle = \sum_i \sqrt{\alpha_i} \, | i \, i \, i \, i \rangle \; , \tag{3.67}$$

the multi-partite concurrence $C^{(4)}$ may adopt finite values:

$$C^{(4)}(\Psi_{\text{GHZ}}) = 2 \left(\left(\sum_i \alpha_i \right)^2 - \sum_i \alpha_i^2 \right) = 2 \sum_{i \neq j} \alpha_i \alpha_j \; . \tag{3.68}$$

In particular, $C^{(4)}(\Psi_{\text{GHZ}})$ is maximal for equal α_i, and it vanishes if and only if all but one of the pre-factors α_i vanish, *i.e.* if the state is separable. Thus, it turns out that $C^{(4)}$ characterises a special kind of p-partite correlations.

For an intuitive understanding of the various multi-partite concurrences it would be helpful to have a complete characterisation of the correlations that a general multi-partite concurrence can describe. The systematic investigation of all kinds of pure states that is required for the above characterisation could be facilitated by a - still missing - generalisation of the Schmidt decomposition, eq. (2.9), for pure states of arbitrary multi-partite systems. Unless no such complete characterisation is available, it will be difficult to properly interprete the concurrences proposed in this chapter. However, in turn, our concurrences can also be helpful for finding such a characterisation, or for extending the concept of the Schmidt decomposition to multi-partite systems. For example, one can consider two states $|\Psi\rangle$ and $|\Phi\rangle$, and two multi-partite concurrences C_1 and C_2. The two given states necessarily contain qualitatively different kinds of quantum correlations if $C_1(\Psi) > C_1(\Phi)$ and $C_2(\Psi) < C_2(\Phi)$, since both inequalities together imply that none of the two states can be prepared starting from the other one, and using only LOCC. On the other hand, if any multi-partite concurrence coincides for two given states $|\Psi\rangle$ and $|\Phi\rangle$, it is likely that both states are locally equivalent - *i.e.* they are related to each other via a local unitary operation.

Chapter 4

Applications of our theory

In the preceding chapter we have collected a set of operational tools to access the non-classical correlations of arbitrary mixed quantum states of finite dimension - characterised by their concurrence. Our formal treatment spans the entire range from an approximation-free description for the numerical quantification, over lower bounds that can be tightened numerically, to an easily tractable, purely algebraic estimate of the degree of entanglement of a quasi-pure quantum state which is typically dealt with in experiments. However, our approach was largely based on physical intuition, and so far we cannot come up with mathematically precise error bounds. Often, however, the latter are only available in full mathematical rigour under rather restrictive assumptions - whilst we are seeking for robust quantities which, beyond formal consistency, can cope with requirements which stem from real-world experiments.

Therefore, we now have to test our novel tools under realistic conditions, and we will do so by monitoring the time evolution of entanglement - quantified by concurrence - of two families of quantum states under non-vanishing environment coupling - *i.e.* in the presence of decoherence. These two families are states emerging from random time evolutions, and states describing a real ion trap experiment [20, 59]. The rather excellent performance of our entanglement estimates, in monitoring the time evolution of concurrence over long time scales, for both classes of states, will demonstrate the versatility of our approach.

4.1 Random evolutions

In order to construct some random states, we consider a bipartite system and a third system serving as environment. The bipartite system is initially prepared in a maximally entangled pure state $1/\sqrt{d}\sum_{i=1}^{d}|ii\rangle$, *i.e.* it is not entangled with the environment. Then we apply some random unitary

evolution

$$\mathcal{U}_{\rm se}(t) = \exp(i(\alpha_{\rm se}H_{\rm se} + \alpha_{\rm s}H_{\rm s} \otimes \mathbb{1}_e)t) \tag{4.1}$$

with a randomly chosen hermitian matrix $H_{\rm se}$ acting on the entire system including the environment, and a second randomly chosen hermitian matrix $H_{\rm s}$ acting only on the bipartite system, but not on the environment. All elements of $H_{\rm se}$ and $H_{\rm s}$ are determined independently under the constraint of hermiticity. Any real entry is obtained as $\sin(r)$, with a random integer r, where the a priori probability is the same for any integer $0 \leq r < 10^{15}$ [69].

Tracing out the environment leads to a mixed state of the bipartite system. The second hermitian matrix $H_{\rm s}$ in particular describes the interaction between the subsystems of the bipartite system. This interaction does not change the mixing of the bipartite system state, however it can change its entanglement. The constant real parameters $\alpha_{\rm se}$ and $\alpha_{\rm s}$ allow to fix a certain behaviour of the system dynamics. The parameter $\alpha_{\rm se}$ fixes the strength of the system-environment interaction and therefore characterises the order of magnitude for the increase of mixing of the system state, whereas $\alpha_{\rm s}$ specifies the time-scale of a unitary evolution that causes a repeated de- and increase of concurrence.

In the following we will discuss the time evolution of concurrence of states obtained that way, as a function of the scaled time $\alpha_{\rm se}t$, for different values of $\alpha_{\rm se}$ and $\alpha_{\rm s} = 10^{-6}$. The degree of mixing of ϱ will be characterised by the von Neumann entropy $S = -{\rm Tr}\varrho\ln\varrho$ of the system state. In addition, we also monitor the time evolution of the largest eigenvalue of ϱ, because of its close connection to the initial assumptions for the derivation of the quasi-pure approximation (chapter 3.5).

The upper panels in figs. 4.1 and 4.2 show upper (eq. (3.35), solid line) and lower (eq. (3.48), dashed line) bounds of concurrence, together with concurrence in quasi-pure approximation (eq. (3.59), dotted line) for two different random time evolutions. The interaction hamiltonians $H_{\rm se}$ and $H_{\rm s}$ are the same in both cases, but the coupling constant $\alpha_{\rm se}$ in fig. 4.2 is larger by a factor 5 as compared to its value $\alpha_{\rm se} = 10^{-8}$ in fig. 4.1. Therefore, mixing increases slower in fig. 4.1 than in fig. 4.2. The degree of mixing is characterised by both the largest eigenvalue of ϱ, depicted by a double-dot-dashed line, and the von Neumann entropy of ϱ, indicated by a dash-dotted line.

Concurrence in quasi-pure approximation can not always be distinguished from the optimised lower bound in the upper panels. Therefore the difference of these two quantities is depicted in the lower panels with a solid line. Also the difference of the numerically optimised lower bound and the best algebraic bound (dashed line) is plotted. Over almost the entire time interval displayed in fig. 4.1 and for short times in fig. 4.2, where mixing is not too large, both differences are about two orders of magnitude smaller

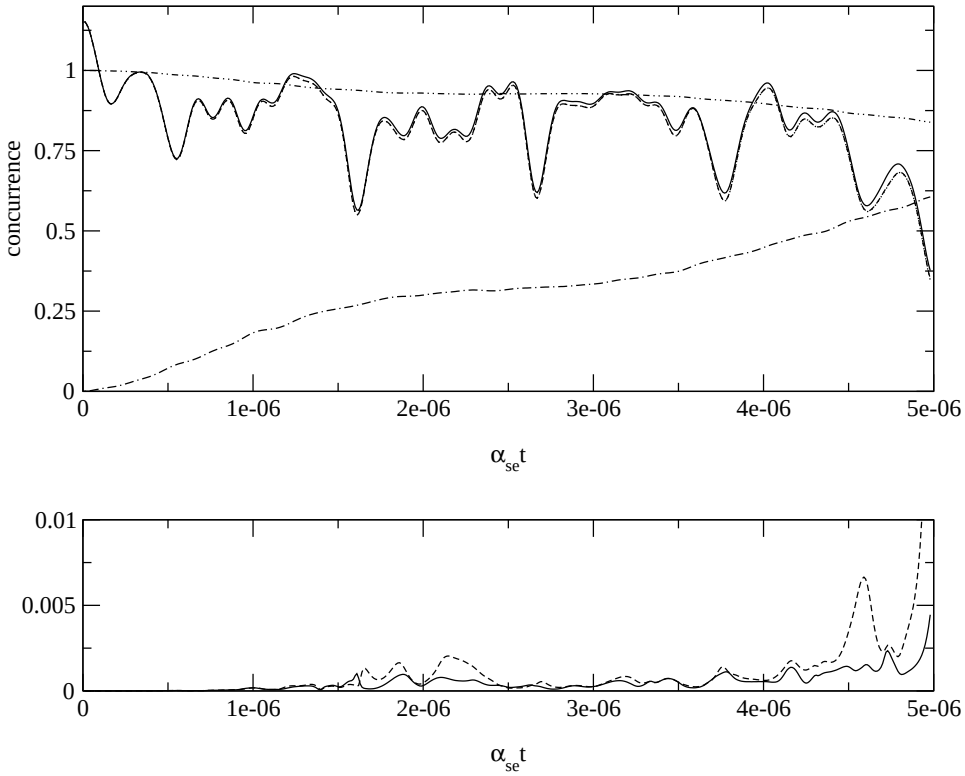

Figure 4.1: Top panel: Upper bound (eq. (3.35), solid line) and numerically optimised lower bound (eq. (3.48), dashed line) of concurrence of a 3×3 state vs. scaled time $\alpha_{\rm se}t$. The state ϱ is initially prepared as maximally entangled, with concurrence $c = 2/\sqrt{3}$. Then it is subject to a randomly chosen time evolution with $\alpha_{\rm se} = 10^{-8}$, leading to a finite degree of mixing. The difference between upper and lower bound allows for a rather tight estimate of concurrence. The relevant parameters characterising the state ϱ are its largest eigenvalue (double-dot-dashed line) and its von Neumann entropy (dash-dotted line). The differences of the optimised bound and the quasi-pure approximation, eq. (3.59), and between the optimised lower bound and the best algebraic lower bound, eq. (3.49)), are indicated in the lower plot, by the solid and the dashed line, respectively.

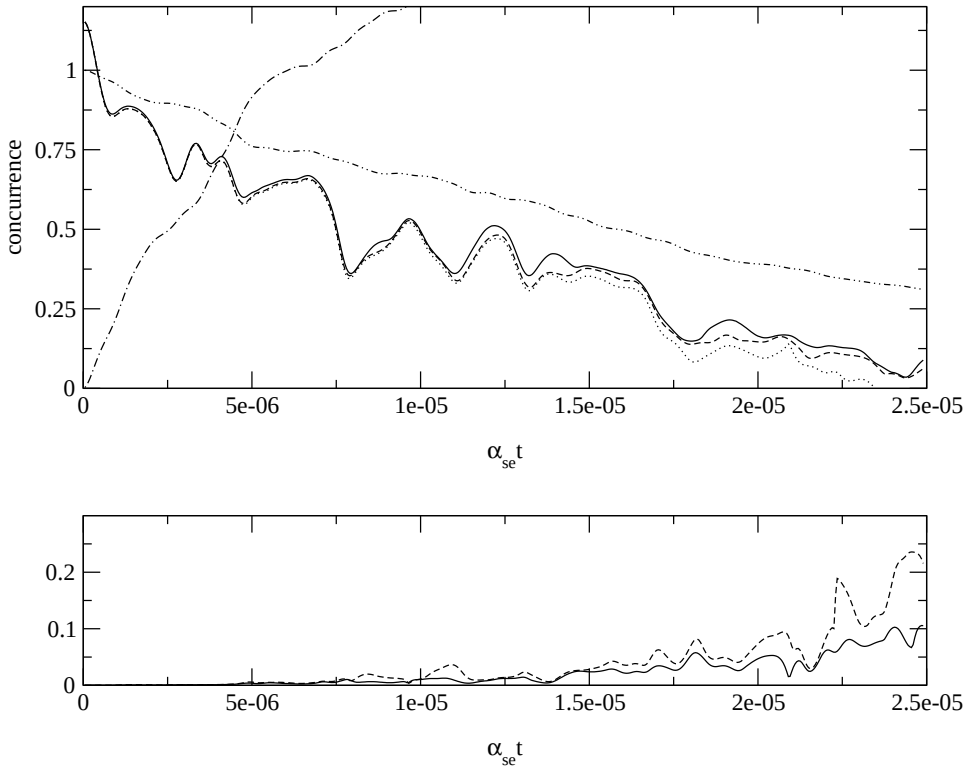

Figure 4.2: Top panel: Upper bound (eq. (3.35), solid line), numerically optimised lower bound (eq. (3.48), dashed line), and concurrence in quasi-pure approximation (eq. (3.59), dotted line), for a 3×3 state subject to a random time evolution. As in fig. 4.1 the state was initially prepared as maximally entangled. However, due to a larger environment coupling ($\alpha_{\rm se} = 5\ 10^{-8}$) mixing occurs faster than in fig. 4.1. Whereas the difference between upper and lower bound is hardly discernible in fig. 4.1, it becomes visible in the present case. With increasing degree of mixing even the difference between the lower bound and the quasi-pure approximation (bottom panel, solid line) becomes apparent. Yet, even for a rather large degree of mixing and almost vanishing concurrence, upper and lower bound still allow for a reliable estimation of concurrence. Also the quasi-pure approximation (discrepancy with respect to the optimised lower bound indicated by the dashed line in the lower plot) provides a satisfactory approximation of concurrence

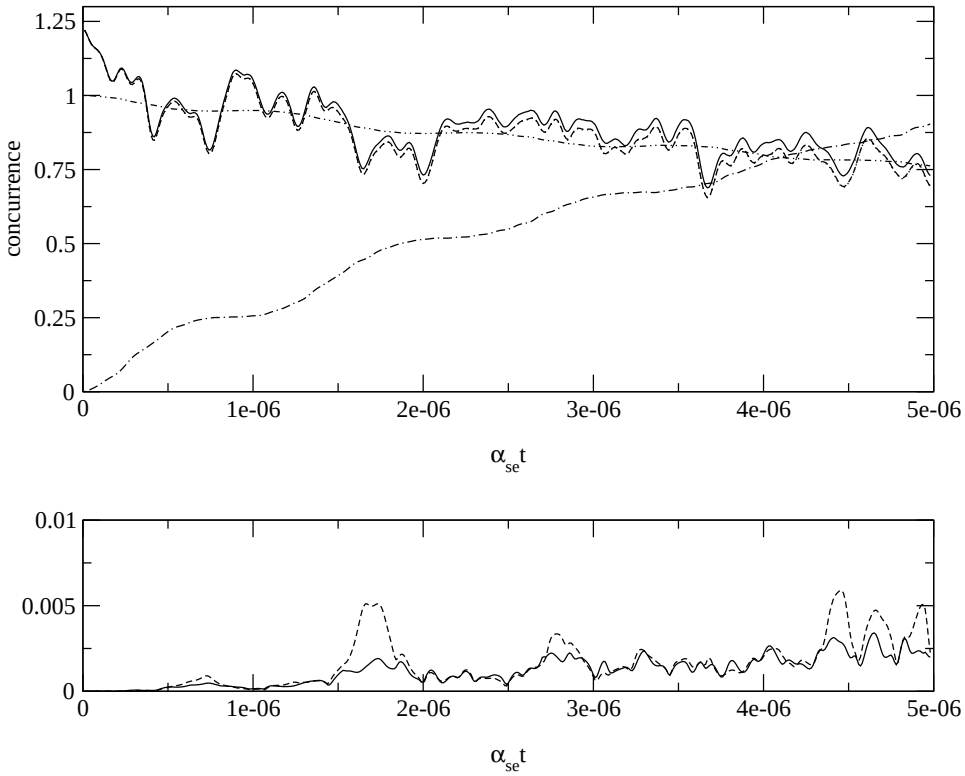

Figure 4.3: Top panel: Upper bound (eq. (3.35), solid line) and lower bound (eq. (3.48), dashed line) for an initially maximally entangled 4×4 state and subject to a random time evolution with $\alpha_{\rm se} = 10^{-8}$. The double-dot-dashed line shows the largest eigenvalue of the state, the dash-dotted line its von Neumann entropy. The differences between optimised lower bound and concurrence in quasi-pure approximation, eq. (3.59), as well as the difference of optimised lower bound and best algebraic bound, eq. (3.49), are shown in the lower graph, by the solid and the dashed line, respectively.

than concurrence itself. Only for states with rather small concurrence and a large degree of mixing there is a significant difference between the two lower bounds and between the bounds and the quasi-pure approximation. It is remarkable that both in fig. 4.1 as well as in fig. 4.2 the quasi-pure approximation of concurrence is always smaller than the optimised lower bound. Since this will also be observed in figs. 4.3, 4.4 and 4.5, we conjecture that the quasi-pure approximation indeed is a lower bound of concurrence.

Fig 4.3 shows a similar plot as the preceding ones for a 4×4 system. Environment coupling is determined by $\alpha_{\rm se} = 10^{-8}$, such that the degree of mixing remains moderate during the entire time evolution, as indicated by the von Neumann entropy (dash-dotted line) and the largest eigenvalue of ϱ (double-dot-dashed line). Upper (eq. (3.35), solid line) and lower bound (eq. (3.48), dashed line) define a rather narrow interval that allows for a reliable estimate of concurrence. Both concurrence in quasi-pure approximation, eq. (3.59), and the best algebraic lower bound, eq. (3.49), can hardly be distinguished from the numerically optimised lower bound, eq. (3.48), in the upper plot of fig. 4.3. Therefore, the difference of optimised, eq. (3.48), and algebraic bound (eq. (3.49), solid line), as well as the difference of optimised bound and quasi-pure approximation of concurrence (eq. (3.59), dashed line) are once again plotted in the lower graph of fig. 4.3.

The upper panels of figs. 4.4 and 4.5 show upper and lower bounds for the concurrence of a 2×4 system. The initially maximally entangled states acquire some finite mixing due to a randomly chosen time evolution. The increase of mixing in fig. 4.5 is faster ($\alpha_{\rm se} = 5\ 10^{-8}$) than that in fig. 4.4 ($\alpha_{\rm se} = 10^{-8}$). In both plots, upper and lower bound allow for a rather precise quantification of concurrence. In the lower plot of fig. 4.4 the difference of the numerically optimised lower bound and concurrence in quasi-pure approximation (solid line) is about three orders of magnitude smaller than the actual value of concurrence. The difference of optimised lower bound and the best algebraic lower bound (dashed line) is of a comparable size during nearly the entire time evolution. Only during a rather short interval where concurrence exhibits a dip, ($\alpha_{\rm se} \simeq 3 \cdot 10^{-6}$), this difference increases to about one percent of the actual value of concurrence. Nonetheless, even then the algebraic lower bound provides a rather tight interval together with the upper bound.

In fig. 4.5 these differences grow larger with increasing degree of mixing of ϱ. However, during the entire time evolution, upper and lower bound provide a satisfactory estimate of concurrence. Again, the quasi-pure approximation gives a rather good estimate of concurrence, albeit the states hardly satisfy the requirements for the approximation in a major part of the considered time interval.

For all random states considered above, the difference between upper and lower bound was small enough to quantify concurrence satisfactorily. There

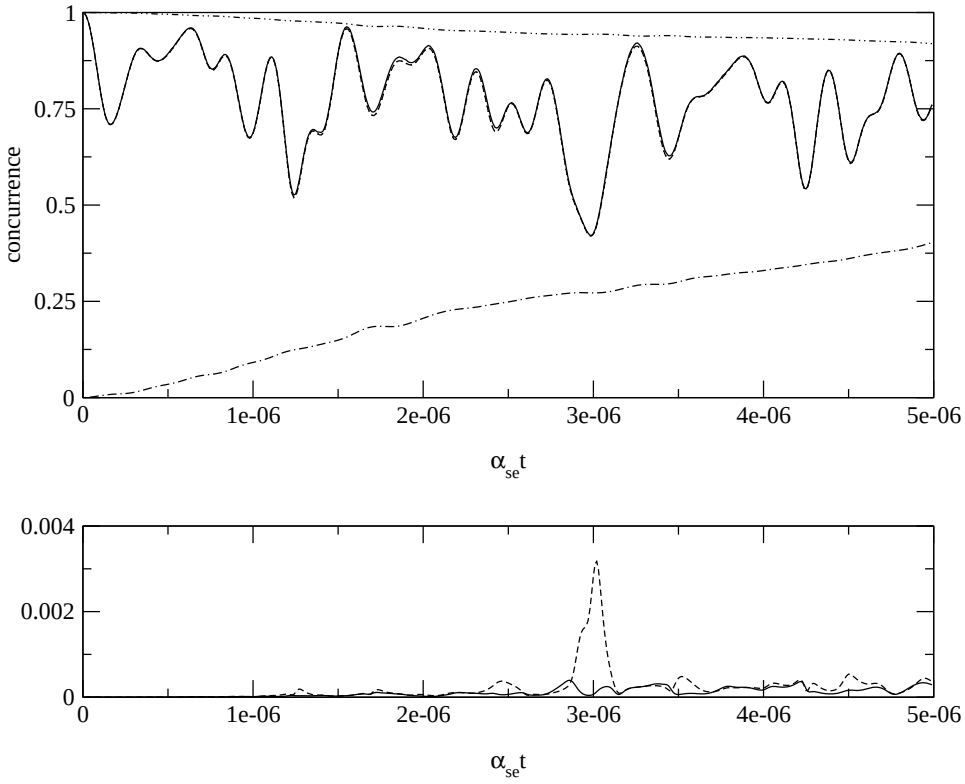

Figure 4.4: Top panel: Upper bound (eq. (3.35), solid line) and lower bound (eq. (3.48), dashed line) for a initially maximally entangled 2×4 state, subject to a random time evolution with $\alpha_{\rm se} = 10^{-8}$. Upper and lower bounds are hardly discernible. The double-dot-dashed line shows the largest eigenvalue of ϱ, whereas the dash-dotted line indicates its von Neumann entropy. In the lower panel, the difference of lower bound and concurrence in quasi-pure approximation, eq. (3.59) together with the difference between the optimised lower bound and best algebraic lower bound, eq. (3.49), is plotted, by the solid and the dashed line, respectively.

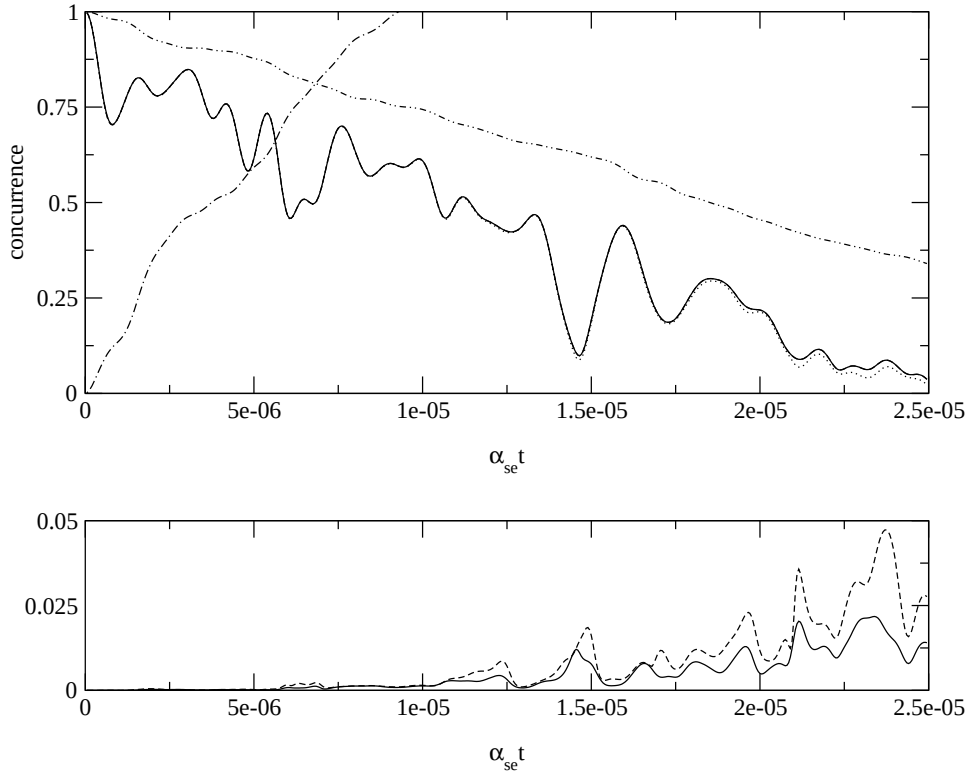

Figure 4.5: Top panel: upper bound (eq. (3.35), solid line), lower bound (eq. (3.48), dashed line), and concurrence in quasi-pure approximation (eq. (3.59), dotted line) for a initially maximally entangled 2×4 state. The random time evolution with $\alpha_{\rm se} = 5 \cdot 10^{-8}$ leads to a faster increase of mixing as compared to fig 4.4. Notwithstanding, upper and lower bound provide a rather tight estimation of concurrence during the entire evolution. The quasi-pure approximation provides a reliable measure of concurrence over the entire evolution, albeit its formal conditions of validity are certainly not fulfilled any more for large times, in the present example. The differences between the numerically optimised lower bound and the quasi-pure approximation, and between the optimised lower bound and the best algebraic bound, eq. (3.49), are plotted in the lower graph, as solid and dashed lines, respectively.

is a clear tendency that the interval grows with decreasing concurrence and increasing degree of mixing. The quasi-pure approximation provides a good estimation of concurrence even for rather strongly mixed states. For states with a moderate degree of mixing concurrence in quasi-pure approximation nearly coincides with the numerically optimised lower bound. In general the quasi-pure approximation seems not to exceed the optimised lower bound.

The temporal effort required to generate the data shown in figs. 4.1 - 4.5 differs significantly for the different quantities. The fastest is the quasi-pure approximation - only a few seconds are required for one run with 500 states, on the time series. The construction of the matrices T^α required for the gradient, eq. (3.40), and the lower bound, eq. (3.47), needs a few minutes for one run. Once the matrices T^α are constructed, the optimised lower bound, eq. (3.48), is obtained in another few seconds. As mentioned above in the discussion following eq. (3.43) and in figs. 3.1 and 3.2, a perfect convergence of the gradient procedure can be hard to achieve and requires a rather small step size. However, even if the procedure does not converge completely, it gives a good estimate of the actual value of concurrence. Though - even if one is satisfied with incomplete convergence - the temporal effort is significantly larger than that required for the evaluation of the quasi-pure approximation and the lower bound. Depending on the degree of mixing and the dimensions of the system, a run with 500 time steps took a couple of hours or even a few days, as for example in the case of fig. 4.2.

4.2 Trapped ions

One of the most prominent experimental systems used for the investigation of entangled states are ions stored in a linear Paul trap [70]. Such traps provide experimental means of trapping charged particles and manipulating individual ions coherently with lasers, such that arbitrary bi- and multi-partite states can be prepared and investigated. Trapped ions are isolated from environmental influences to a certain extent. However, due to their finite charge, they are sensitive to thermal electromagnetic fields. Therefore, the preparation of entangled states cannot be expected to work perfectly. In chapters 4.2.1 and 4.2.2 we will therefore investigate how a finite environment coupling influences the generation of quantum correlations - characterised by the theoretical tools developed above.

In a Paul trap, ions with mass m are stored with the help of an oscillating electric quadrupole field that - in the long time average - acts as a three-dimensional, attractive trapping potential which is harmonic in very good approximation,

$$V = \frac{1}{2} m \left(\omega_x^2 x^2 + \omega_y^2 y^2 + \omega_z^2 z^2 \right) . \tag{4.2}$$

The amplitude and frequency of the oscillating quadrupole field can be chosen such that the *trap frequency* ω_z is small compared to ω_x and ω_y. Accordingly, the z-axis is called the *trap axis*. The ions are confined in the trapping potential, though repel each other by their mutual coulomb repulsion. Due to this interaction the motion of different ions is coupled, such that the ions perform collective oscillations. If the trap frequency ω_z does not exceed a certain threshold value, the ions line up in a linear chain along the trap axis, such that the motion along the trap axis is independent of that perpendicular to it [70].

A well controllable, state-sensitive interaction between the ions is required in order to prepare arbitrary states. The Coulomb interaction is not viable for this purpose, since it is independent of the internal electronic states of the ions. Dipole-dipole interaction is state sensitive, however, the distance between neighbouring ions is too large for this interaction to be significant. Thus, some further means has to be found that enables the preparation of arbitrary electronic states of the ions. In the following, we will sketch how a state sensitive interaction between two or more ions can be engineered with the help of lasers and collective oscillations.

For p stored ions, there are p different collective oscillatory modes called *phonon modes* [70]. However, only one of the phonon modes is used for the scheme of preparing entangled states that we will focus on. Since the state of all the other modes remains unchanged, and since the phonon modes are non-interacting as long as the trapping potential is harmonic, we can restrict our considerations to just one single mode. In addition, the electronic structure of each ion will be mimicked by a two-level system.

In order to manipulate the states of the ions, they are illuminated with coherent electromagnetic radiation. The Hamiltonian H_I describing the interaction between the driving field and the ions reads

$$H_I = \sum_i \hbar\Omega_R(\vec{r}_i)(\sigma_+^i + \sigma_-^i)\cos(\vec{k}\vec{r}_i - \nu t) \ , \tag{4.3}$$

where $\Omega_R(\vec{r}_i)$ is the Rabi frequency at the position $\vec{r}_i$ of the i-th ion. The driving field, with space and time dependence $\cos(\vec{k}\vec{r}_i - \nu t)$, couples to an ion via its *dipole operator* $(\sigma_+^i + \sigma_-^i)$, where σ_+^i and σ_-^i are the raising and lowering operators acting on the two-level system that represents the ion i.

Illuminating an ion can lead to several transitions. During a *carrier transition*, the state of the phonon mode remains unchanged, whereas during a *sideband transition* one *phonon* is created or annihilated. A sideband transition with a resonance frequency that exceeds that of the carrier frequency by an integer multiple of one phonon frequency is called *blue sideband* transition. The resonance frequency of a *red sideband* is smaller than that of the carrier transition by an integer multiple of a phonon frequency.

The matrix element that describes a carrier transition is proportional to Ω_R - that of a sideband transition is proportional to $\eta^l\Omega_R$, where the

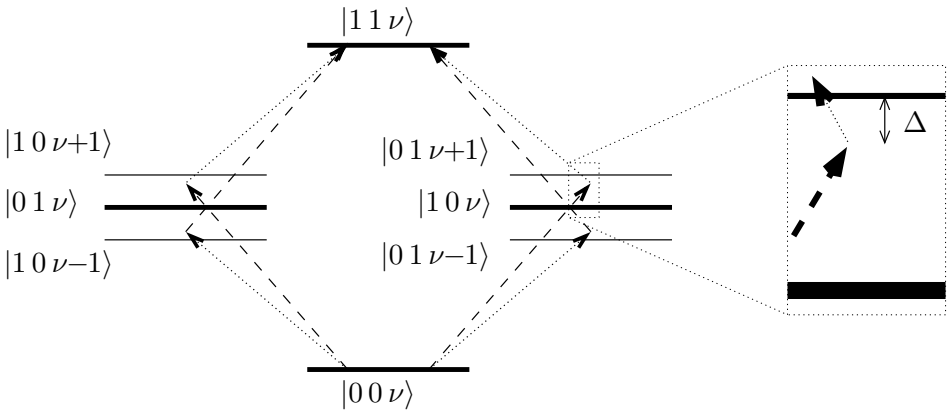

Figure 4.6: Illustration of a scheme for creating a maximally entangled state $(|0\,0\rangle{+}i|1\,1\rangle)/\sqrt{2}$. Two ions are illuminated simultaneously with two electromagnetic fields. One (dashed arrows) is red detuned with respect to the blue sideband with detuning Δ. The second one (dotted arrows) is blue detuned with respect to the red sideband. Both sideband transitions are not driven resonantly, however the two photon process $|0\,0\rangle \leftrightarrow |1\,1\rangle$ is resonant, since the absolute value of the detunings of both transitions coincide. Thus, starting with the initial state $|0\,0\rangle$, one can create a coherent superposition of the states $|0\,0\rangle$ and $|1\,1\rangle$.

Lamb Dicke parameter $\eta = \sqrt{\hbar k^2/(2m\omega_z)}$ [19] is the ratio of the driving field's wavelength and a mean oscillator displacement, and the integer l counts the number of created or annihilated phonons. The experiments we are interested in are usually performed in a parameter regime where η is significantly smaller than one. Since a sideband transition of l-th order is suppressed by the factor η^l, sideband transitions of an order higher than first, where two or more phonons are created or annihilated, can be neglected in this regime.

Many schemes that provide a state-dependent interaction between two ions require the phonon-mode to be cooled to the ground state [17]. Here we follow an approach that imposes less severe restrictions to the phonon state and also works for thermal distributions [20].

In particular, this scheme allows for the preparation of arbitrary multipartite states. In general a sequence of different laser pulses is required for the preparation of an arbitrary state. Though, Greenberger-Horne-Zeilinger (GHZ) states [6]

$$|\Psi_{\mathrm{GHZ}}\rangle = \frac{1}{\sqrt{2}}\left(|0\ldots0\rangle + e^{i\varphi}|1\ldots1\rangle\right) \tag{4.4}$$

can be prepared with only two pulses that are applied simultaneously. In order to create such GHZ-states, all ions are initially prepared in a separable pure state. Which state is required depends on the number of ions. Then

all ions are illuminated simultaneously with two electromagnetic fields. One is red detuned with respect to the blue sideband transition, *i.e.* the field frequency is a little smaller than the resonance frequency of the blue sideband transition. The second field is blue detuned with respect to the red sideband. The absolute value of the *detuning* Δ, *i.e.* the difference of field frequency and transition frequency is the same in both cases, as indicated in fig. 4.6 for the case of two ions.

Due to the finite detuning Δ, the probability for a one-photon process, *e.g.* $|0\,0\,\nu\rangle \leftrightarrow |0\,1\,\nu{\pm}1\rangle$ is small. However, the two-photon process $|0\,0\rangle \leftrightarrow |1\,1\rangle$ is resonant, such that a coherent superposition of the states $|0\,0\rangle$ and $|1\,1\rangle$ can be created. When both of these two states have the same weight, a state with the structure defined in eq. (4.4) is realised.

The same scheme can be applied for any number of trapped ions - here we will sketch it for three and four ions - the generalisation for more ions is then straightforward.

Since the state of two ions is changed simultaneously in the described two photon process, the three-ion-state $|0\,0\,0\rangle$ can never evolve into $|1\,1\,1\rangle$. Therefore, each ion has to be prepared in a coherent superposition of its ground state $|0\rangle$ and its excited state $|1\rangle$, such that the initial, separable three ion state reads $((|0\rangle + |1\rangle)/\sqrt{2})^{\otimes 3}$. Fig. 4.7 shows the corresponding level scheme for three trapped ions together with the light-induced transitions that lead to the generation of the final state $(|0\,0\,0\rangle + |1\,1\,1\rangle)/\sqrt{2}$.

In the case of four ions, the initially prepared, separable state reads $|0\,0\,0\,0\rangle$. During one two-photon process, this state evolves into states alike $|0\,0\,1\,1\rangle$, with two ions exited and the other two in their ground state. In a second process, these states eventually evolve into $|1\,1\,1\,1\rangle$, such that the final state $(|0\,0\,0\,0\rangle - |1\,1\,1\,1\rangle)/\sqrt{2}$ is of the GHZ type of eq. (4.4).

Since the detuning Δ is finite, there remains a finite probability for one-photon processes to occur, and since a phonon is created or annihilated during a one-photon process, the internal states of the ions become correlated with the phonon state while the ions are illuminated. However, at the end of the illumination, all one-photon processes interfere destructively with each other [20], such that finally only the two-photon processes contribute. Since a two-photon process is composed from a red and a blue sideband transition, only virtual phonons are exchanged. Accordingly, the electronic and motional degrees of freedom of the ions are uncorrelated at the end of the preparation scheme. However, during the preparation process they are, what gives rise to an environment coupling that may decrease the success probability of the preparation process.

Choosing proper electronic levels of the ions, decoherence of these levels themselves can be neglected on the timescale of the state preparation. However, the motional degrees of freedom couple to thermal electric fields,

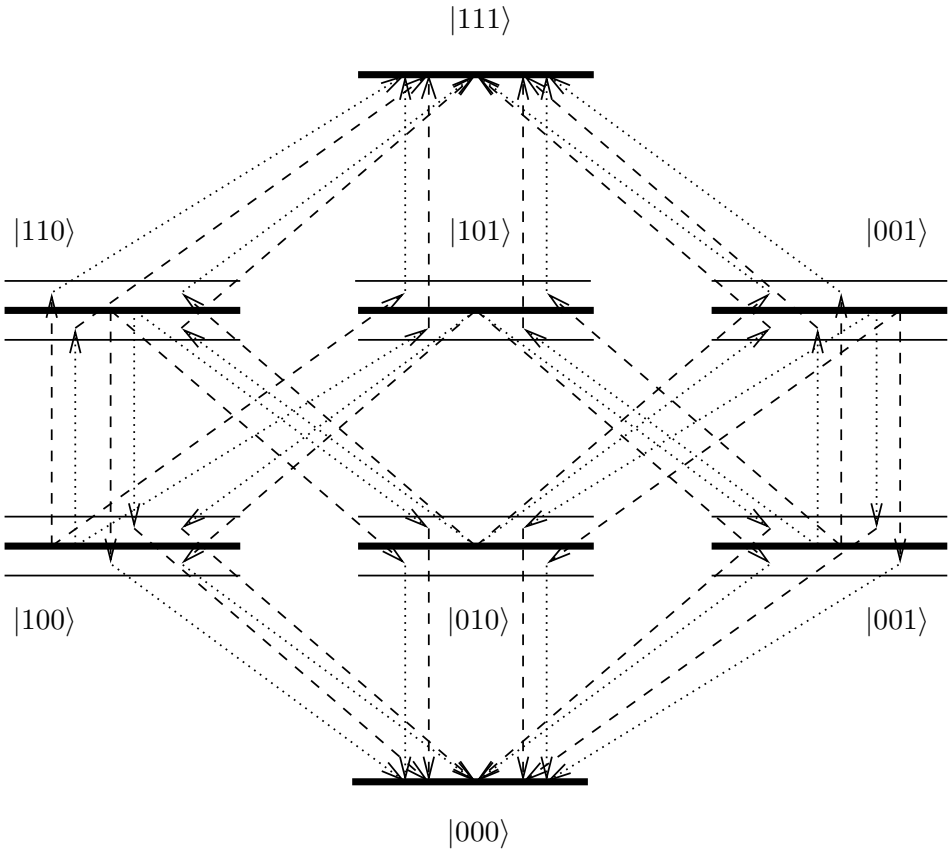

Figure 4.7: The three ion GHZ state $(|0\,0\,0\rangle + |1\,1\,1\rangle)/\sqrt{2}$ can be prepared starting out from the separable state $((|0\rangle + |1\rangle)/\sqrt{2})^{\otimes 3}$. The driven transitions are indicated - the dashed arrows show a transition that is slightly red detuned with respect to the blue sideband, whereas the dotted arrows show a transition that is slightly blue detuned with respect to the red sideband. Neither of these transitions is resonant itself. However, the two photon process composed of both of these transitions is resonant.

since the ions are charged. The interaction between the phonon mode and an environmental field is described by the interaction Hamiltonian $H_{\rm pe}$

$$H_{\rm pe} = \sum_i \hbar\Omega_i \left(a\ b_i^\dagger + a^\dagger b_i\right)\ , \tag{4.5}$$

where a and $a^\dagger$ are the phonon annihilation and creation operators, $b_i^\dagger$ and b_i are the creation and annihilation operators for the different environmental modes, and Ω_i are the corresponding coupling constants.

Since the environmental modes are not observed, only the reduced dynamics of the phonon mode is of interest. Tracing over all environmental degrees of freedom, and performing a Markov limit, one obtains a *master equation* [71],

$$\frac{\partial\varrho}{\partial t} = -\frac{\gamma}{2}(n_t+1)\left(\left[a^\dagger, a\varrho\right] - \left[a, \varrho a^\dagger\right]\right) - \frac{\gamma}{2}n_t\left(\left[a, a^\dagger\varrho\right] - \left[a^\dagger, \varrho a\right]\right)\ , \tag{4.6}$$

that describes the reduced dynamics of the phonon mode. The mean photon number of the environmental field at the phonon frequency is denoted by n_t, and γ is the decay constant. The temperature corresponding to the motional state of the ions is usually small compared to the environment temperature, such that the latter can be assumed to be infinite. *I.e.* one can perform the limit $n_t \to \infty$, keeping the product $\gamma n_t =: \Gamma$ constant. In this limit the above master equation simplifies to

$$\frac{\partial\varrho}{\partial t} = \Gamma\left(a\varrho a^\dagger + a^\dagger\varrho a - (a^\dagger a - \frac{1}{2})\varrho - \varrho(a^\dagger a - \frac{1}{2})\right)\ , \tag{4.7}$$

which implies a linear growth of the phonon occupation number, what is also observed experimentally [72]. This supports the validity of the above limit.

As long as the system state decomposes into a direct product of a state describing the electronic degrees of freedom and a phonon state, any non-unitary dynamics of the phonon mode does not influence the electronic state at all. However, since the electronic and the phonon state are indeed coupled during the preparation process, also the electronic states acquires a finite degree of mixing. Therefore, the preparation of GHZ-states cannot be expected to be perfect, if one assumes a finite environment coupling Γ.

To check upon the quality of the preparation of the GHZ-correlations under non-vanishing environment coupling, we numerically integrated the master equation, eq. (4.7), for several numbers of ions, and for different coupling constants Γ [73]. In the next chapters 4.2.1 and 4.2.2 we will discuss the entanglement properties of the generated states using our theory derived above.

4.2.1 Bipartite correlations

We start with the case of three ions, where we will determine the quantum correlations between one ion and the residual two. Fig. 4.8 shows upper (solid line) and lower bound (dashed line) of concurrence for three different coupling constants Γ. We compare the case of vanishing coupling to the cases of $\Gamma = 2 \cdot 10^{-4}\omega_z$ and $\Gamma = 4 \cdot 10^{-4}\omega_z$, which correspond to realistic values in current laboratory experiments [59]. Even for $\Gamma = 0$, the electronic state of the ions gets mixed, as indicated by the largest eigenvalue (dash-dotted line) and the von Neumann entropy (dotted line) of the state. This is due to a finite occupation of states with a phonon number different than that of the initial state, such that electronic and phonon state do not decompose into a direct product. However, when concurrence is maximal, the phonon state equals the initial phonon state, the electronic state is not correlated with the phonon state at all, and the electronic state is pure. At this moment upper and lower bound coincide exactly.

For different times, and for finite values of Γ, there is a gap between upper and lower bound. Yet, concurrence is still quantified rather precisely. Equally so by the quasi-pure approximation and the best algebraic lower bound, as apparent from the plot of their mismatch with the numerically optimised lower bound in the lower graph of the figure.

During the temporal evolution the mixing in- and decreases, such that there is a finite difference between upper and lower bound of concurrence. Notwithstanding a tendency towards a slight growth of the gap with rising coupling constant Γ, concurrence can be estimated reliably - the difference between the optimised lower bound and concurrence in quasi-pure approximation (solid line), as well as that of the optimised bound and the best algebraic bound (dashed line) are smaller than one percent of the actual value of concurrence. *I.e.* both the algebraic bound and the quasi-pure approximation allow for a good estimation of concurrence for all considered environment couplings.

Thus we can use the quasi-pure approximation to compare the precision of the preparation of quantum correlations for larger numbers of ions. Fig. 4.9 shows the bipartite concurrence that characterises the correlations between one ion and all other stored ions, for total ion numbers 4, 6, and 8, and for environment coupling constants $\Gamma = 1 \cdot 10^{-4}\omega_z$ and $\Gamma = 2 \cdot 10^{-4}\omega_z$. For a given decay rate Γ, the maximally achievable quantum correlations drop with increasing number of ions. This decrease is due to non-resonant sideband transitions that cause some detrimental entanglement between the electronic states and the phonon mode. Though, they are neglected in the idealised scheme. There are transitions of second and higher order - neglecting them is equivalent to assuming η infinitesimally small. Moreover, there are also first order transitions that are not taken into account by performing a rotating wave approximation in the laser-ion interaction, eq. (4.3), [71].

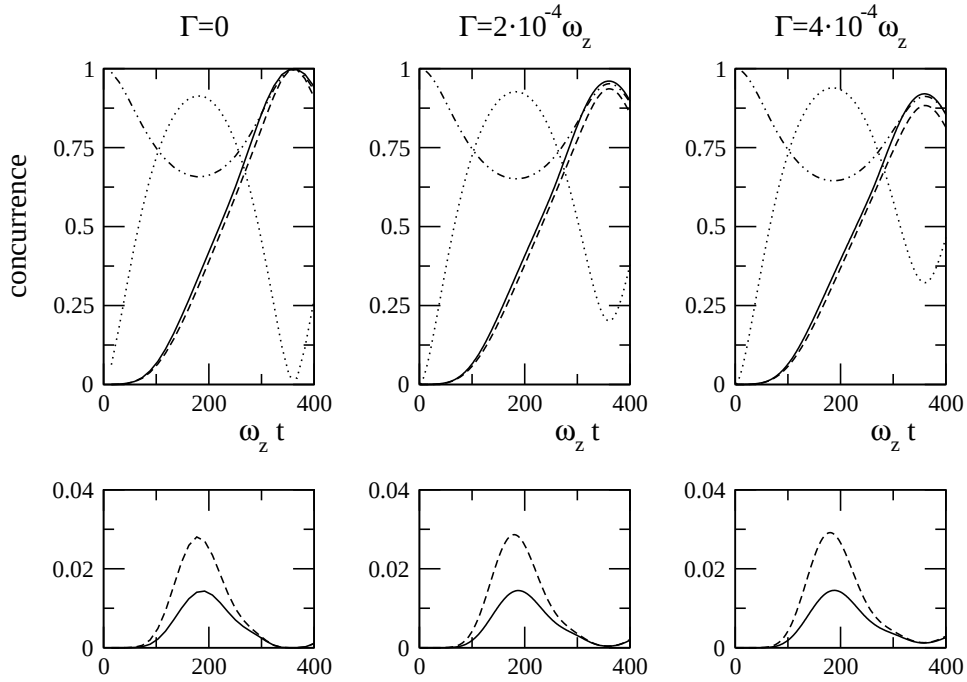

Figure 4.8: Top panel: Upper (eq. (3.35), solid line) and lower bound (eq. (3.48), dashed line) of concurrence, characterising the quantum correlations between one and the other two trapped ions. In the case of vanishing environment coupling, concurrence reaches its ideal value. For finite environment coupling Γ, there is a decrease in the produced entanglement. Even in the case of vanishing Γ the electronic state of the ions gets mixed to a finite degree, as indicated by the largest eigenvalue (dashed-dotted line) and the von Neumann entropy (dotted line) of the electronic states. For non-vanishing environment coupling there is a small difference between upper and lower bound when the maximum concurrence is achieved. However, the gap still allows for a rather precise estimation of concurrence. Both, concurrence in quasi-pure approximation, eq. (3.59), and the best algebraic lower bound, eq. (3.49), are only insignificantly smaller than the optimised lower bound, as apparent from the lower panel, where the corresponding differences are plotted as solid (quasi-pure) and dashed lines (algebraic lower bound), respectively.

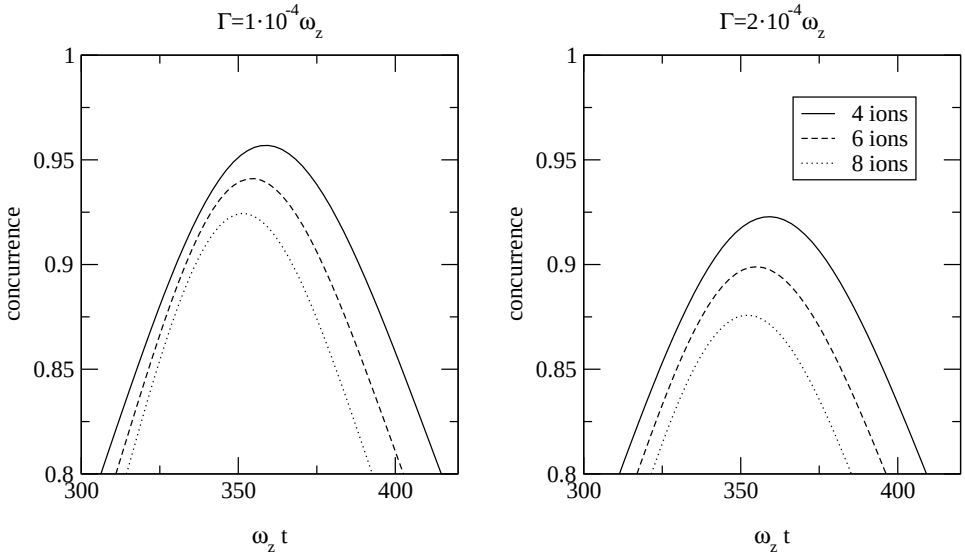

Figure 4.9: Concurrence in quasi-pure approximation, eq. (3.59), for one ion that is entangled by tailored laser pulses (see chapter 4.2) with all other ions stored in a linear Paul trap. We show the cases of 4, 6, and 8 ions, for two different environment coupling constants $\Gamma = 1 \cdot 10^{-4}\omega_z$ and $\Gamma = 2 \cdot 10^{-4}\omega_z$. The maximally achievable correlations decrease with increasing Γ and ion number.

However, our numerical simulations - that include these transitions - show, that they do cause finite errors that lead to the observed decrease of the maximal concurrence. Since the number of such detrimental transitions increases with the number of stored ions, the scalability of the preparation scheme proposed in [71] will crucially depend on the scaling behaviour of the maximally achievable entanglement with the length of the ion chain, at fixed Γ. A detailed study of this behavior is currently under way [73].

4.2.2 Multi-partite correlations

In the previous chapter we were concerned with bipartite correlations in an ion chain, for a specific partition. Here, we will focus on real multi-partite correlations, which we characterise in terms of our multi-partite concurrence C introduced chapter 3.6. Of course, we have to bear in mind that the monotonicity of C under LOCC still has the status of a conjecture - which we are confident, however, to prove in the near future.

The experimental setup we are considering allows to prepare the four-partite state $(|0000\rangle + |1111\rangle)/\sqrt{2}$. The specific kind of correlations contained in such a GHZ-state can be characterised by the multi-partite concurrence $C^{(4)}$ defined in chapter 3.6, as given in eq. (3.65). Since the ions are described as two-level systems, this particular multi-partite concurrence can be computed exactly, and purely algebraically.

Figure 4.10 shows the four-partite GHZ-type correlations as a function of time, for four stored ions, with a typical experimental value [59] of the Lamb-Dicke parameter, $\eta = 0.15$. In contrast to the bipartite correlations shown in fig. 4.8, that take finite values at the very beginning, four-partite correlations start growing only after a finite time. This is due to the fact that, at the beginning of the preparation process, correlations are different from the ones contained in GHZ states as defined in eq. (4.4) - and the multi-partite concurrence considered here is insensitive to such correlations.

However, after a delay of about $160 - 190\ \omega_z t$, depending on Γ, $C^{(4)}$ starts growing towards its maximum, achieved after approx. $360\ \omega_z t$. As expected, $C^{(4)}$ decreases with increasing coupling constant Γ, as depicted for Γ ranging from 0 to $2.5 \cdot 10^{-3}\omega_z$.

Note that, even in the case of vanishing environment coupling (solid line), the correlations are not perfect - $C^{(4)}$ remains smaller than one. This is due to the finite value of the Lamb-Dicke parameter η, giving rise to additional two-photon and higher order processes that cause transitions to levels which are neglected in the derivation [71] of the idealised scheme, and thereby decrease the precision of the preparation process. Though, a comparably pronounced drop of concurrence is not observed for bipartite correlations, as shown in fig. 4.8, where concurrence adopts its ideal value one, for $\Gamma = 0$. We attribute this to a stronger sensitivity of multi-partite correlations as compared to bipartite ones.

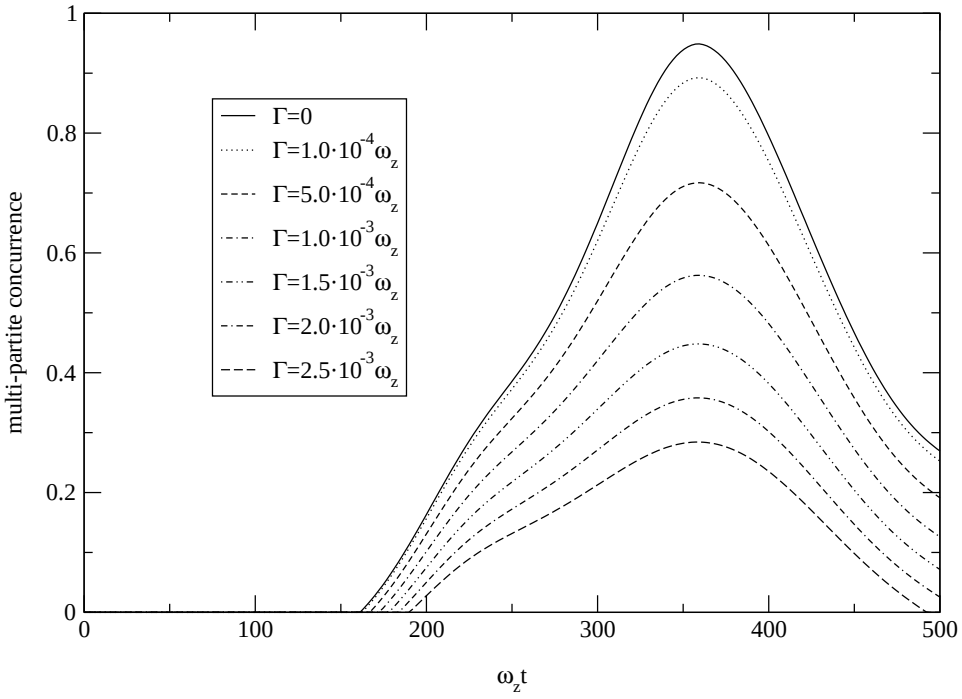

Figure 4.10: Four-particle GHZ-type correlations, eq. (3.65), created in an ion trap with four stored ions. In contrast to the case of bipartite correlations depicted in figure 4.8, non-vanishing four-particle GHZ-type correlations build up only after a finite time. Even in the case without environment coupling ($\Gamma = 0$), no perfect correlations are obtained. Due to the finite Lamb-Dicke parameter ($\eta = 0.15$), there are detrimental non-resonant transitions which are neglected in the idealised picture [71], but which *do* become relevant for realistic experimental parameters. The maximally achievable correlations decrease with increasing environment coupling Γ. Since the ions are described as two-level systems, multi-partite concurrence can be calculated purely algebraically.

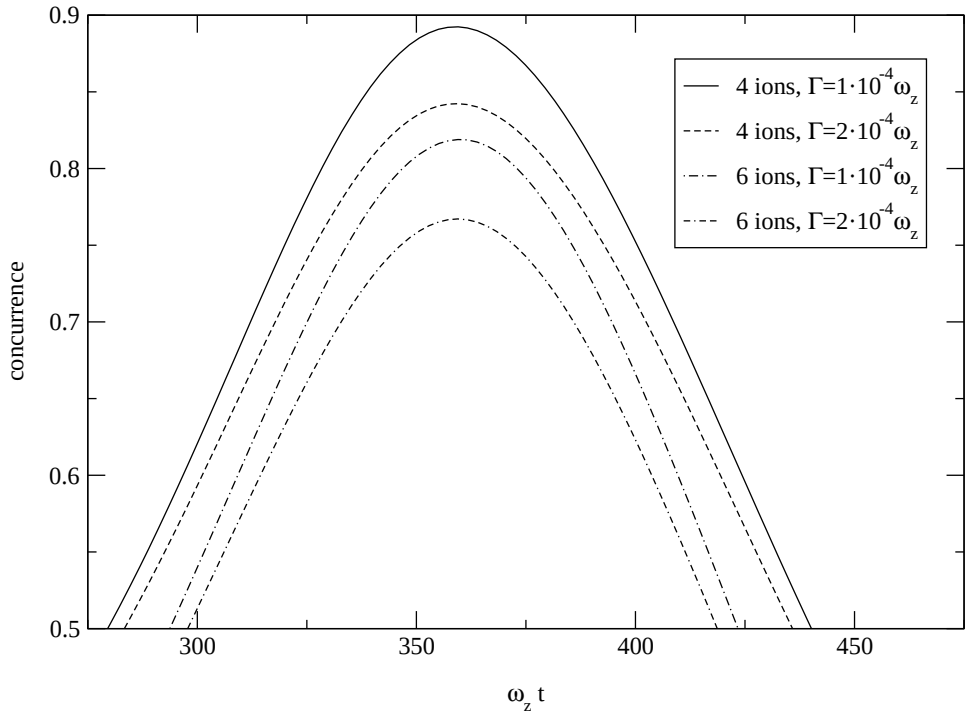

Figure 4.11: Four- and six-partite concurrence, eq. (3.64), with $p = 4,\ 6$, that characterises GHZ-type correlations, for two different environment coupling constants $\Gamma = 1 \cdot 10^{-4}\omega_z$ and $\Gamma = 2 \cdot 10^{-4}\omega_z$, as a function of the scaled time $\omega_z t$. Similarly as in the case of bipartite correlations shown in fig. 4.9, the maximally achievable quantum correlations are weaker for 6 ions than for 4 at given Γ.

It is important to state that the interpretation of fig. 4.11 is not as unambiguous as one might think on a first glance. Whilst $C^{(4)}$ decreases with growing Γ, one has to keep in mind that it only quantifies a specific class of quantum correlations. It therefore is not evident to what extent the GHZ-correlations decay into classical correlations, and to what extent different quantum correlations build up at the expense of the here desired ones.

Since we have already seen above that, at a given environment coupling, the preparation of bipartite quantum correlations deteriorates with increasing ion number, we also compare the creation of multi-partite correlations for 4 and 6 trapped ions. Fig. 4.11 shows the corresponding multi-partite concurrences for $\Gamma = 1 \cdot 10^{-4}\omega_z$ and $\Gamma = 2 \cdot 10^{-4}\omega_z$. Also in this case it is apparent that correlations strongly decrease with increasing ion number. As for the bipartite case, more data for larger ion numbers are required to decide whether the scheme discussed here is scalable - *i.e.*, whether is can be applied to arbitrary ion numbers, or whether - given some finite environment coupling - there is a maximum length of the ion chain such that no correlation of GHZ type can be created at all. However, the present data already show that the performance of the preparation scheme is limited. Even for vanishing environment coupling, where the idealised scheme predicts perfect correlations, the maximum concurrence is significantly smaller than its ideal value one.

Chapter 5

Beyond reduced density matrices

So far we extracted all information on the entanglement of a given quantum state from reduced density matrices. Since entanglement of mixed states was quantified by the entanglement of a suitably chosen set of pure states, the techniques using reduced density matrices - as formulated in eq. (3.13) - could also be applied to mixed states. For bipartite states, *all* information about quantum correlations can be extracted from the reduced density matrices, as argued in chapter 2.1.1, and in chapter 3.6 we saw that the approach of using reduced density matrices can also be extended to multi-partite systems. However, it is doubtful whether states of multi-partite systems can be characterised *completely* with the recourse to reduced density matrices.

In this chapter we derive an alternative approach to quantify bipartite entanglement, with a self-evident generalisation to systems composed of an arbitrary number of parties.

5.1 Technical tools

The present approach is based one a suitably chosen set of coherent states, that we will define in chapter 5.1.1 and which allows us to define suitable Husimi functions in chapter 5.1.2. These functions will be constructed such that their degree of localisation allows deduce some classes of entanglement monotones, what we will do in chapter 5.2.

5.1.1 Coherent states

Properly chosen classes of coherent states will be crucial in the following analysis. According to a general group-theoretical approach [74], one can define $SU(N)$-*coherent states* $|\alpha\rangle$ in terms of generators J_-^i and J_+^i ($i =$

$1, \ldots, N-1$) of $SU(N)$, acting on a reference state $|0\rangle$:

$$|\alpha\rangle = e^{\left(\vec{\gamma}\vec{J}_+ - \vec{\gamma}^*\vec{J}_-\right)}|0\rangle \ . \tag{5.1}$$

Thus, any coherent state $|\alpha\rangle$ is parametrised by $N-1$ complex numbers γ_i. We are considering $SU(N)$ coherent states in an N-dimensional Hilbert space $\mathcal{H}$. Since they are defined by the application of a general $SU(N)$ element on the reference state, each state of $\mathcal{H}$ is a coherent state - if we identify states that differ from each other only by an overall phase. This would not be the case if we were considering $SU(N)$ coherent states in a Hilbert space of dimension larger than N.

Coherent states as defined above provide a resolution of the identity

$$\int d\mu(\alpha)|\alpha\rangle\langle\alpha| = \mathbb{1} \ , \tag{5.2}$$

where $d\mu(\alpha)$ is an infinitesimal volume element that we explicitly derive in the appendix A.1. However, coherent states are not only complete - as necessary for the above resolution of the identity - but even over-complete.

The concept of $SU(N)$-coherent states can be generalised to groups with product structure [75], *e.g.* $SU(n_1) \times SU(n_2)$. Similarly to the case of $SU(N)$ coherent states, we define product group coherent states in terms of generators of the product group, *i.e.* in terms of a product of generators of the subgroups. A general $SU(n_1) \times SU(n_2)$ coherent state reads, for example,

$$|\alpha_{n_1\times n_2}\rangle = e^{\left(\vec{\gamma}_{n_1}\vec{J}_+^{n_1} - \vec{\gamma}_{n_1}^*\vec{J}_-^{n_1}\right)} \otimes e^{\left(\vec{\gamma}_{n_2}\vec{J}_+^{n_2} - \vec{\gamma}_{n_2}^*\vec{J}_-^{n_2}\right)}|0\rangle \ , \tag{5.3}$$

with vectors $\vec{J}_+^{n_1}$ and $\vec{J}_-^{n_1}$ containing the generators of $SU(n_1)$ and vectors $\vec{J}_+^{n_2}$ and $\vec{J}_-^{n_2}$ containing the generators of $SU(n_2)$, respectively. In the case of $SU(N)$ coherent states, all states of the corresponding Hilbert state were coherent states. In order to achieve a similar correspondence for product group coherent states, we will use them in Hilbert spaces with the proper tensor product structure. For example, the $SU(n_1)\times SU(n_2)$ coherent states mentioned above will be defined in a Hilbert space $\mathcal{H}$ that decomposes into the tensor product of an n_1-dimensional subspace $\mathcal{H}_1$ and an n_2-dimensional subspace $\mathcal{H}_2$. Requiring the reference state $|0\rangle$ to be separable ensures that exactly the separable states in $\mathcal{H}_1 \otimes \mathcal{H}_2$ are coherent states.

The generalisation of such a construction of coherent states to systems decomposing into p subsystems, each of which is described by an n_i-dimensional Hilbert space, is straightforward. Choosing a reference state $|0\rangle = |0_1\rangle \otimes \cdots \otimes |0_p\rangle$ allows to define $SU(N_1) \otimes \cdots \otimes SU(N_p)$ coherent states such that exactly the p-separable states, *i.e.* states of the form $|\phi_1\rangle \otimes \cdots \otimes |\phi_p\rangle$, are coherent states. This way of distinguishing separable pure states from entangled ones will eventually allow us to construct quantities that can serve as separability criteria and even satisfy the proper behaviour under LOCC, such that they are entanglement monotones.

5.1.2 Husimi function

Any density matrix ϱ can be represented by its Husimi function $H_\varrho(\alpha)$ [76], which is defined as its expectation value with respect to coherent states $|\alpha\rangle$:

$$H_\varrho(\alpha) = \langle\alpha|\varrho|\alpha\rangle \ . \tag{5.4}$$

A Husimi function completely characterises a given state ϱ, although it contains only diagonal elements of ϱ. For a complete set of states $\{|\psi_i\rangle\}$, all matrix elements $\langle\psi_i|\varrho|\psi_j\rangle$ are needed for an unambiguous description of some state ϱ. It is the over-completeness of the coherent states [74] which causes a complete characterisation of ϱ by its diagonal elements alone.

We will be especially interested in the localisation properties of the Husimi functions $H_\Psi(\alpha)$ of pure states $|\Psi\rangle$, in the phase space generated by the $\vec{J}_+^i$ and $\vec{J}_-^i$ in eq. (5.3). In the case of a mono-partite two-level system, this phase space is equivalent to the well known Bloch sphere, whereas it is equivalent to the product of two Bloch spheres for a bipartite two level system. In higher dimensional systems, the phase space is equivalent to the corresponding generalisations of such products of spheres.

The localisation of a given Husimi representation can be quantified by means of the Wehrl entropy

$$S_W = -\int d\mu \ H \log H \ . \tag{5.5}$$

According to a conjecture due to Lieb [77, 78], the Wehrl entropy is minimal exactly for Husimi functions representing coherent states, *i.e.* for $H_{\tilde{\alpha}}(\alpha) = \langle\alpha|\tilde{\alpha}\rangle\langle\tilde{\alpha}|\alpha\rangle$. This conjecture is unproven for the very general case, *i.e.* for arbitrary groups with dimensions that do not necessarily coincide with that of the considered Hilbert space. However, it is widely believed to be true [79], which supports the expectation that it holds true for the cases of product group coherent states that we are considering here.

Since we are interested in distinguishing separable states from entangled ones, we will choose exactly the coherent states that we defined in chapter 5.1.1. If we define Husimi functions with the help of these state, the Lieb conjecture suggests that the Wehrl entropy of Husimi functions representing coherent - *i.e.* separable - states is minimal. Thus one can expect - and we will prove it in chapter 5.2 - that, indeed, S_W can be used to distinguish separable states from entangled ones, and that, it even is an entanglement monotone.

Though, as mentioned in chapter 2.2.2, a single monotone does not - except for the case of two-level systems - completely characterise correlations of a pure state, since it does not allow to reconstruct all Schmidt coefficients defined in eq. (2.9). However, as we will show in chapter 5.2, Wehrl entropy is not the only entanglement monotone that can be derived using Husimi functions. Our present approach will rather allow to construct a hierarchy

of monotones that characterises all quantum correlations of pure bipartite states, in arbitrary dimensions.

The Lieb conjecture implies that the Wehrl entropy of a p-partite Husimi function is minimal exactly for separable, *i.e.* p-separable states. Thus one can expect the Wehrl entropy of such Husimi functions to characterise all correlations, in particular also those of ν-separable states with $\nu < p$. This implies that is has different properties our multi-partite concurrence, 3.6. In the sequel of eq. (3.65), we found for an exemplary four-partite concurrence that such a quantity cannot quantify any bi- or tri-separable states, and that it can only account for special types of four-partite correlations. Although not shown for the very general case, one cannot expect that there is a multi-partite concurrence that can characterise all kinds of quantum correlations, as argued in chapter 3.6. Thus, possible monotones derived from a multi-partite Husimi function can be expected to be independent from our multi-partite concurrences, such that both classes of quantities provide different - complementary - information.

5.1.3 Moments of the Husimi function

In the following we consider pure states of bipartite systems. Due to the Schmidt decomposition given in eq. (2.9), we can assume $\dim(\mathcal{H}_1) = \dim(\mathcal{H}_2) = p$ without loss of generality.

As argued in chapter 5.1.1, we will use $SU(d) \times SU(d)$ coherent states $|\alpha\rangle$ given as the direct product of $SU(d)$-coherent states,

$$\underbrace{|\alpha\rangle}_{SU(d)\times SU(d)-\text{coherent}} = \underbrace{|\alpha_1\rangle}_{SU(d)-\text{coherent}} \otimes \underbrace{|\alpha_2\rangle}_{SU(d)-\text{coherent}} , \tag{5.6}$$

since this set provides a natural distinction between separable and entangled states. The Husimi function H_Ψ of a bipartite state $|\Psi\rangle$ is then given by

$$H_\Psi(\alpha_1, \alpha_2) = \langle\alpha_1| \otimes \langle\alpha_2|\Psi\rangle\langle\Psi|\alpha_1\rangle \otimes |\alpha_2\rangle , \tag{5.7}$$

where $|\alpha_1\rangle$ and $|\alpha_2\rangle$ are $SU(d)$ coherent states.

The Wehrl conjecture implies that Husimi functions representing coherent states have strongest possible localisation in phase space and that all Husimi functions representing states that are no coherent states are less strongly localised. In the original conjecture [78], the localisation is quantified by the Wehrl entropy, eq. (5.5). Evaluating it straightforwardly is rather involved due to the logarithm under the integral. We will evaluate it indirectly, treating first the statistical moments

$$m_q = \int d\mu(\alpha_1)\; d\mu(\alpha_2)\; \Big(H_\Psi(\alpha_1, \alpha_2)\Big)^q \tag{5.8}$$

of the Husimi representation H_Ψ of the considered state $|\Psi\rangle$. In chapter 5.2.2 we will show that knowledge of these moments allows to derive a

closed expression for S_W, without direct integration over the logarithm in eq. (5.5). Furthermore, the detour via the moments, instead of computing the Wehrl entropy directly, will allow us to derive the additional entanglement monotones that are required for the complete characterisation of $|\Psi\rangle$. We will discuss these moments in some detail in chapters 5.2.1 and 5.2.3.

Since the moments $m_q(\Psi)$ are invariant under the action of the considered group, it is always possible to express $m_q(\Psi)$ as a function of the invariants of ϱ under this group. Since $SU(d) \times SU(d)$ describes local unitary transformations, these invariants are just the Schmidt coefficients λ_i, defined in eq. (2.9). The derivation of the explicit result [80] in terms of the Euler Gamma function

$$m_q(\Psi) = \left(\frac{d!\Gamma(q+1)}{\Gamma(d+q)}\right)^2 \mu_{q,d} \,, \quad \text{with} \quad \mu_{q,d} = \sum_{i=1}^{d} \frac{\lambda_i^{q+d-1}}{\prod_{j=1, j\neq i}^{d} (\lambda_i - \lambda_j)} \,, \tag{5.9}$$

is sketched in Appendix A.1. According to eq. (A.13), the quantity $\mu_{q,d}$ can be expressed via the following integral expression

$$\mu_{q,d} = \frac{\Gamma(q+d)}{\Gamma(q+1)} \int d^d\!x \; \delta(\|\vec{x}\|_1 - 1) \; \left(\vec{\lambda}\vec{x}\right)^q \,, \tag{5.10}$$

where $d^d\!x$ is a short hand notation for $\prod_{i=1}^{d} dx_i$.

Using this representation, one can easily derive the Jacobi matrix J of $\mu_{q,d}$ with elements

$$J_{ij} = \frac{\partial^2 \mu_{q,d}}{\partial\lambda_i \partial\lambda_j} \,. \tag{5.11}$$

The explicit expression for the Jacobian reads

$$J(\mu_{q,d}) = \frac{\Gamma(q+d)}{\Gamma(q+1)} q(q-1) \int d^d\!x \; \delta(\|\vec{x}\|_1 - 1) \; \left(\vec{\lambda}\vec{x}\right)^{q-2} \; \vec{x} \; \vec{x}^T \,, \tag{5.12}$$

where $\vec{x}\,\vec{x}^T$ denotes the dyadic product, *i.e.* a positive semi-definite quantity with exactly one non-vanishing eigenvalue equal to $\sum x_i^2$. The corresponding eigenvector is $\vec{x}$ itself. Since the integration contains contributions from all vectors $\vec{x}$ with unit 1-norm, the integral is positive definite. Due to the prefactor $(q-1)$ it is clear that $\mu_{q,d}$ is convex for $q > 1$, and concave for $0 < q < 1$. Consequently, there is a unique minimum for $q > 1$, and a unique maximum for $0 < q < 1$, that is obtained for $\vec{\lambda} = \vec{\lambda}_*$ - the vector of Schmidt coefficients describing a maximally entangled state as introduced in chapter 2.1.1.

5.1.4 Monotonicity under LOCC

If the moments m_q are supposed to serve as a basis for constructing entanglement monotones, they have to show the proper monotonous behaviour

under LOCC operations, *i.e.* they have to be either Schur concave or Schur convex as defined in eq. (2.25).

In this chapter we will show that $\mu_{q,d}$ is Schur convex for $q > 1$, and Schur concave for $0 < q < 1$. This will allow us to prove that the quantities derived from the moments in chapter 5.2 hereafter are proper entanglement monotones.

As shown in eq. (A.28), $\mu_{q,d}$ can be expressed as

$$\mu_{q,d} = \frac{\Gamma(q+d)}{\Gamma(q+1)} \int d^d x \; \delta(\|\vec{x}\|_1 - 1) \; \left(\vec{\lambda}\vec{x}\right)^q \; . \tag{5.13}$$

Using this integral expression, one obtains

$$\partial_s \mu_{q,d} = (\lambda_1 - \lambda_2) \frac{\Gamma(q+d)}{\Gamma(q+1)} \int d^d x \; \delta(\|\vec{x}\|_1 - 1) \; \left(\vec{\lambda}\vec{x}\right)^{q-1} (x_1 - x_2) \; , \tag{5.14}$$

with the differential operator $\partial_s = (\lambda_1 - \lambda_2)(\partial/\partial\lambda_1 - \partial/\partial\lambda_2)$. Remember that the choice of the first two components in the preceding equation is arbitrary, as argued in the sequel of eq. (2.25).

The integration can be divided into one integration over the domain $x_1 > x_2$, and a second one over $x_1 < x_2$:

$$\begin{aligned} \partial_s \mu_{q,d} &= (\lambda_1 - \lambda_2) \frac{\Gamma(q+d)}{\Gamma(q+1)} \int_{x_1 > x_2} d^d x \; \delta(\|\vec{x}\|_1 - 1) \; \left(\vec{\lambda}\vec{x}\right)^{q-1} (x_1 - x_2) \\ &+ (\lambda_1 - \lambda_2) \frac{\Gamma(q+d)}{\Gamma(q+1)} \int_{x_1 < x_2} d^d x \; \delta(\|\vec{x}\|_1 - 1) \; \left(\vec{\lambda}\vec{x}\right)^{q-1} (x_1 - x_2) \; . \end{aligned} \tag{5.15}$$

Exchanging x_1 and x_2 in the second term, one gets

$$\begin{aligned} \partial_s \mu_{q,d} &= (\lambda_1 - \lambda_2) \frac{\Gamma(q+d)}{\Gamma(q+1)} \int_{x_1 < x_2} d^d x \; \delta(\|\vec{x}\|_1 - 1) \; (x_1 - x_2) \\ &\left(\left(\lambda_1 x_1 + \lambda_2 x_2 + \sum_{i=3}^{d} \lambda_i x_i \right)^{q-1} - \left(\lambda_2 x_1 + \lambda_1 x_2 + \sum_{i=3}^{d} \lambda_i x_i \right)^{q-1} \right) \; . \end{aligned} \tag{5.16}$$

Now one can distinguish the three cases $\lambda_1 = \lambda_2$, $\lambda_1 > \lambda_2$, and $\lambda_1 < \lambda_2$. In the first case one has $\partial_s \mu_{q,d} = 0$, due to the prefactor $(\lambda_1 - \lambda_2)$. For the other cases we can make use of the fact that the integration is restricted to the domain $x_1 - x_2 \geq 0$. Using $\lambda_1 - \lambda_2 \lesseqgtr 0$, one can multiply both left- and right-hand-sides of these two inequalities, and immediately gets

$$\lambda_1 x_1 + \lambda_2 x_2 \lesseqgtr \lambda_1 x_2 + \lambda_2 x_1 \; . \tag{5.17}$$

Since power functions are monotonously increasing for positive exponents, and monotonously decreasing for negative exponents, the integrand is non-negative for $q > 1$, and non-positive for $0 < q < 1$, in the case $\lambda_1 > \lambda_2$.

For $\lambda_1 < \lambda_2$, the integrand in non-positive for $q > 1$ and non-negative for $0 < q < 1$. Due to the prefactor $(\lambda_1 - \lambda_2)$, one obtains

$$\begin{aligned}(\lambda_1 - \lambda_2)\left(\frac{\partial \mu_{q,d}}{\partial \lambda_1} - \frac{\partial \mu_{q,d}}{\partial \lambda_2}\right) \geq 0 \ , \quad \text{for } q > 1, \text{ and} \\ (\lambda_1 - \lambda_2)\left(\frac{\partial \mu_{q,d}}{\partial \lambda_1} - \frac{\partial \mu_{q,d}}{\partial \lambda_2}\right) \leq 0 \ , \quad \text{for } 0 < q < 1,\end{aligned} \tag{5.18}$$

independently of the values of λ_1 and λ_2. Thus, $\mu_{q,d}$ is indeed Schur convex for $q > 1$, and Schur concave for $0 < q < 1$. Knowing that $\mu_{q,d}$ is monotonous under LOCC operations, we can use this quantity as a basis for deriving entanglement monotones.

5.2 Entanglement monotones

As mentioned earlier in chapter 2.1.1, a set of $d-1$ independent entanglement monotones is required in order to characterise the quantum correlations of pure bipartite states completely. Knowledge of the moments for arbitrary real q allows to construct complete hierarchies of monotones. $d-1$ independent monotones then determine the Schmidt coefficients of a given state.

5.2.1 Rescaled monotones

The main advantage of concurrence with respect to other entanglement measures is that it defines a function, eq. (3.13), that is linear in some of its arguments, and antilinear in all others. This property enabled an elegant generalisation for mixed states in chapter 3.2. The rescaled moments defined as

$$M_q = \frac{1}{1-q}(\mu_{q,d} - 1) \ , \tag{5.19}$$

also define such (anti-)linear functions for integer values of q. Moreover, independently of q, they vanish for separable states, and adopt their maximal value for maximally entangled states. Furthermore, according to eq. (5.18), they are also Schur concave for $q > 0$, since the prefactor $1/(1-q)$ changes its sign at $q = 1$.

In fig. 5.1, M_q is plotted for $d = 3$ and for several values of q. The Schmidt vector $\vec{\lambda}_*$, which identifies maximally entangled states, refers to the centre of the triangle which describes the domain of regular Schmidt vectors with $\|\vec{\lambda}\|_1 = 1$. Separable states described by $\vec{\lambda}_s$ correspond to the corners of the triangle.

M_q can be interpreted as a measure of the distance between a point describing a given state and the point describing a maximally entangled state. If the distance vanishes, the entanglement is maximal - and if the

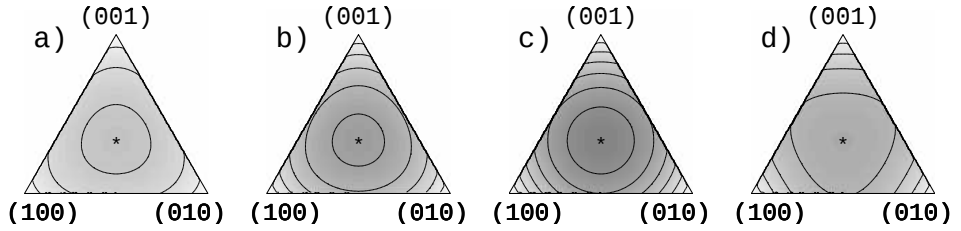

Figure 5.1: Rescaled moments M_q (grey-scaled plots with contour lines) as a function of two independent variables for $d = 3$, $q = 1/2$ (a), $q = 1$ (b), $q = 2$ (c), and $q = 5$ (d). The moments M_q are maximal at the centre $\vec{\lambda}_* = [1/3, 1/3, 1/3]$, and minimal at the corners.

distance is maximal, the corresponding state is separable. Different values of q refer to different norms of that distance. For example, $q = 2$ refers to the regular Euclidean norm, such that lines of equal moments M_q are circles centred around $\vec{\lambda}_*$.

5.2.2 Wehrl entropy

The most commonly used quantity to quantify the localisation of Husimi functions is the Wehrl entropy $S_W(\Psi)$, for which the original Lieb conjecture was formulated [78]. Generalising eq. (5.5) for bipartite systems, $S_W(\Psi)$ is defined as

$$S_W(\Psi) = -\int d\mu(\alpha_1) d\mu(\alpha_2)\; H_\Psi(\alpha_1, \alpha_1)\; \ln H_\Psi(\alpha_1, \alpha_2)\;. \tag{5.20}$$

Since eq. (5.9) provides closed expressions for the moments m_q for arbitrary positive q, we can derive S_W quite easily. Using $\partial H^q/\partial q = H^q \ln H$, one gets

$$S_W(\Psi) = -\lim_{q\to 1} \frac{\partial m_\Psi(\varrho)}{\partial q}\;. \tag{5.21}$$

Performing the limit one can express the Wehrl entropy in terms of the Schmidt vector $\vec{\lambda}$ as $S_W = Q(\vec{\lambda}) + 2C_d$, with the *subentropy* [81]

$$Q(\vec{\lambda}) = -\sum_{i=1}^{d} \frac{\lambda_i^d \log \lambda_i}{\prod_{j=1, j\neq i}^{d} (\lambda_i - \lambda_j)} \tag{5.22}$$

and an additive constant C_d that can be expressed in terms of the digamma function [82] $\Psi_d(x)$:

$$C_d = \Psi_d(d+1) - \Psi_d(2) = \sum_{k=2}^{d} \frac{1}{k}\;, \quad \text{with} \quad \Psi_d(x) = \frac{\partial \ln \Gamma(x)}{\partial x}\;. \tag{5.23}$$

Similarly to the representation of the moments, as given in eq. (5.10), the subentropy can be expressed as [81]

$$Q(\vec{\lambda}) = -d! \left(C_d + \int d^d x \; \delta(\|\vec{x}\|_1 - 1) \; (\vec{\lambda}\vec{x}) \ln(\vec{\lambda}\vec{x}) \right) , \tag{5.24}$$

as we show in eq. (A.38). Using this representation, one can express the Jacobi matrix of the subentropy as

$$J(Q) = -d! \int d^d x \; \delta(\|\vec{x}\|_1 - 1) \; \frac{\vec{x} \; \vec{x}^T}{\vec{\lambda}\vec{x}} . \tag{5.25}$$

Invoking the same arguments as in the case of $J(\mu_{q,d})$, one finds that J is negative definite. Consequently, Q has a unique maximum obtained for $\vec{\lambda} = \vec{\lambda}_*$, *i.e.* for maximally entangled states. Its minimal value C_d is realised for vectors of Schmidt coefficients $\vec{\lambda}_s$, representing separable states.

Since entanglement monotones are scaled such that they assign the value zero to separable states, we subtract the Wehrl entropy of a separable state and obtain the *Wehrl entropy excess*

$$\Delta S_W(\Psi) = S_W(\Psi) - S_W(\Psi_s) = Q(\vec{\lambda}) . \tag{5.26}$$

This quantity vanishes exactly for separable states, is positive for all entangled states, and maximal for maximally entangled states.

Schur concavity of the Wehrl entropy excess ΔS_W can be directly inferred from eq. (5.18), what implies that the derivative of $\mu_{q,d}$ with respect to q is Schur convex for $q = 1$. Since ΔS_W can be expressed as $\Delta S_W = -\lim_{q\to 1} \partial\mu_{q,d}/\partial q$, we obtain

$$(\lambda_1 - \lambda_2) \left(\frac{\partial \Delta S_W}{\partial \lambda_1} - \frac{\partial \Delta S_W}{\partial \lambda_2} \right) = -\partial_s \left. \frac{\partial \mu_{q,d}}{\partial q} \right|_{q=1} \leq 0 . \tag{5.27}$$

Thus ΔS_W is Schur concave. Alternatively Schur concavity can also be derived directly from eq. (5.24), invoking similar arguments as in chapter 5.1.4, where we proved the Schur concavity respectively convexity of $\mu_{q,d}$.

5.2.3 Rényi-Wehrl entropy

Wehrl entropy itself is - as a single scalar quantity - not sufficient to completely characterise a state in arbitrary dimensions. Though it can be generalised as to provide a sufficient number of independent monotones. Analogously to the Rényi entropy S_R [83], one defines the *Rényi-Wehrl entropy*

$$S_q = \frac{1}{1-q} \; \ln \; m_q . \tag{5.28}$$

Since the moments m_q have a unique maximum for $q > 1$, and a unique minimum for $0 < q < 1$, and since the logarithm is a monotonous function,

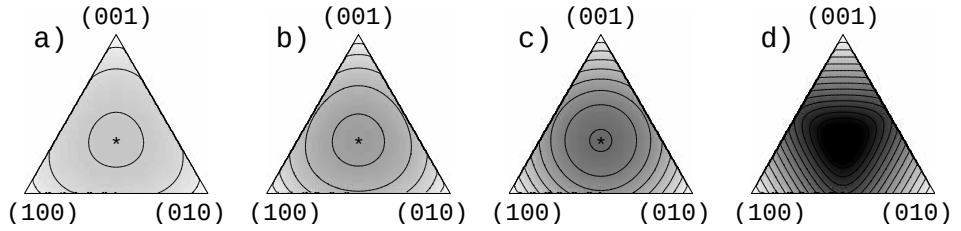

Figure 5.2: Rényi-Wehrl entropy excess ΔS_q, eq. (5.29), as a function of two independent variables for $d = 3$, $q = 1/2$ (a), $q = 1$ (b), $q = 2$ (c), and $q = 10$ (d). Grey scale reflects the values ΔS_q: the higher q, the larger the maximum at the centre $\vec{\lambda}_* = (1/3, 1/3, 1/3)$ - which refers to maximally entangled states.

S_q has a unique maximum which is met at $\vec{\lambda} = \vec{\lambda}_*$, *i.e.* for maximally entangled states, whereas its minimal value is obtained for separable states.

Analogously to the above, the *Rényi-Wehrl entropy excess* ΔS_q is defined by subtracting the Rényi-Wehrl entropy of a separable state,

$$\Delta S_q(\Psi) = \frac{1}{1-q} \ln \sum_{i=1}^{d} \frac{\lambda_i^{q+d-1}}{\prod_{j=1, j\neq i}^{d} (\lambda_i - \lambda_j)} \ . \tag{5.29}$$

As for the Schur convexity of the Rényi-Wehrl entropy excess, it is again convenient to make use of properties of $\mu_{q,d}$. Since $\Delta S_{W,q}$ can be expressed as $\Delta S_q = 1/(1-q) \ \ln \mu_{q,d}$, one obtains

$$\partial_s \Delta S_q = \frac{1}{1-q} \frac{1}{S_q} \partial_s \mu_{q,d} \ . \tag{5.30}$$

With S_q non-negative, eq. (5.18) allows to conclude that ΔS_q is Schur concave

$$(\lambda_1 - \lambda_2) \left(\frac{\partial \Delta S_q}{\partial \lambda_1} - \frac{\partial \Delta S_q}{\partial \lambda_2} \right) \leq 0 \ , \tag{5.31}$$

i.e. that the Rényi-Wehrl entropy excess is an entanglement monotone.

5.3 Towards multi-partite systems

The approach of quantifying entanglement of pure states has a self evident formal generalisation to systems consisting of more than just two parties. Analogously to choosing $SU(N) \times SU(N)$ coherent states in the case of bipartite systems one can choose $SU(n_1) \times \ldots \times SU(n_p)$ coherent states for p-partite systems. This latter class of coherent states is separable with respect

to any subsystem. Thus the Wehrl conjecture implies that the localisation properties of the corresponding Husimi functions provides a measure for the inseparability of p-partite quantum states, sensitive to all correlations, in contrast to the proposed multi-partite concurrence (chapter 3.6) that only accounts for special classes of quantum correlations.

On the other hand, there will be nontrivial complications when it comes to the calculation of the statistical moments, and of the associated entropies of such multi-partite Husimi representations, as well as in the proof of the monotonicity under LOCC of these quantities.

All moments of a Husimi function can be expressed as a function of invariants of the group used to construct the coherent states. In the case of bipartite systems, these are the Schmidt coefficients (chapter 2.1.1). For multi-partite systems, in general, not all invariants are known, and a representation analogous to the Schmidt decomposition, eq. (2.9), is not available.

Therefore, whilst there is no obvious reason why the above characterisation of entanglement by a quasi probability representation of bipartite quantum states cannot be extended to multi-partite states, it is equally certain that other techniques than those built upon in the bipartite case will have to be developed.

If, however, the generalisation is performed, one can apply the theory derived in chapter 3 for concurrence also to a quantity related to the second moment of a multi-partite Husimi function. The basic requirement that was necessary for our treatment of mixed states was that concurrence was the square root of a function of four arguments, which is linear in two and anti-linear in the other two arguments.

This property is also satisfied by the following Husimi concurrence c_H defined on the basis of the second moment of a multi-partite Husimi function H as

$$c_H = \sqrt{\left|\langle\psi|\psi\rangle\right|^2 - \int d\mu \; H^2} \; . \tag{5.32}$$

In analogy to eq. (3.16) one can define a Husimi concurrence tensor A_H with elements

$$\left[A_H\right]_{jk}^{lm} = \langle\psi_j|\psi_l\rangle\langle\psi_k|\psi_m\rangle - \int d\mu \langle\alpha|\psi_j\rangle\langle\psi_l|\alpha\rangle\langle\alpha|\psi_k\rangle\langle\psi_m|\alpha\rangle \; . \tag{5.33}$$

As also in the case of concurrence, eq. (3.11), the Husimi concurrence of a pure state can be expressed as the square root of a completely diagonal element of A_H, where all four indices coincide. Therefore, the tensor A_H provides a basis for deriving a gradient iteration, eq. (3.40), lower bound, eq. (3.48), and quasi-pure approximation, eq. (3.59), for the corresponding Husimi concurrence as the tensor A did for regular concurrence. What remains to show is the positivity of A_H.

Chapter 6

Outlook

It was the aim of the present work to characterise the entanglement of mixed quantum states - which naturally occur in any experimental realisation. As opposed to most treatments hitherto available, we were seeking for a theoretical framework which is equally general as versatile, such as to be applicable in arbitrary, finite dimensions, for arbitrary states, and to allow for an explicit quantitative evaluation - by numerical and/or algebraic means. This program was fully accomplished for bipartite states, with some generalisations to multi-partite systems - where two conjectures remain to be rigorously proven. More specifically, we formulated several bounds on the concurrence of mixed bipartite quantum states in arbitrary dimensions, *i.e.* of an entanglement measure which so far could be reliably calculated only for two-level systems. In particular, we derived a *lower bound* which not only serves as a separability criterion, but, importantly together with already available upper bounds, yields rather accurate estimates of the actual value of concurrence. Furthermore, we have seen that a suitable approximation, which can be evaluated purely algebraically and was inspired by the generic experimental scenario, shows excellent agreement with the optimal bounds for the overwhelming majority of examples which we have tested here. Thus, we provide a formalism which allows, for the first time, for a *quantitative and efficient* assessment of concurrence of arbitrary bipartite quantum states.

Alternatively to our treatment of the concurrence of mixed states, we also outlined a characterisation of the quantum correlations of pure bipartite states through the localisation properties of suitably defined Husimi representations.

The versatility of our tools, including its multi-partite generalisations, is illustrated by some examples on the time evolution of the entanglement of various, also experimentally accessible states under non-vanishing environ-

ment coupling. As a byproduct, we found that a prominent proposal for the creation of multi-partite entangled states in ion traps may suffer considerably from some oversimplifications in the underlying model as the number of ions is increased.

This nicely illustrates how, given a readily calculable entanglement measure, one can access the dynamical evolution of entanglement under realistic experimental conditions, rather than only studying the static entanglement properties of various, more or less abstract sets of quantum states. Whilst we have not yet elaborated this aspect in detail in the present thesis, we are confident that our contribution indicates the ultimate route to an equally systematic as intuitive understanding of quantum entanglement - only if we understand the dynamics of entanglement under incoherent forcing will we be able to appreciate the relevant part of its static characterisations.

Appendix A

Derivation of the moments

A.1 Moments of the Husimi function

In this chapter we will derive closed expressions for the moments of the Husimi function H_Ψ. As already mentioned, every pure state belonging to a d-dimensional Hilbert space is a $SU(d)$ coherent state and vice versa. Therefore we can parametrise all $SU(d)$ coherent states as

$$|\alpha\rangle = \Big(1 - \sum_{i=1}^{d-1} x_i\Big)^{1/2} |0\rangle + \sum_{i=1}^{d-1} \sqrt{x_i} e^{i\varphi_i} |i\rangle \ , \tag{A.1}$$

with $0 \leq x_i \leq 1 - \sum_{j=i+1}^{d-1} x_j$ and $d\mu = d!/(2\pi)^{d-1} \prod_{i=1}^{d-1} dx_i \, d\varphi_i$. The states $|i\rangle$, $i = 0, \ldots, d-1$, form an orthonormal basis.

Since the moments are invariant under local unitary transformations, one can assume the state $|\Psi\rangle$ to be given in its Schmidt form

$$|\Psi\rangle = \sum_{\nu} \sqrt{\lambda_\nu} |\nu_1\rangle \otimes |\nu_2\rangle \ , \tag{A.2}$$

without loss of generality. The Husimi function H_Ψ of state $|\Psi\rangle$ with respect to $SU(d) \otimes SU(d)$-coherent states $|\alpha\rangle = |\alpha_1\rangle \otimes |\alpha_1\rangle$ ($|\alpha_1\rangle \in \mathcal{H}_1$, $|\alpha_2\rangle \in \mathcal{H}_2$) reads

$$H_\Psi^{(2)} = \sum_{\nu,\mu=1}^{d} \sqrt{\lambda_\nu \lambda_\mu} \langle \alpha_1 | \nu_1 \rangle \langle \mu_1 | \alpha_1 \rangle \ \langle \alpha_2 | \nu_2 \rangle \langle \mu_2 | \alpha_2 \rangle \ . \tag{A.3}$$

The overlap elements $\langle \nu | \alpha \rangle$ are given by

$$\langle 0 | \alpha \rangle = \left(1 - \sum_{i=1}^{d-1} x_i \right)^{\frac{1}{2}} \quad \text{and} \quad \langle \nu | \alpha \rangle = \sqrt{x_\nu} e^{i\varphi_\nu} \ , \quad \text{for} \quad i > 0 \ . \tag{A.4}$$

In the following we will restrict ourselves for a while to integer q. To evaluate eq. (5.8) for the moments m_q, we have to integrate separately over both subsystems. Due to the symmetry of the Schmidt decomposition with respect

to both subsystems, the moments can be expressed as

$$m_q = \sum_{\substack{\nu_1 \dots \nu_q = 1 \\ \mu_1 \dots \mu_q = 1}}^{d} \sqrt{\lambda_{\nu_1} \dots \lambda_{\nu_q} \lambda_{\mu_1} \dots \lambda_{\mu_q}} \big(f_q(\mathcal{N}_1, \dots, \mathcal{N}_d, \mathcal{M}_1, \dots, \mathcal{M}_d) \big)^2 \ , \tag{A.5}$$

with

$$f_q = \int d\mu(\alpha) \langle \alpha | \nu_1 \rangle \langle \mu_1 | \alpha \rangle \langle \alpha | \nu_2 \rangle \langle \mu_2 | \alpha \rangle \dots \langle \alpha | \nu_q \rangle \langle \mu_q | \alpha \rangle \ . \tag{A.6}$$

The integers $\mathcal{N}_i$ and $\mathcal{M}_i$ count how often the states $|\nu_i\rangle$ and $\langle \mu_i|$ appear in the integrand on the right-hand side of eq. (A.6). Now f_q can be expressed as

$$\begin{aligned} f_q &= \frac{d!}{(2\pi)^{d-1}} \left(\prod_{i=1}^{d-1} \int_0^{x_i^{(max)}} dx_i \int_0^{2\pi} d\varphi_i \ e^{i(\mathcal{N}_i - \mathcal{M}_i)\varphi_i} x_i^{\frac{1}{2}(\mathcal{N}_i + \mathcal{M}_i)} \right) \\ & \quad (1 - \sum_{j=1}^{d-1} x_j)^{q - \frac{1}{2}\sum_{\chi=1}^{d-1} \mathcal{N}_\chi + \mathcal{M}_\chi} \ , \end{aligned} \tag{A.7}$$

where the integrations over x_i are performed in increasing order of i, and the upper limit of the integration is given by $x_i^{(max)} = 1 - \sum_{j=i+1}^{d-1} x_j$. It is useful to first perform the φ_i integrations, that lead to $\delta_{\mathcal{N}_i, \mathcal{M}_i}$ terms, so that one gets

$$f_q = d! \prod_{i=1}^{d-1} \int_0^{x_i^{(max)}} dx_i \ x_i^{\mathcal{N}_i} \ \delta_{\mathcal{N}_i, \mathcal{M}_i} \ (1 - \sum_{j=1}^{d-1} x_j)^{q - \sum_{\chi=1}^{d-1} \mathcal{N}_\chi} \ . \tag{A.8}$$

In chapter A.1.1 we will explicitly perform the x_i-integrations. Anticipating the result given in eq. (A.21), we obtain

$$f_q = d! \ \frac{\left(\prod_{i=1}^{d-1} (\mathcal{N}_i!) \right) \left(q - \sum_{i=1}^{d-1} \mathcal{N}_i \right)!}{(q + d - 1)!} \ \delta_{\mathcal{N}_i, \mathcal{M}_i} \ . \tag{A.9}$$

Thus one obtains for the moments

$$\begin{aligned} m_q &= \left(d! \frac{\left(\prod_{i=1}^{d-1} (\mathcal{N}_i!) \right) \left(q - \sum_{i=1}^{d-1} \mathcal{N}_i \right)!}{(q + d - 1)!} \right)^2 \\ & \quad \sum_{\substack{\nu_1 \dots \nu_q = 1 \\ \mu_1 \dots \mu_q = 1}}^{d} \sqrt{\lambda_{\nu_1} \dots \lambda_{\nu_q} \lambda_{\mu_1} \dots \lambda_{\mu_q}} \ \delta_{\mathcal{N}_i, \mathcal{M}_i} \ . \end{aligned} \tag{A.10}$$

The $\delta_{\mathcal{N}_i, \mathcal{M}_i}$-terms assure that there are only integer powers of the λ_{ν_i}. To further evaluate eq. (A.10), one just has to count how many terms with fixed

powers occur. Using simple combinatorics one then can see that there are

$$\left(\frac{q!}{\left(\prod_{i=1}^{d-1}(\mathcal{N}_i)!\right)\left(q-\sum_{i=1}^{d-1}\mathcal{N}_i\right)!} \right)^2 \tag{A.11}$$

terms containing the expression $\lambda_1^{\mathcal{N}_1}\lambda_2^{\mathcal{N}_2}\ldots\lambda_{d-1}^{\mathcal{N}_{d-1}}\lambda_d^{q-\sum_{i=1}^{d-1}\mathcal{N}_i}$. Consequently, we finally get

$$m_q = \left(\frac{d!\;q!}{(q+d-1)!}\right)^2 \sum_{\mathcal{N}_1=0}^{q}\sum_{\mathcal{N}_2=0}^{q-\nu_1}\cdots\sum_{\mathcal{N}_{d-1}=0}^{q-\sum_{i=1}^{d-2}\mathcal{N}_i} \lambda_1^{\mathcal{N}_1}\lambda_2^{\mathcal{N}_2}\ldots\lambda_{d-1}^{\mathcal{N}_{d-1}}\lambda_d^{q-\sum_{i=1}^{d-1}\mathcal{N}_i}\;. \tag{A.12}$$

Using eq. (A.22) that we will prove in chapter A.1.2, this simplifies to

$$m_q = \left(\frac{d!\Gamma(q+1)}{\Gamma(q+d)}\right)^2 \sum_{i=1}^{d} \frac{\lambda_i^{q+d-1}}{\prod\limits_{\substack{j=0\\ j\neq i}}^{d}\lambda_i-\lambda_j}\;. \tag{A.13}$$

So far we were restricting ourselves to integer values of q, what was crucial for the evaluation of eq. (A.8). Since eq. (A.13) holds true for all positive integers, and integers are dense at infinity, eq. (A.13) has a unique analytic extension to real q. And because all terms in eq. (A.13) are defined also for real q, we can conclude that eq. (A.13) indeed is this extension.

A.1.1 x-integrations

To perform the integrations in eq. (A.8), we need to define an auxiliary function

$$g_q(\beta,d) = \prod_{i=1}^{d-1}\int_0^{\tilde{x}_i^{(max)}(\beta)} dx_i\;\; x_i^{\mathcal{N}_i}(\beta-\sum_{j=1}^{d-1}x_j)^{q-\sum_{\chi=1}^{d-1}\mathcal{N}_\chi}\;, \tag{A.14}$$

with $\tilde{x}_i^{(max)}(\beta) = \beta - \sum_{j=i+1}^{d-1}x_j$. For $\beta = 1$, $g_q(1,d)$ coincides with f_q as given in eq. (A.8). According to its definition, $g_q(\beta,d)$ satisfies the following relation

$$g_q(\beta,d) = \int_0^{\beta} dx_{d-1}\;\; x_{d-1}^{\mathcal{N}_{d-1}} g_{q-\mathcal{N}_{d-1}}(\beta-x_{d-1},d-1)\;, \tag{A.15}$$

connecting the quantities g_q that refer to different dimensions d. For $d=2$ only one single integration has to be performed, what can be done straightforwardly

$$g_q(\beta,2) = \int_0^{\beta} dx_1\; x_1^{\mathcal{N}_1}(\beta-x_1)^{q-\mathcal{N}_1} = \beta^{q+1}\;\frac{\mathcal{N}_1!(q-\mathcal{N}_1)!}{(q+1)!}\;, \tag{A.16}$$

with q integer. For $d > 2$ several similar integrations have to be performed. Therefore we will invoke inductive arguments to show that

$$g_q(\beta, d) = \beta^{(q+d-1)} \; \frac{(\prod_{i=1}^{d-1} \mathcal{N}_i!)(q - \sum_{i=1}^{d-1} \mathcal{N}_i)!}{(q+d-1)!} \; . \tag{A.17}$$

Assuming that eq. (A.17) holds true for $g_q(\beta, d-1)$, and making use of eq. (A.15), one gets

$$\begin{aligned} g_q(\beta, d) &= \int_0^\beta dx_{d-1} \; x_{d-1}^{\mathcal{N}_{d-1}} (\beta - x_{d-1})^{q+d-2-\mathcal{N}_{d-1}} \\ &\qquad \frac{(\prod_{i=1}^{d-2} \mathcal{N}_i!)(q - \mathcal{N}_{d-1} - \sum_{i=1}^{d-2} \mathcal{N}_i)!}{(q+d-2-\mathcal{N}_{d-1})!} \end{aligned} \tag{A.18}$$

Using further eq. (A.16), one obtains

$$\begin{aligned} f_q = g_q(\beta, d) &= \beta^{q+d-1} \frac{\mathcal{N}_{d-1}!(q+d-2-\mathcal{N}_{d-1})!}{(q+d-1)!} \\ &\qquad \frac{(\prod_{i=1}^{d-2} \mathcal{N}_i!)(q - \sum_{i=1}^{d-1} \mathcal{N}_i)!}{(q+d-2-\mathcal{N}_{d-1})!} \; . \end{aligned} \tag{A.19}$$

Finally, several terms in the factorials cancel, such that one ends up with

$$g_q(\beta, d) = \beta^{q+d-1} \frac{(\prod_{i=1}^{d-1} \mathcal{N}_i!)(q - \sum_{i=1}^{d-1} \mathcal{N}_i)!}{(q+d-1)!} \; , \tag{A.20}$$

i.e. eq. (A.17) also holds for $g_q(\beta, d)$. At last, we can set β equal to unity and obtain

$$f_q = g_q(1, d) = \frac{(\prod_{i=1}^{d-1} \mathcal{N}_i!)(q - \sum_{i=1}^{d-1} \mathcal{N}_i)!}{(q+d-1)!} \; , \tag{A.21}$$

which provides the required closed expression for f_q.

A.1.2 $\mathcal{N}$-summation

We still have to show that the $(d-1)$-fold sum in eq. (A.12) can be replaced by the single sum in eq. (A.13), *i.e.*

$$\sum_{\mathcal{N}_1=0}^{q} \sum_{\mathcal{N}_2=0}^{q-\nu_1} \cdots \sum_{\mathcal{N}_{d-1}=0}^{q-\sum_{i=1}^{d-2} \mathcal{N}_i} \lambda_1^{\mathcal{N}_1} \lambda_2^{\mathcal{N}_2} \ldots \lambda_{d-1}^{\mathcal{N}_{d-1}} \lambda_N^{q-\sum_{i=1}^{d-1} \mathcal{N}_i} = \sum_{i=1}^{d} \frac{\lambda_i^{q+d-1}}{\prod_{\substack{j=1 \\ j \neq i}}^{d} \lambda_i - \lambda_j} =: \mu_{q,d} \; . \tag{A.22}$$

This can be done by induction.

However, before doing so, it is useful to first show, again by induction, that $\mu_{-1,d} = 0$. For $d = 2$ this can be checked easily. For $d > 2$ we have

$$\begin{aligned}
\mu_{-1,d} &= \sum_{\substack{i=1\\ i\neq j}}^{d} \frac{\lambda_i^{d-3}}{\prod_{\substack{k=1\\ k\neq i,j}}^{d}(\lambda_i-\lambda_k)} \frac{\lambda_i}{\lambda_i-\lambda_j} + \frac{\lambda_j^{d-2}}{\prod_{\substack{k=1\\ k\neq j}}^{d}(\lambda_j-\lambda_k)} \\
&= \sum_{\substack{i=1\\ i\neq j}}^{d} \frac{\lambda_i^{d-3}}{\prod_{\substack{k=1\\ k\neq i,j}}^{d}(\lambda_i-\lambda_k)} + \sum_{\substack{i=1\\ i\neq j}}^{d} \frac{\lambda_j\lambda_i^{d-3}}{\prod_{\substack{k=1\\ k\neq i}}^{d}(\lambda_i-\lambda_k)} + \frac{\lambda_j\lambda_i^{d-2}}{\prod_{\substack{k=1\\ k\neq j}}^{d}(\lambda_j-\lambda_k)} \\
&= \sum_{\substack{i=1\\ i\neq j}}^{d} \frac{\lambda_i^{d-3}}{\prod_{\substack{k=1\\ k\neq i,j}}^{d}(\lambda_i-\lambda_k)} + \lambda_j \sum_{i=1}^{d} \frac{\lambda_i^{d-3}}{\prod_{\substack{k=1\\ k\neq i}}^{d}(\lambda_i-\lambda_k)} \; . \qquad \text{(A.23)}
\end{aligned}$$

The first term equals $\mu_{-1,d-1}(\lambda_1, \ldots, \lambda_{j-1}, \lambda_{j+1}, \ldots, \lambda_d)$, *i.e.* it vanishes by assumption. Eq. (A.23) holds for any choice of the index j. Therefore we can subtract eq. (A.23) from itself for different choices of j

$$0 = (\lambda_j - \lambda_l) \sum_{i=1}^{d} \frac{\lambda_i^{d-3}}{\prod_{\substack{k=1\\ k\neq i}}^{d}(\lambda_i-\lambda_k)} \; . \qquad \text{(A.24)}$$

Equality holds for arbitrary values of λ_j and λ_l, in particular for $\lambda_j \neq \lambda_l$. Therefore the sum has to vanish identically, which proves that also $\mu_{-1,d}$ vanishes.

Now we can come back to the proof of eq. (A.22). For $d = 2$ it is just a straightforward calculation to show that

$$\sum_{\nu=0}^{q} \lambda_1^{\nu}\lambda_2^{q-\nu} = \frac{\lambda_1^{q+1}}{\lambda_1-\lambda_2} + \frac{\lambda_2^{q+1}}{\lambda_2-\lambda_1} = \mu_{q,d} \; , \qquad \text{(A.25)}$$

what can be checked by multiplication with $\lambda_1 - \lambda_2$. Assuming that eq. (A.22) is true for $d-1$, we obtain

$$\mu_{q,d} = \sum_{\nu=0}^{q} \mu_{q-\nu,d-1}\lambda_d^{\nu} \; . \qquad \text{(A.26)}$$

The summation over ν can be performed, making use of the assumption,

eq. (A.22), once again, but this time for $d = 2$:

$$\begin{aligned} m_{q,d} &= \sum_{i=1}^{d-1} \frac{\lambda_i^{d-2}}{\prod_{\substack{j=1 \\ j\neq i}}^{d-1}(\lambda_i - \lambda_j)} \frac{\lambda_i^{q+1} - \lambda_d^{q+1}}{\lambda_i - \lambda_d} \\ &= \sum_{i=1}^{d} \frac{\lambda_i^{q+d-1}}{\prod_{\substack{j=1 \\ j\neq i}}^{d}(\lambda_i - \lambda_j)} - \lambda_d^{q+1} \sum_{i=1}^{d} \frac{\lambda_i^{d-2}}{\prod_{\substack{j=1 \\ j\neq i}}^{d}(\lambda_i - \lambda_j)} \frac{\lambda_i^{q+1} - \lambda_d^{q+1}}{\lambda_i - \lambda_d} \end{aligned} \tag{A.27}$$

We now use $\mu_{-1,d} = 0$, what implies that the second term vanishes. It immediately follows that the assumption as given in eq. (A.22) holds true for arbitrary d.

A.2 Integral representation

Here we show that $\mu_{q,d}$ can be expressed by the integral expression

$$\mu_{q,d} = \frac{\Gamma(q+d)}{\Gamma(q+1)} \int_\Delta dx\ \delta(\|\vec{x}\|_1 - 1)\ (\vec{\lambda}\vec{x})^q\ , \tag{A.28}$$

where dx is a short hand notation for $\prod_i dx_i$. In order to do so, we introduce some new quantity $f_{q,d}(a,b)$, defined as

$$f_{q,d}(a,b) = \frac{\Gamma(q+d)}{\Gamma(q+1)} \delta(\|\vec{x}\|_1 - (1-a))\ (\vec{\lambda}\vec{x} + b)^q\ , \tag{A.29}$$

such that the original quantity can be expressed as $\mu_{q,d} = f_{q,d}(0,0)$. Different values of d are related via

$$f_{q,d}(a,b) = \frac{\Gamma(q+d)}{\Gamma(q+d-1)} \int_0^{1-a} dx_{d-1}\ f_{q,d-1}(a + x_{d-1}, b + x_{d-1}\lambda_d)\ . \tag{A.30}$$

We now show by induction that

$$f_{q,d}(a,b) = \sum_{i=1}^{d} \frac{((1-a)\lambda_i + b)^{q+n-1}}{\prod_{\substack{j=1 \\ j\neq i}}^{d}(\lambda_i - \lambda_j)}\ , \tag{A.31}$$

for arbitrary real a and b. Setting a and b to zero will then yield eq. (A.28).

For $d = 2$, it is straightforward to check that eq. (A.31) is satisfied:

$$\begin{aligned} f_{q,2}(a,b) &= \frac{\Gamma(q+2)}{\Gamma(q+1)} \int_0^{1-a} dx_1((1-a-x_1)\lambda_2 + x_1\lambda_1 + b)^q \\ &= (q+1)\int_0^{1-a} ((\lambda_1-\lambda_2)x_1 + b + (1-a)\lambda_2)^q \\ &= \frac{((\lambda_1-\lambda_2)x_1 + b + (1-a)\lambda_2)^{q+1}}{(\lambda_1-\lambda_2)}\Big|_0^{1-a} \\ &= \frac{((1-a)\lambda_1 + b)^{q+1} - ((1-a)\lambda_2 + b)^{q+1}}{\lambda_1-\lambda_2} \ . \end{aligned} \tag{A.32}$$

Thus the assumption, eq. (A.31), holds for $d = 2$. For $d > 2$ we use eqs. (A.30) and (A.31) and obtain

$$\begin{aligned} f_{q,d}(a,b) &= \frac{\Gamma(q+d)}{\Gamma(q+d-1)} \int_0^{1-a} dx_{d-1} \\ &\quad \sum_{i=1}^{d-1} \frac{((1-a-x_{d-1})\lambda_i + b + x_{d-1}\lambda_d)^{q+d-2}}{\prod_{\substack{j=1\\ j\neq i}}^{d}(\lambda_i-\lambda_j)} \ . \end{aligned} \tag{A.33}$$

Carrying out the integral one obtains

$$\begin{aligned} f_{q,d}(a,b) &= \frac{\Gamma(q+d)}{\Gamma(q+d-1)} \\ &\quad \sum_{i=1}^{d-1} \frac{1}{\prod_{\substack{j=1\\ j\neq i}}^{d}(\lambda_i-\lambda_j)} \ \frac{((\lambda_d-\lambda_i)x_{d-1} + (1-a)\lambda_i + b)^{q+d-1}}{(q+d-1)(\lambda_d-\lambda_i)}\Big|_0^{1-a} \\ &= \sum_{i=1}^{d-1} \frac{((1-a)\lambda_i + b)^{q+d-1}}{\prod_{\substack{j=1\\ j\neq i}}^{d}(\lambda_i-\lambda_j)} + \sum_{i=1}^{d-1} \frac{((1-a)\lambda_{d-1} + b)^{q+n-1}}{(\lambda_{d-1}-\lambda_i)\prod_{\substack{j=1\\ j\neq i}}^{d}(\lambda_i-\lambda_j)} \ . \end{aligned} \tag{A.34}$$

We are done if we manage to show that

$$\sum_{i=1}^{d-1} \frac{1}{(\lambda_d-\lambda_i)\prod_{\substack{j=1\\ j\neq i}}^{d-1}(\lambda_i-\lambda_j)} = \frac{1}{\prod_{\substack{j=1\\ j\neq d}}^{d}(\lambda_d-\lambda_j)} \ , \tag{A.35}$$

or, equivalently, if the polynomial $P(\lambda_d)$ defined as

$$P(\lambda_d) = \sum_{i=1}^{d-1} \frac{\prod_{j=1}^{d-1}(\lambda_d - \lambda_j)}{(\lambda_d - \lambda_i)\prod_{\substack{j=1 \\ j\neq i}}^{d-1}(\lambda_i - \lambda_j)} = \sum_{i=1}^{d-1}\prod_{\substack{j=1 \\ j\neq i}}^{d-1}\frac{\lambda_d - \lambda_j}{\lambda_i - \lambda_j} \tag{A.36}$$

is identical to unity. The polynomial $P(\lambda_d)$ is of order not higher than $d-2$. We can evaluate it for $d-1$ different values of λ_d, namely at $\lambda_d = \lambda_k$ with $k = 1, \ldots, d-1$, and get

$$P(\lambda_k) = \prod_{j\neq k}\frac{\lambda_k - \lambda_j}{\lambda_k - \lambda_j} = 1 \ , \tag{A.37}$$

since all terms in the summation over i with $i \neq k$ vanish, because of the term $\lambda_k - \lambda_j$ in the numerator, with $j = 1, \ldots, i-1, i+1, \ldots, d-1$. The only polynomial of order not higher than $d-2$, adopting the value 1 at $d-1$ different points, is the zeroth order polynomial equal to unity. Therefore we conclude that $P \equiv 1$ and thus complete our proof.

Now we can easily reproduce [81] an analogous integral representation of the subentropy Q. Since Q can be expressed as $Q = -\lim_{q\to 1}\partial m_{q,d}/\partial q$, we obtain

$$\begin{aligned} Q &= -\lim_{q\to 1}\frac{\partial}{\partial q}\frac{\Gamma(q+d)}{\Gamma(q+1)}\int_\Delta d^d x\ (\vec{\lambda}\vec{x})^q \\ &= -\lim_{q\to 1}\frac{\Gamma(q+d)}{\Gamma(q+1)}\quad\left(\int_\Delta d^d x\ (\vec{\lambda}\vec{x})^q \ln\vec{\lambda}\vec{x}\right) - \\ &\qquad\qquad -(\Psi_d(q+d) - \Psi_d(q+1))\int_\Delta d^d x\ (\vec{\lambda}\vec{x})^q\Bigg) \\ &= -d!\left(\int_\Delta d^d x\ \vec{\lambda}\vec{x}\ln\vec{\lambda}\vec{x} - (\Psi_d(q+d) - \Psi_d(q+1))\right) \quad . \end{aligned} \tag{A.38}$$

Bibliography

[1] F. Schwabl, *Quantenmechanik* (Springer Verlag, Berlin, 1998).

[2] A. Einstein, B. Podolsky, and N. Rosen, *Can Quantum-Mechanical Description of Physical Reality Be Considered Complete ?*, Phys. Rev. **47**, 777 (1935).

[3] C. Papaliolios, *Experimental Test of a Hidden-Variable Quantum Theory*, Phys. Rev. Lett. **18**, 622 (1967).

[4] J. S. Bell, *On the Einstein-Podolski-Rosen Paradox*, Physics **1**, 195 (1964).

[5] J. F. Clauser, M. A. Horne, A. Shimony, and R. A. Holt, *Proposed Experiment to Test Local Hidden-Variable Theories*, Phys. Rev. Lett. **23**, 880 (1969).

[6] D. M. Greenberger, M. A. Horne, A. Shimony, and A. Zeilinger, *Bell's theorem without inequalities*, Am. J. Phys. **58**, 1131 (1990).

[7] J.-W. Pan, D. Bouwmeester, M. D. H. Weinfurter, and A. Zeilinger, *Experimental test of quantum nonlocality in three-photon Greenberger-Horne-Zeilinger entanglement*, Nature **403**, 515 (2000).

[8] R. P. Feynman, *Simulating physics with computers*, Int. J. Theor. Phys. **21**, 467 (1982).

[9] D. Deutsch, *Quantum theory, the Church-Turing Principle and the Universal Quantum Computer*, Proc. R. Soc. Lond. A **425**, 73 (1985).

[10] I. L. Chuang, N. Gershenfeld, and M. Kubinec, *Experimental implementation of fast quantum searching*, Phys. Rev. Lett **80**, 3408 (1998).

[11] F. Schmidt-Kaler, H. Häffner, M. Riebe, S. Gulde, G. P. T. Lancaster, T. Deuschle, C. Becher, C. F. Roos, J. Eschner, and R. Blatt, *Realization of the Cirac-Zoller controlled-NOT quantum gate*, Nature **422**, 408 (2003).

[12] D. Leibfried, B. DeMarco, V. Meyer, D. Lucas, M. Barrett, J. Britton, W. M. Itano, B. Jelenkovi, C. Langer, T. Rosenband, and D. J. Wineland, *Experimental demonstration of a robust, high-fidelity geometric two ion-qubit phase gate*, Nature **422**, 412 (2003).

[13] L. P. Hughston, R. Jozsa, and W. K. Wootters, *A complete classification of quantum ensembles having a given density matrix*, Phys. Lett. A **183**, 14 (1993).

[14] C. H. Bennet and G. Brassard, *Quantum cryptography: Public key distribution and coin tossing*, Proceedings of IEEE International Conference on Computers, Systems and Signal Processing 175 (1984).

[15] D. Bouwmeester, J.-W. Pan, K. Mattle, M. Eibl, H. Weinfurter, and A. Zeilinger, *Experimental quantum teleportation*, Nature **390**, 575 (1997).

[16] T. Jennewein, C. Simon, G. Weihs, H. Weinfurter, and A. Zeilinger, *Quantum Cryptography with Entangled Photons*, Phys. Rev. Lett. **84**, 4729 (2000).

[17] J. I. Cirac and P. Zoller, *Quantum Computations with Cold Trapped Ions*, Phys. Rev. Lett. **74**, 4091 (1995).

[18] C. Monroe, D. M. Meekhof, B. E. King, W. M. Itano, and D. J. Wineland, *Demonstration of a Fundamental Quantum Logic Gate*, Phys. Rev. Lett. **75**, 4714 (1995).

[19] Q. A. Turchette, C. S. Wood, B. E. King, C. J. Myatt, D. Leibfried, W. M. Itano, C. Monroe, and D. J. Wineland, *Deterministic Entanglement of Two Trapped Ions*, Phys. Rev. Lett. **81**, 3631 (1998).

[20] K. Mølmer and A. Sørensen, *Multiparticle Entanglement of Hot Trapped Ions*, Phys. Rev. Lett. **82**, 1835 (1999).

[21] T. Calarco, J. I. Cirac, and P. Zoller, *Entangling ions in arrays of microscopic traps*, Phys. Rev. A **63**, 062304 (2001).

[22] K. Eckert, J. Mompart, X. X. Yi, J. Schliemann, D. Bruß, G. Birkl, and M. Lewenstein, *Quantum computing in optical microtraps based on the motional states of neutral atoms*, Phys. Rev. A **66**, 042317 (2002).

[23] J. Mompart, K. Eckert, W. Ertmer, G. Birkl, and M. Lewenstein, *Quantum Computing with Spatially Delocalized Qubits*, Phys. Rev. Lett. **90**, 147901 (2003).

[24] D. Jaksch, H.-J. Briegel, J. I. Cirac, C. W. Gardiner, and P. Zoller, *Entanglement of Atoms via Cold Controlled Collisions*, Phys. Rev. Lett **82**, 1975 (1999).

[25] O. Mandel, M. Greiner, A. Widera, T. Rom, T. W. Hänsch, and I. Bloch, *Controlled Collisions for Multiparticle Entanglement of Optically Trapped Atoms*, Nature **425**, 937 (2003).

[26] W. K. Wootters, *Entanglement of Formation of an Arbitrary State of Two Qubits*, Phys. Rev. Lett. **80**, 2245 (1998).

[27] T. Wellens and M. Kuś, *Separable approximation for mixed states of composite quantum systems*, Phys. Rev. A **64**, 052302 (2001).

[28] B.-G. Englert and N. Metwally, *Remarks on 2-q-bit states*, Appl. Phys. B **72**, 35 (2001).

[29] M. Reed and B. Simon, *Methods of modern mathematical physics* (Academic press, London, 1980).

[30] R. F. Werner, *Quantum states with Einstein-Podolsky-Rosen correlations admitting a hidden-variable model*, Phys. Rev. A **40**, 4277 (1989).

[31] P. A. Horn and C. R. Johnson, *Matrix Analysis* (Cambridge University Press, New York, 1985).

[32] M. Horodecki, P. Horodecki, and R. Horodecki, *Separability of mixed states: necessary and sufficient conditions*, Phys. Lett. A **223**, 1 (1996).

[33] A. Peres, *Separability Criterion for Density Matrices*, Phys. Rev. Lett. **77**, 1413 (1996).

[34] M. Horodecki, P. Horodecki, and R. Horodecki, *Mixed-State Entanglement and Distillation: Is there a 'Bound' Entanglement in Nature?*, Phys. Rev. Lett. **80**, 5239 (1998).

[35] P. Horodecki, M. Horodecki, and R. Horodecki, *Bound entanglement can be activated*, Phys. Rev. Lett. **82**, 1056 (1999).

[36] G. Vidal, *Entanglement monotones*, J. Mod. Opt **47**, 355 (2000).

[37] K. Kraus, *General state changes in quantum theory*, Ann. Phys. **64**, 311 (1971).

[38] K. Kraus, *States, Effects and Operations* (Springer Verlag, Berlin, 1983).

[39] K. E. Hellwig and K. Kraus, *Pure operations and measurements*, Commun. Math. Phys. **11**, 214 (1969).

[40] K. E. Hellwig and K. Kraus, *Operations and measurements II*, Commun. Math. Phys. **16**, 142 (1970).

[41] M. A. Nielsen, *Conditions for a Class of Entanglement Transformations*, Phys. Rev. Lett. **83**, 436 (1999).

[42] T. Ando, *Majorization, Doubly Stochastic Matrices, and Comparison of Eigenvalues*, Linear Algebra Appl. **118**, 163 (1989).

[43] C. H. Bennet, D. P. DiVincenzo, J. A. Smolin, and W. K. Wootters, *Mixed-state entanglement and quantum error correction*, Phys. Rev. A **54**, 3824 (1996).

[44] A. Uhlmann, *Fidelity and concurrence of conjugated states*, Phys. Rev. A **62**, 032307 (2000).

[45] E. Schrödinger, *Probability relations between separated systems*, Proc. Cambridge Philos. Soc **32**, 446 (1936).

[46] A. Uhlmann, *Optimizing entropy relative to a channel or a subalgebra*, Open Sys. & Inf. Dyn. **5**, 209 (1998).

[47] V. Vedral and M. Plenio, *Entanglement measures and purification procedures*, Phys. Rev. A **57**, 1619 (1998).

[48] D. Bruß, *Characterizing entanglement*, J. Math. Phys. **43**, 4237 (2002).

[49] M. Horodecki, *Entanglement measures*, Quant. Inf. Comp. **1**, 3 (2002).

[50] M. Horodecki, P. Horodecki, and J. Oppenheim, *Reversible transformations from pure to mixed states and the unique measure of information*, Phys. Rev. A **67**, 062104 (2003).

[51] G. Vidal and R. F. Werner, *A computable measure of entanglement*, Phys. Rev. A **65**, 032314 (2002).

[52] C. H. Bennett, D. P. DiVincenzo, J. A. Smolin, and W. K. Wootters, *Mixed-state entanglement and quantum error correction*, Phys. Rev. A **54**, 3824 (1996).

[53] S. Hill and W. K. Wootters, *Entanglement of a Pair of Quantum Bits*, Phys. Rev. Lett. **78**, 5022 (1997).

[54] E. W. Weisstein, *Concise Encyclopedia of Mathematics* (CRC press, London, 1999).

[55] B. M. Terhal and K. G. H. Vollbrecht, *Entanglement of formation for Isotropic states*, Phys. Rev. Lett **85**, 2625 (2000).

[56] K. Życzkowski, *Volume of the set of separable states. II*, Phys. Rev. A **60**, 3496 (1999).

[57] K. Audenaert, F. Verstraete, and B. D. Moor, *Variational characterizations of separability and entanglement of formation*, Phys. Rev. A **64**, 052304 (2001).

[58] A. Łozinski, A. Buchleitner, K. Życzkowski, and T. Wellens, *Entanglement of* $2 \times K$ *quantum systems*, Euro Phys. Lett. **62**, 168 (2003).

[59] C. A. Sackett, D. Kielpinski, B. E. King, C. Langer, V. Meyer, C. J. Myatt, M. Rowe, Q. A. Turchette, W. M. Itano, D. J. Wineland, and C. Monroe, *Experimental entanglement of four particles*, Nature **404**, 256 (2000).

[60] S. Osnaghi, P. Bertet, A. Auffeves, P. Maioli, M. Brune, J. M. Raimond, and S. Haroche, *Coherent Control of an Atomic Collision in a Cavity*, Phys. Rev. Lett. **87**, 037902 (2001).

[61] W. K. Wootters, *Entanglement of formation and concurrence*, Quant. Inf. Comp. **1**, 27 (2001).

[62] P. Rungta, V. Buzek, C. M. Caves, M. Hillery, G. J. Milburn, and W. K. Wootters, *Universal state inversion and concurrence in arbitrary dimensions*, Phys. Rev. A **64**, 042315 (2001).

[63] E. Beckenbach and R. E. Bellmann, *Inequalities* (Springer Verlag, Berlin, 1971).

[64] F. Mintert, M. Kuś, and A. Buchleitner, *Concurrence of mixed quantum states in arbitrary dimensions*, submitted to Phys. Rev. Lett. (2003).

[65] P. Horodecki, *Separability criterion and inseparable mixed states with positive partial transposition*, Phys. Lett. A **232**, 333 (1997).

[66] W. H. Press, S. A. Teulosky, W. T. Vetterling, and B. P. Flannery, *Numerical Recipies* (Cambridge University Press, Camebridge, 1999).

[67] W. Dür, G. Vidal, and J. I. Cirac, *Three qubits can be entangled in two inequivalent ways*, Phys. Rev. A **62**, 062314 (2000).

[68] V. Coffman, J. Kundu, and W. K. Wootters, *Distributed Entanglement*, Phys.Rev. A **61**, 052306 (2000).

[69] G. Krüger, *Programmieren in C* (Addison-Wesley, Bonn, 1995).

[70] P. K. Ghosh, *Ion Traps* (Oxford University Press, Oxford, 1995).

[71] K. Mølmer and A. Sørensen, *Entanglement and quantum computation with ions in thermal motion*, Phys. Rev. A **62**, 022311 (2000).

[72] Q. A. Turchette, D. Kielpinski, B. E. King, D. Leibfired, D. M. Meekhof, C. J. Myatt, M. A. Rowe, C. A. Sackett, W. M. Itano, C. Monroe, and D. J. Wineland, *Heating of trapped ions from the quantum ground state*, Phys. Rev. A **61**, 063418 (2000).

[73] A. Carvalho, F. Mintert, and A. Buchleitner, *in preparation*, .

[74] A. Perelomov, *Generalized Coherent States and their Applications* (Springer Verlag, Berlin, 1986).

[75] A. Wehrl, *On the relation between classical and quantum-mechanical entropy*, Rep. Math. Phys. **16**, 353 (1979).

[76] K. Husimi, *Some formal properties of density matrices*, Proc. Phys. Math. Soc. Jpn. **22**, 264 (1940).

[77] A. Wehrl, *General properties of entropy*, Rev. Mod. Phys. **50**, 221 (1978).

[78] E. H. Lieb, *Proof of an Entropy Conjecture of Wehrl*, Comm. Math. Phys. **62**, 35 (1978).

[79] S. Gnutzmann and K. Życzkowski, *Rényi–Wehrl entropies as measures of localization in phase space*, J. Phys. A **34**, 10123 (2001).

[80] F. Mintert and K. Życzkowski, *Wehrl entropy, Lieb conjecture and entanglement monotones*, Phys. Rev. A **69**, 022317 (2004).

[81] R. Jozsa, D. Robb, and W. K. Wootters, *Lower bound for accessible information in quantum mechanics*, Phys. Rev. A **49**, 668 (1994).

[82] M. Abramowitz and I. A. Stegun, *Handbook of Mathematical Functions with Formulas, Graphs, and Mathematical Table* (Dover Publications, Inc., Mineola, NY, 1984).

[83] A. Rényi, *Proc. of the Fourth Berkeley Symp. Math. Statist. Prob. 1960,Vol. I* (University of California Press, Berkeley, 1961), p. 547.